ANL-7208
Reactor Technology
(TID-4500)
AEC Research and
Development Report

ARGONNE NATIONAL LABORATORY
9700 South Cass Avenue
Argonne, Illinois 60439



# ZPR-9 ASSEMBLIES NO. 6-9 CRITICAL EXPERIMENTS

by

R. C. Doerner, W. G. Knapp,
R. A. Karam, and D. K. Butler

Reactor Physics Division



March 1967

## DISCLAIMER

# TABLE OF CONTENTS

TABLE OF CONTENTS

# TABLE OF CONTENTS

# LIST OF FIGURES

# LIST OF FIGURES

## LIST OF FIGURES

# LIST OF FIGURES

# LIST OF TABLES

# LIST OF TABLES

# ZPR-9 ASSEMBLIES NO. 6-9 CRITICAL EXPERIMENTS

by

R. C. Doerner, W. G. Knapp,
R. A. Karam, and D. K. Butler

## I. INTRODUCTION

A series of fast critical assemblies was studied in the Argonne ZPR-9 facility in support of the Laboratory's design effort in the fast-reactor, nuclear-propulsion program. Historically, critical experiments have been used to provide engineering design parameters for a mockup or prototype reactor. This approach was neither practical nor desirable in the rocket program since the engineering work was done essentially simultaneously with the physics effort. Rather, an attempt was made primarily to provide integral measurements as checkpoints for cross-section sets that were generated for the program and, secondarily, to provide data to test the utility of simple, one-dimensional, multigroup diffusion theory in the program. A major objective of the present report is to present the results of a series of critical experiments emphasizing the important differences between measurements made in metal- and oxide-fueled cores and between aluminum, $Al_2O_3$, and BeO as a reflector material. This is the third of four topical reports describing a two year program of study.

Studies directed towards an evaluation of tungsten cross sections relative to $U^{238}$ (Assemblies No. 1-4) have been reported in ANL-7007[1] and ANL-7010.[2]

Four aluminum-reflected assemblies were studied in which the neutronically familiar $U^{238}$ diluent material was gradually replaced by increasing amounts of tungsten. As an anchor point for these measurements, the core of Assembly No. 1 was the extensively studied 7:1 volume ratio of a $U^{238}$ diluent material to $U^{235}$ fuel, but having an aluminum reflector. A comparison of data obtained on these assemblies to corresponding measurements in the reference reactor (ZPR-3 Assemblies No. 11 and 22; ZPR-6 Assembly No. 1; 7:1 volume ratio of $U^{238}$ diluent to $U^{235}$ fuel with a $U^{238}$ reflector) yields some of the pertinent information regarding the neutronics of the aluminum reflector, particularly the effects of large downscattering characteristic of aluminum. In subsequent assemblies, one-fourth, one half, and all of the $U^{238}$ diluent material was replaced by tungsten. In addition to a set of standard measurements performed on these systems (critical mass, Rossi-alpha, central fuel, and material worths), a limited number of studies were made of the effects of sample size on the reactivity worth of boron and of hydrogenous materials in a fast spectrum.

Measurements related to the effects of changing core diluent compositions have been reported in ANL-7207[3] and ANL-7110.[4] In the series of assemblies discussed in these reports, the standard measurements were repeated in a very dense and heavily absorbing tungsten-rhenium-diluted core (Assembly No. 4B); a moderately dense tungsten-carbon-diluted core with a fairly soft spectrum (Assembly No. 5), and a dilute core (Assembly No. 6) typical of rocket engines with approximately 25% porosity. Assembly No. 6 is used as a reference for the studies reported in the present work. The last report of the series[5] will review much of the analytical effect and how it relates to the experimental measurements as a whole.

The sections that follow describe the assemblies and present the results of the basic experiments.[6] Measurements specifically related to the control and propellant problems are given in Sections III and IV. Sections V and VI, respectively, present the spatially dependent reaction rates and reactivity traverses. Section VII then discusses results of the measurements according to experiment type.

In the assemblies studied, Assembly No. 6 was a $U^{235}$ metal-fueled (~10 v/o), tungsten-diluted (~35 v/o) core, having an essentially infinite aluminum metal reflector. The core composition of Assembly No. 7 was the same, but the reflector was changed to $Al_2O_3$. In both assemblies, about 50% of the core volume consisted of 45% density aluminum. In Assembly No. 9, sufficient $Al_2O_3$ replaced the aluminum diluent in the core to give a U:O atom ratio of 1:2 in order to simulate an oxide-fueled, oxide-reflected system. In the last (chronologically) assembly to be studied in this series (Assembly No. 8), the oxide-fueled core of Assembly No. 9 was surrounded by a nominal 10-cm-thick BeO reflector. It was found necessary, in this case, to isolate the assembly from its surroundings by a 40-cm-thick, aluminum metal isolation blanket. For safety reasons, the 10-cm thickness was chosen to limit the thermal power spike at the core-reflector interface, and an aluminum metal axial reflector was used to provide a negative prompt power coefficient. Table XXXII summarizes the assemblies studied in this report.

# II. CRITICAL EXPERIMENTS

This section provides details of the various assemblies and the values for some of the measured parameters. For comparison, Assembly No. 6 will be used as a reference in later sections, but detailed measurements will not be repeated here. (These have been reported in ANL-7207.)

## A. Assembly No. 7

Assembly No. 7 was the first oxide-reflected system to be studied in the ZPR-9 program and represents an intermediate step between the hard-spectrum reflector of aluminum metal and the soft-spectrum reflector of beryllium. Two versions of Assembly No. 7, which differed in their critical mass by about 10 kg of $U^{235}$, were in effect. The first had a nominal 37.5-cm-thick $Al_2O_3$ reflector, and in this were made the central-worth, fuel-edge, and Rossi-alpha measurements. In the preparatory measurements for the boron-sleeve experiment, 37.5-cm $Al_2O_3$ as a radial reflector was not infinite, and in fact even a 50.1-cm-thick $Al_2O_3$ reflector did not isolate the assembly from its environment. For this reason, a 12.8-cm-thick, aluminum metal isolation sleeve around the radial surface of the 50.1-cm-thick oxide reflector constituted the second version of Assembly No. 7.

### 1. Description

A reasonably symmetric and cylindrical geometry was obtained in Loading 18. Figure 1 shows a geometric outline of this loading for the stationary half. Drawers occupying a full matrix position were loaded in the following sequence from east to west*: WAFWAWA-FWAWFAWAWFA, where W and A represent 1/8-in.-thick columns of tungsten and 45% density aluminum, respectively, and F represents 1/16-in.-thick columns of fully enriched (93%) $U^{235}$ fuel. Further details regarding these materials are contained in the appendix. In the horizontally loaded half-drawers indicated in Fig. 1, the same sequence was followed starting from the top and going downwards. In all the half-drawers, one-half of the core material was replaced by $Al_2O_3$. In the movable half, a fully loaded drawer was in

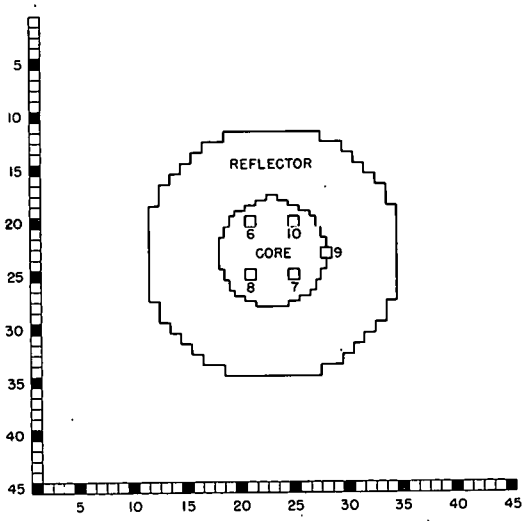


112-7759

Fig. 1. Geometric Outline, Assembly No. 7, Loading 18, Stationary Half.

*All ZPR-9 assemblies are loaded as horizontal cylinders with a north-south central axis. The stationary half is the north half of the assembly.

M-2823* and a half-loaded drawer in M-1823, the reverse of that shown in Fig. 1 for the stationary half.

2. Critical Properties

While the outer regions of the core were being cylindricized, but before the aluminum metal was replaced by $Al_2O_3$ in the axial reflector, measurements of the core-material worth at the radial core-reflector interface gave a value of 17.7 Ih/kg of $U^{235}$. Edge worth measurements are always made by replacing core material (fuel + diluent) by reflector material. Numerical values for the worth correspond to the reactivity change per kg of $U^{235}$ change in such a replacement. Some variation in edge worth is expected, depending on the side of the core in which the replacement is made and hence on the amount of tungsten between the outermost fuel plate and the innermost reflector material. Smaller variations are expected because of varying radii of the outermost drawers.

After the axial reflector was changed to $Al_2O_3$, edge worths ranged from 12 Ih/kg of $U^{235}$ for horizontally loaded quarter drawers at the bottom of the core to 16 Ih/kg for vertically loaded full drawers at the core sides. Similarly, the addition of 1.4 kg of fuel more or less homogeneously at the core surface gave the value of 19 Ih/kg, while an analagous removal of 5.5 kg of $U^{235}$ gave an edge worth of 24 Ih/kg. A factor of two variation is considerably larger than the general past experience would indicate, but can be attributed to possible small changes in core-reflector geometry made between the different measurements. An unweighted average of all the measurements gives the fuel-edge worth of 18.21 Ih/kg of $U^{235}$.

Critical properties of Loading 18 are listed on the bottom part of Table XXXII. The quoted core length includes a 1.5-mm air gap plus the 0.75-mm-thick aluminum drawer fronts in each half.

The critical mass is determined by compensating for the excess reactivity (151.2 Ih) by removal of (151.2 Ih/18.2 Ih/kg = 8.3 kg) peripheral fuel. Since the atom density of fuel is fixed, the corresponding critical radius can be determined immediately. These results are given in column 6 of Table XXXIV. Also included in that table is the $k_{eff}$ of the experimental assembly in which excess reactivity (in Ih) is converted to k by the calculated constant listed in Table XXXII. Atom densities in units of $10^{24}$ atoms/cm$^3$ for the core and reflector region are given in Table XXXIII.

3. Central Worths of Nonhydrogenous Materials

Central reactivity worths of a large number of the samples were measured in Loading 15, a loading essentially the same as Loading 18. Results

*Notation for drawer identification is a letter (M or S) for movable or stationary half, and two numbers designating row and column.

for nonhydrogenous materials are given in Table I. The central worths of rhenium and of crystalline boron were measured independently on different days. For both cases, the error in the measurements is approximately ±0.2 Ih. The two measurements of $Gd_2O_3$ were made within several hours of each other and without separating the halves between measurements. The error in this case is ~±0.05 Ih.

TABLE I. Central Worths of Nonhydrogenous Materials in Assembly No. 7

| Material[a] | Sample Weight, g | Δρ, Ih | Δρ/ΔM, Ih/kg |
|---|---|---|---|
| Rhenium | 1266.9 | -58.0<br>-59.5 | -45.8<br>-46.9 } 46.4 ± 0.2 |
| Be[b] | 114.309 | -0.265 | -2.3 ± 2.6 |
| Tungsten | 1052.0 | -11.6 | -11.0 ± 0.3 |
| Carbon | 103.0 | 2.67 | 25 ± 3 |
| $WO_2$[b] | 78.370 | -0.659 | -8.4 ± 3.8 |
| $B^{10}$[c] | 29.29 | -72.0 | -2460 ± 10 |
| $B_4C$[d] | 59.62 | -13.9 | -234 ± 5 |
| Gold | 1183.6 | -23.7 | -20.0 ± 0.3 |
| $U^{238}$[b] | 507.555 | -1.35 | -2.7 ± 0.6 |
| $U^{235}$[b] | 134.980 | 23.8 | 176 ± 2 |
| $UO_2$[b] | 106.500 | 0.515 | 4.8 ± 2.8 |
| Crystalline B[b] | 75.200 | -37.5<br>-37.7 | -498<br>-502 } -500 ± 4 |
| $Eu_2O_3$[b] | 34.2 | -2.41 | -70 ± 9 |
| $Gd_2O_3$ | 59.20 | 0.458<br>0.350 | 7.74<br>5.91 } 6.8 ± 5.1 |
| $Y_2O_3$[b] | 81.5 | 2.95 | 36 ± 4 |
| $Dy_2O_3$[b] | 104.7 | 1.96 | 19 ± 3 |
| $U^{233}$[e] | 283.60 + 8.32 g $U^{238}$ | 85.0 | 300 ± 2 |
| Gadolinium | 397.930 | -16.5 | -41.4 ± 0.7 |
| Europium | 324.93 | -52.4 | -161 ± 1 |
| Lucite | 59.153 | 25.8 | 435 ± 5 |

[a] All samples occupy a 5 x 5 x 2.5-$cm^3$ volume at the center of the core and are unclad unless otherwise noted.
[b] Clad in 0.032-in.-thick Type 1100 aluminum.
[c] Clad in 0.064-in.-thick Type 304 stainless steel. Samples also contained 2.23 g of $B^{11}$ plus 1.78 g of impurities, mostly Ni, Ca, Al, Fe, Mg, Mn, and Si.
[d] Unclad hot pressure plates of $B_4C$ containing 0.78 g of impurity. Boron is 19.57 w/o $B^{10}$ and 80.43 w/o $B^{11}$.
[e] $U^{233}$ plates have an inner cladding of 0.015-in. aluminum and a center cladding of 0.015-in. Type 304 stainless steel.

Although it is difficult to assign errors to a given set of central-worth measurements, these errors rarely exceed ±0.3 Ih and depend rather sensitively on the individual reactor operator who determines the critical rod position. Smaller errors in the absolute magnitude of the measurement are introduced by errors in rod calibration and possibly the value of $\beta_{eff}$ (or equivalently, the prompt-neutron lifetime) used in converting measured periods to reactivities through the inhour equation. We take the position here, that unless there is motivation for doing otherwise, all errors in the measurement are ±0.3 Ih. In the case of $U^{233}$, the automatic sample changer could not accommodate the oversized $U^{233}$ plates, and an error of ±0.5 Ih is assigned to the measurement. No correction was made for the 8.32 g of $U^{238}$ impurities in the sample.

### 4. Central Worth of Hydrogen

The central worth of hydrogen-containing materials is shown in Table II. A correction for carbon in all samples was made using 0.025 Ih/g of carbon. Polyethylene samples were made by laying 1 x 2 x 0.020-in.-thick strips of material in 2 x 2 x 1-in. aluminum cans. (Physical properties of polyethylene are given in the appendix.) Although small variations in the hydrogen worth between samples is noted, these are not statistically significant. These data indicate that the average central hydrogen worth is 3.71 Ih/g and that the spectrum in Assembly No. 7 is such that the central hydrogen worth is not severely self-shielded.

TABLE II. Central Worths of Polyethylene in Assembly No. 7

| Sample | | Constituent Weights, g | | Correction for Carbon, Ih | Hydrogen Worth,[b] Ih/g |
|---|---|---|---|---|---|
| Weight, g | Worth,[a] Ih | Hydrogen | Carbon | | |
| 59.153 | 32.96 | 8.458 | 50.695 | 1.28 | 3.73 ± 0.03 |
| 53.918 | 30.07 | 7.710 | 45.992 | 1.16 | 3.75 ± 0.03 |
| 49.116 | 27.70 | 7.023 | 42.092 | 1.05 | 3.69 ± 0.03 |
| 5.020 | 2.75 | 0.718 | 4.282 | 0.11 | 3.68 ± 0.29 |
| | | | | | avg: 3.71 |

[a]All measurements were made during the same reactor run and have an estimated error of ±0.20 Ih.
[b]Assumes an error of ±11% in carbon.

### 5. Central Worths of Boron-Lucite Mixtures

The central worths for varying mixtures of boron and Lucite are shown in Table III. The first four items shown in this table were mixtures of fine powders of crystalline boron and Lucite that filled the standard

2 x 2 x 1-in. aluminum sample can, while the next three were powders that were compressed under high temperature and at high pressure, to form small pellets approximately 1 in. in diameter by 1/4 in. thick. In Table III, the first column lists the weight percent of the sample, which was boron. The subsequent columns list the weight of the sample and its measured reactivity worth in the center of the core. Because the measurements extended over several days, the error associated with column 3 is estimated to be ±0.2 Ih. The next two columns list the gram weights for the constituent parts of each sample. A correction is then applied to the measured worth for the effects of the Lucite. Since the measurements with hydrogen did not show any sample size effects, it was assumed that the Lucite in each sample had a constant worth per gram (0.435 ± 0.005 Ih/g). What remains is the apparent worth of boron in the sample, and this is shown in the last column. Comparing this to the central worth for pure boron (500 Ih/g as listed in Table I), we see that the boron in the presence of hydrogen has a somewhat enhanced or higher apparent worth per gram of material.

TABLE III. Central Worths of Boron-Lucite Mixtures

| Sample | | | Constituent | | | |
|---|---|---|---|---|---|---|
| | | | Weights, g | | | |
| % Boron | Weight, g | Measured Worth, Ih | Boron | Lucite | Worth of Lucite,[a] Ih | Apparent Boron Worth, Ih/g |
| 20 | 27.232 | -1.15 ± 0.05 | 5.446 | 21.785 | 9.476 ± 0.653 | 1.95 ± 0.12 |
| 40 | 31.307 | -6.023 ± 0.05 | 12.522 | 18.784 | 8.171 ± 0.375 | 1.133 ± 0.03 |
| 50 | 28.893 | -4.007 ± 0.05 | 14.447 | 14.447 | 6.284 ± 0.433 | 0.712 ± 0.03 |
| 70 | 33.578 | -10.66 ± 0.05 | 23.505 | 10.073 | 4.381 ± 0.302 | 0.641 ± 0.01 |
| 25 P[b] | 19.939 | -2.79 ± 0.05 | 4.985 | 14.954 | 6.504 ± 0.448 | 1.864 ± 0.09 |
| 50 P[b] | 19.854 | -5.88 ± 0.05 | 9.927 | 9.927 | 10.198 ± 0.297 | 1.027 ± 0.03 |
| 75 P[b] | 19.275 | -7.96 ± 0.05 | 14.591 | 4.818 | 2.095 ± 0.144 | 0.685 ± 0.01 |
| 100 P[c] | 75.200 | -37.55 ± 0.10 | 75.200 | 0 | 0 | 0.500 ± 0.004 |

[a]Based on measured worth of Lucite (0.435 ± 0.005) being constant with size and density. Error associated with Lucite is ±0.03 Ih/g.
[b]P = pellet.
[c]Crystalline boron, taken from Table I.

## 6. Kinetic Properties

According to the statistical model of a point critical reactor, the correlation in time between detected events from correlated neutron chains decreases exponentially with time. In all the assemblies studied in the ZPR-9 program, there has been evidence of at least two and possibly three exponentials in the Rossi-alpha data. Further evidence of more than a single decay component in the Rossi-alpha measurements has been seen on several of the ZPR-3 experiments in which the reflector spectrum was considerably different (softer) than the core spectrum. Rossi-alpha measurements made in Assembly No. 7 indicate that the oxide reflector strongly enhances the faster decaying component in the measured alpha values.

Following the fundamental mode statistical model, it has been the customary practice to identify the major decay component ($\alpha_3$) with $\beta_{eff}/\ell$, where $\ell$ is the prompt-neutron lifetime of the assembly as a whole.

Because of instrument limitation associated with the electronic equipment used in the measurements on the earlier assemblies (minimum time per channel ~16 $\mu$sec), only the predominant component, $\alpha_3$, was measured. Table IV lists the values of the three measured components in the Rossi-alpha as well as the calculated $\beta_{eff}$ and $\ell$ values for Assembly No. 7. It has been the general experience within the ZPR-9 program to underestimate the calculated prompt-neutron lifetime by some 30-40%. In part, this is the consequence of the particular cross-section sets that have been used in the calculations, as well as the tendency for the one-dimensional diffusion code to calculate a harder real-flux spectrum than that which actually exists, even when the best cross sections available are used.

TABLE IV. Kinetic Properties of Assembly No. 7

| Measured Rossi-alpha, $sec^{-1}$ | | | $\beta_{eff}$, Calculated | Prompt Lifetime, nsec | |
|---|---|---|---|---|---|
| $\alpha_1$ | $\alpha_2$ | $\alpha_3$ | | Measured | Calculated |
| $(8.58 \pm 0.92) \times 10^5$ | $(6.86 \pm 0.58) \times 10^4$ | $(1.51 \pm 0.10) \times 10^3$ | 0.00660 | 4370 | 3110 |

## 7. Second Version of Assembly No. 7

Through a series of experiments, to be reported in Section III, the reactivity worth of both boron and fuel at or near the core-reflector interface was found to depend rather sensitively on position. This led to adding 12.6 cm of $Al_2O_3$ to the radial reflector (exhausting the supply of this material) and a 12.87-cm-thick sleeve (two-drawer thickness) of aluminum metal around the radial reflector in order to isolate the assembly from its environment. In this geometry, fuel-edge and boron worths were found to be independent of geometry. The critical properties of Loading 71, referred to earlier as the second version of Assembly No. 7, are listed in Table XXXII, and the geometric outline of the assembly is shown in Fig. 2. The only measurements made in this loading were the spatial distribution of reaction rates and reactivities as determined by the traverse mechanism. These will be reported in Sections V and VI, respectively.

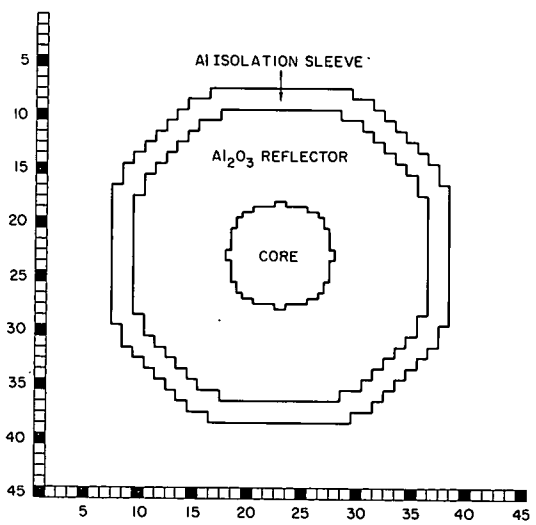


112-7751

Fig. 2. Geometric Outline, Assembly No. 7, Loading 71.

## B. Assembly No. 9

The main objective of Assembly No. 9 was to determine the effects of the oxide, relative to its metal as a fuel. Except for the replacement for some of the 45% density aluminum by $Al_2O_3$, the core composition and reflector properties of Assembly No. 9 were essentially those of Assembly No. 7.

### 1. Description

Each drawer was loaded with 10-in.-long columns of materials in the following sequence from east to west: WOFWAWOFWAWOFWAWFO, where W, O, and A represent 1/8-in.-thick columns of tungsten, $Al_2O_3$, and 45%-density aluminum metal, respectively, and F represents 1/16-in.-thick columns of the fully enriched $U^{235}$ fuel. Additional data related to these materials and their weights are given in the appendix. As for Assembly No. 7, each 10-in.-long column consisted of two 2 x 3-in. pieces plus two 2 x 2-in. pieces, laid end to end. Loading to critical was done in a straightforward manner starting with approximately one-third of the critical mass followed by a multiplication measurement and an addition of approximately one-third of the remaining fuel, etc. Loading 7 was reasonably cylindrical and critical with an excess reactivity of 106.2 Ih. The geometric outline of a stationary half of Loading 7 is shown in Fig. 3. Both the radial and axial reflectors were high-density $Al_2O_3$ having thicknesses of 50.825 and 35.56 cm, respectively. The two-drawer-thick aluminum metal isolation blanket found necessary on Assembly No. 7 was retained for Assembly No. 9.

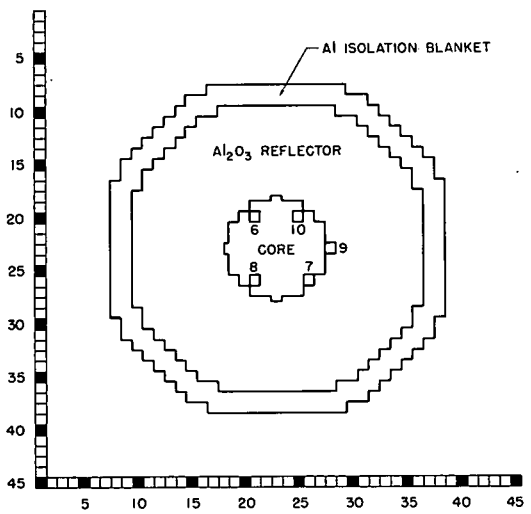


112-7757

Fig. 3. Geometric Outline, Assembly No. 9, Loading 7.

### 2. Critical Properties

Fuel-edge worth was determined through a series of measurements in which half-loaded drawers* replaced reflector drawers in various radial positions around the core. In the first of these measurements, vertically loaded half-drawers were exchanged with reflector drawers on the east and west sides (in positions 22-18 and 24-28 of the stationary half and in positions 24-18 and 22-28 of the movable half; see Fig. 3). This added 84 Ih of reactivity or 30.47 Ih/kg of $U^{235}$. In the next measurement, the same fuel drawers were relocated to positions 45° off the horizontal axis in matrix

* The other half of the drawer was loaded with reflector material.

positions 20-27 and 26-19 in the stationary half and 20-19 and 26-27 in the movable half; 90 Ih of reactivity (32.65 Ih/kg of $U^{235}$) were gained. In the last measurement of the series, the half-drawers were horizontally loaded and placed at the top and bottom of the core in positions 18-22 and 28-24 in the movable half and 18-24 and 28-22 in the stationary half. This added 92 Ih of reactivity (33.375 Ih/kg of $U^{235}$). An unweighted average of the three measurements gives a value of 33.16 Ih/kg of fuel at the core edge. Compensating for the excess reactivity of Loading 7 by the removal of fuel from the core edge yields a critical mass of 192.4 kg. The critical properties of Assembly No. 9, Loading 7 are summarized in Table XXXII.

### 3. Central Worths of Nonhydrogenous Materials

Central material worths relative to void were determined for the same series of samples as was used in Assembly No. 7. These are listed in Table V. In the measurements for which an error is listed, the

TABLE V. Central Worths of Nonhydrogenous Materials in Assembly No. 9

| Material | Sample Weight, g | Measured Worth, Ih | Sample Worth, Ih/kg |
|---|---|---|---|
| Lucite | 72.970 | 27.3 ± 0.1 | 376 ± 2 |
| Carbon | 103 | 1.16 ± 0.11 | 12.1 ± 2.9 |
| $Al_2O_3$ | 226.4 | -0.232 ± 0.038 | -0.63 ± 0.17 |
| $U^{235}$ | 134.980 | 28.1 ± 0.1 | 206.7 ± 0.6 |
| $U^{238}$ | 507.555 | -2.91 ± 0.12 | -5.7 ± 0.2 |
| Gadolinium | 12.8144 | -0.73 ± 0.10 | -57 ± 8 |
| $Gd_2O_3$ | 59.2 | -2.77 ± 0.10 | -46.8 ± 1.7 |
| $WO_2$ | 78.3702 | -0.95 ± 0.10 | -12.1 ± 1.3 |
| Natural Boron | 75.2 | -49.1 ± 0.2 | -653 ± 3 |
| $Y_2O_3$ | 81.5 | 0.36 ± 0.09 | 4.4 ± 1.1 |
| $Dy_2O_3$ | 104.7 | -4.28 ± 0.09 | -40.9 ± 0.9 |
| $Eu_2O_3$ | 34.2 | -6.13 ± 0.13 | -179 ± 4 |
| $B_4C$ | 83.509 | -45.4 ± 0.3 | -543 ± 3 |
| Tungsten | 1108 | -17.7 ± 0.2 | -15.9 ± 0.2 |
| BeO | 177.7 | 3.79 ± 0.09 | 21.3 ± 0.5 |
| Beryllium | 114.3087 | 6.37 ± 0.09 | 55.7 ± 0.8 |
| 1100 Aluminum | 166.9 | -0.58 ± 0.12 | -3.5 ± 7 |
| $B^{10}$ | 29.2 | -89.7 ± 0.2 | -3704 ± 7 |
| Rhenium | 1266.9 | -74.5 ± 0.3 | -58.8 ± 0.2 |
| Rhenium | 39.581 | | -70.7 ± 7.5 |
| Gadolinium | 29.841 | | -71 ± 10 |
| Gadolinium | 448.432 | | -56.9 ± 0.7 |
| Dysprosium | 32.262 | | -62.2 ± 9.4 |
| Dysprosium | 484.471 | | -51.2 ± 0.6 |
| Europium | 20.59 | | -237 ± 14 |
| Europium | 304.34 | | -220 ± 1 |
| $B^{10}$ | 0.775 | -2.923 ± 0.052 | -3770 ± 67 |
| $U^{233}$ | 142.53 | 51.2 | 359 ± 2 |

measured worth was determined from the change in reactor periods associated with sample in and sample out. Periods were determined by on-line computer least-squares fit of the d.c. signal from one of the reactor monitoring channels to a single exponential. Measured periods were then converted to reactivities through the inhour equation. The errors listed for the measured worths in Table V have their origin in the least-squares fitting process of the data. More detail on this technique of measurement is given in Refs. 7-9. The seven metals near the end of the table were high-purity metal plates, which were too large to be accommodated by the sample changer. To make these measurements, the sample had to be introduced manually into a void region in the center of the core. This requires two separate determinations of the critical rod positions (one for the void, the other for the samples), and the error associated with this type of measurement is estimated to be ±0.3 Ih. The next to last item in Table V is a small sample of enriched $B^{10}$ used for reactivity traverses. The quoted worth and error for this sample were determined from the on-line computer solution of the inhour equation using fitted period data, and was made to test the reliability of the reactivity traverse probe measurements reported in Section VI. The last item in the table was a 2 x 2 x 1/4-in.-thick plate of high-purity $U^{233}$. This plate was clad in a welded, 15-mil-thick, aluminum can (5.29 g) plus a 15-mil stainless steel jacket (18.98 g) and contained 4.18 g of impurity, mostly $U^{234}$. No corrections have been made for the iron cladding or impurities in the sample.

### 4. Central Worths of Hydrogen

The measured central worths of several sizes of polyethylene samples are listed in Table VI. The first six polyethylene samples listed were 10- and 20-mil-thick sheets of the material sealed in 2 x 2 x 1-in. aluminum cans. The remaining samples were 2 x 2 x 1-in. blocks of

TABLE VI. Central Worths of Hydrogenous Material in Assembly No. 9

| Material | Sample Weight, g | Measured Worth, Ih | Hydrogen Weight, g | Correction for Carbon[a] | Hydrogen Worth, Ih/g |
|---|---|---|---|---|---|
| Poly-ethylene | 1.999 | 1.43 ± 0.03 | 0.285 | 0.021 | 4.94 ± 0.11 |
| | 4.042 | 3.03 ± 0.08 | 0.578 | 0.042 | 5.17 ± 0.14 |
| | 8.03 | 5.63 ± 0.10 | 1.148 | 0.083 | 4.83 ± 0.09 |
| | 12.01 | 8.40 ± 0.15 | 1.717 | 0.124 | 4.82 ± 0.09 |
| | 16.01 | 10.97 ± 0.14 | 2.289 | 0.165 | 4.72 ± 0.06 |
| | 20.004 | 13.83 ± 0.12 | 2.860 | 0.206 | 4.76 ± 0.04 |
| | 23.973 | 16.87 ± 0.12 | 3.428 | 0.247 | 4.85 ± 0.04 |
| | 29.075 | 19.95 ± 0.11 | 4.157 | 0.299 | 4.73 ± 0.03 |
| | 34.029 | 23.45 ± 0.10 | 4.866 | 0.350 | 4.75 ± 0.02 |
| | 39.051 | 26.37 ± 0.10 | 5.584 | 0.402 | 4.65 ± 0.02 |
| | 43.827 | 29.72 ± 0.07 | 6.267 | 0.451 | 4.67 ± 0.01 |
| | 49.116 | 32.43 ± 0.07 | 7.023 | 0.506 | 4.55 ± 0.01 |
| | 53.918 | 35.72 ± 0.07 | 7.710 | 0.555 | 4.56 ± 0.01 |
| | 58.987 | 38.05 ± 0.06 | 8.435 | 0.608 | 4.44 ± 0.01 |
| Lucite | 72.970 | 27.34 ± 0.11 | 5.837 | | |

[a]Carbon worth assumed constant with sample size with a value of (0.0121 ± 0.0029) Ih/g.

polyethylene in which holes in varying numbers and sizes were drilled through the blocks to provide the different weight samples. These data, corrected for carbon and reduced to the equivalent worth of hydrogen, are shown in the last column of Table VI. Linear extrapolation to zero hydrogen weight gives an infinite-dilution central hydrogen worth of 4.995 Ih/g with an estimated disperson of ±0.090.

### 5. Central Worths of Boron-Lucite Mixtures

The central worths for mixtures of Lucite-boron powder are given in Table VII. Both the powders and the pellet were similar or identical to those used for these measurements in Assembly No. 7 and shown in Table III.

TABLE VII. Central Worths of Boron-Lucite Mixtures in Assembly No. 9

| Percent Boron | Weight, g | Measured Worth, Ih | Constituent Weights, g | | | Self-shielding Factor[b] | Lucite Correction,[d] Ih | Apparent Boron Worth, Ih/g |
|---|---|---|---|---|---|---|---|---|
| | | | Boron | Lucite | Hydrogen | | | |
| 20 | 27.231 | -3.36 ± 0.09 | 5.446 | 21.785 | 1.742 | 0.979 | 8.583 ± 0.171 | -2.19 ± 0.04 |
| 40 | 31.306 | -9.51 ± 0.12 | 12.522 | 18.784 | 1.502 | 0.981 | 7.419 ± 0.148 | -1.38 ± 0.01 |
| 50 | 10.044 | -2.43 ± 0.09 | 5.022 | 5.022 | 0.401 | 0.995 | 2.008 ± 0.040 | -0.88 ± 0.02 |
| 70 | 33.577 | -15.09 ± 0.14 | 23.504 | 10.073 | 0.805 | 0.990 | 4.009 ± 0.080 | -0.82 ± 0.01 |
| 90 | 27.219 | -15.70 ± 0.18 | 24.497 | 2.722 | 0.217 | 0.997 | 1.091 ± 0.022 | -0.69 ± 0.01 |
| 25 P[a] | 19.940 | -3.22 ± 0.10 | 4.985 | 14.955 | 1.196 | 0.985 | 5.922 ± 0.118 | -1.83 ± 0.03 |
| 50 P[a] | 19.856 | -7.32 ± 0.11 | 9.928 | 9.928 | 0.794 | 0.990 | 3.951 ± 0.079 | -1.14 ± 0.01 |
| 75 P[a] | 19.255 | -9.75 ± 0.13 | 14.591 | 4.664 | 0.374 | 0.995 | 1.866 ± 0.037 | -0.80 ± 0.01 |
| 100[c] | 75.2 | -49.08 ± 0.22 | 75.2 | 0 | 0 | - | - | -0.652 ± 0.002 |

[a]P = pellet.
[b]Defined as the ratio of estimated Lucite worth in the sample to its infinitely dilute value.
[c]Crystalline boron, from Table V.
[d]Relative errors in the Lucite correction are assumed to be ±2% from the estimated relative error in infinitely dilute hydrogen.

To determine the correction for Lucite in these samples, we assumed that had measurements of the central hydrogen worth been made using Lucite rather than polyethylene, the results would have been the same. This implies that both the carbon and oxygen worth contributions in Lucite are independent of sample size and density.

Hydrogen worth varied as (a - bx), where a = 4.995 Ih/g, b = 0.06 Ih/g, and x is the hydrogen weight in grams. Thus the 72.97-g sample of Lucite listed in Table VI with 5.837 g of hydrogen had a measured worth (27.34 ± 0.11) Ih and was [4.995 - (0.06)(5.837)]/4.995 = 93% of its infinitely dilute value. It follows then, that infinitely dilute Lucite has a central worth of 403 Ih/kg and a self-shielding factor of 1.00. The sample used in the experiment had a measured worth of 374 Ih with a self-shielding factor of 0.93.

Boron, Lucite, and hydrogen weights for each sample are given in Table VII. Self-shielding factors for the Lucite were then determined from the hydrogen content of each sample. These, in turn, were used to estimate the effective worth of the Lucite in each sample and, hence, the apparent worth of the boron.

## 6. Kinetic Properties

Rossi-alpha measurements in Assembly No. 9 indicate that the predominant decay component in the Rossi-alpha ($\alpha_3$) is associated with the 4.25-$\mu$sec prompt-neutron lifetime. This is very close to the value reported for Assembly No. 7. The $\alpha_1$ component is estimated from the measured data to be greater than $10^6$ sec$^{-1}$ and could not be measured with any statistical precision. The measured values for both $\alpha_2$ and $\alpha_3$ are listed in Table VIII; $\alpha_2$ had a measured value somewhat larger than the equivalent $\alpha_2$ in Assembly No. 7. This may be the consequence of not being able to extract the unique value of $\alpha_1$ from the measured data.

TABLE VIII. Kinetic Parameters for Assembly No. 9

| | |
|---|---|
| Measured Rossi-$\alpha_3$ | $(1.55 \pm 0.02) \times 10^3$ sec$^{-1}$ |
| -$\alpha_2$ | $(1.67 \pm 0.28) \times 10^5$ sec$^{-1}$ |
| Estimated $\alpha_1$ | $>10^6$ sec$^{-1}$ |
| $\beta_{eff}$ (calculated) | 0.00659 |
| $\ell$ ($= \beta_{eff}/\alpha_3$) | $4250 \times 10^{-9}$ sec |

## 7. Core Poison Measurements

Because of their interest to the rocket program, the spatial dependence of the worth of selected rare-earth and refractory metals was determined at various radial positions in the core of Assembly No. 9. In these measurements, the reactivity worth of a single column of metal extending the axial length of a core drawer in each half of the assembly was determined at various radial positions. Each column consisted of five 2 x 2-in.-sq, 1/16-in.-thick plates, loaded end to end and parallel to the fuel columns and was located on the axial centerline of the core drawer in each half of the assembly. The reactivity effect of changing this drawer with a normally loaded drawer was then determined at four different radial positions in the core. The results of measurements using Re, Eu, Gd, and Dy are shown in Table IX for the four different mean radii of the measurement

TABLE IX. Spatial Dependence of Columns of Metal in Assembly No. 9

| Sample Weight, g | Mean Radius, cm | | | | Central Worth, Ih/kg | |
|---|---|---|---|---|---|---|
| | 0.0 | 11.07 | 22.14 | 27.68 | Light Sample | Heavy Sample |
| | Worth of 20-in. Axial Column, Ih/kg | | | | | |
| Re (817.2) | -59.8 | -51.4 | -41.6 | -66.6 | -70.7 | -58.8 |
| Eu (202.9) | -197.1 | -169.5 | -146.4 | -303.6 | -237 | -220 |
| Gd (299.02) | -51.2 | -43.1 | -37.1 | -108.7 | -70.7 | -56.9 |
| Dy (322.91) | -45.5 | -38.7 | -38.1 | -114.3 | -62.2 | -51.2 |

positions. Also included in Table IX are the weights of each column of the various materials. The last two columns in Table IX are the central worths for a heavy and light sample of the same metal measured in the center of the core. The light samples were 20 to 30 g, and the heavy samples ranged from 300 to 1270 g. These last two columns show the effect of sample size on self-shielding. Increasing sample sizes by factors of 10 or more decreases the reactivity worth per gram by approximately 10%, except for the europium. The spatial dependence of the worths for the materials follows very closely the shapes measured for small samples on Assembly No. 7 and reported in Section VI.

## 8. Reflector Worth Studies

The approximate worths of sections of the $Al_2O_3$ reflector were studied. In a practical application, these studies indicate the margin of control available through removal of reflector material as a controlling element. Varying amounts of reflector material were removed from different regions of the reflector, and the worth of $Al_2O_3$ removed was determined relative to a void. Reactivity worths for all measurements were made relative to a calibrated control rod. Table X summarizes the results of these measurements. The columns headed $r_{inner}$ and $r_{outer}$ represent the inner and outer radial distances from the core axis of the voided region, $\theta$ is a solid angle subtended by the voided region as measured in a plane normal to the core axis, $z_1$ and $z_2$ are the boundaries of the voided region in the axial direction relative to $z = 0$ at the core midplane, and $\Delta\rho$ is the reactivity lost by the removal of the reflector material with respect to the reference measurement when no void was present.

TABLE X. Worth of $Al_2O_3$ Reflector Material

| Loading | $r_{inner}$, cm | $r_{outer}$, cm | $\theta$, deg | $z_1$, cm | $z_2$, cm | Worth, Ih | Weight, kg | Worth/Weight, Ih/kg | Void Worth Extrapolated to 360°,[a] % Δk/k |
|---|---|---|---|---|---|---|---|---|---|
| 9-19 | ← Reference measurement; no void → | | | | | | | | |
| 9-18 | 26.55 | 32.09 | 55.2 | 0 | -25.55 | 203.8 | 11.8758 | 17.16 | 3.08 |
| 9-20 | 26.55 | 32.96 | 90 | -20.47 | -25.55 | 27.7 | 3.325 | 8.33 | 0.257 |
| 9-21 | 26.55 | 46.49 | 90 | -20.47 | -25.55 | 95.6 | 17.576 | 5.439 | 0.886 |
| 9-22 | 26.55 | 57.36 | 90 | -20.47 | -25.55 | 130.1 | 31.827 | 4.087 | 1.21 |
| 9-25 | 26.55 | 32.96 | 90 | -15.39 | -25.55 | 75.9 | 6.650 | 11.413 | 0.704 |
| 9-24 | 26.55 | 46.49 | 90 | -15.39 | -25.55 | 204.0 | 35.152 | 5.803 | 1.89 |
| 9-26 | 26.55 | 32.96 | 90 | 0 | 5.08 | 57.0 | 3.325 | 17.142 | 0.529 |
| 9-27 | 26.55 | 46.49 | 90 | 0 | 5.08 | 194.3 | 17.576 | 11.054 | 1.80 |

[a]Uses calculated value of 431.4 Ih/% Δk/k.

In the first measurement, five of the reflector drawers at the top of the movable half were removed from the core-reflector interface region. This produced a voided region extending from $r_{inner} = 26.55$ cm to $r_{outer} = 32.09$ cm and from $z_1 = 0$ to $z_2 = -25.55$ cm with a 55° solid

angle about the core axis. The resulting loss of reactivity was 204 Ih. Extrapolating this loss to a 360° solid angle indicates that the first layer of radial-reflector drawers (2-in.-thick sleeve around half of the core) is worth approximately 3.08 or 0.56% $\Delta k/k$ per cm gap. This measurement was repeated using only the last 2 in. of the reflector material in the drawer ($z_1$ = 20.47 cm to $z_2$ = 25.55 cm). Similar measurements and extrapolations for a two-drawer-thick void ($r_{inner}$ = 26.55 cm, $r_{outer}$ = 46.49 cm) at one end of the movable half ($z_1$ = 15.39 cm to $z_2$ = 25.55 cm) removed a total of 1.89% $\Delta k/k$. Finally, the same measurements repeated at the core mid-plane ($z_1$ = 0, $z_2$ = 5.08 cm) indicated that the first 5 cm of radial reflector had a worth of 0.53% $\Delta k/k$ relative to a void. The second and third from last columns of Table X give the weight of $Al_2O_3$ removed and the worth per kg of the removed material, respectively. The last column of the table lists values of the void worth extrapolated to 360° for each experimentally measured gap.

In an application where the first 5 cm of radial reflector is removed as a sleeve, the measurements would indicate that the first 2 in. of motion would remove 0.26% $\Delta k/k$, the next 2 in., an additional 0.45% $\Delta k/k$; the next 6 in. would remove an additional 2.38% $\Delta k/k$ and the next 2 in. another 0.53% $\Delta k/k$, for a total of 3.61% $\Delta k/k$ for 12 in. of motion. Similarly a 20-cm-thick control element would remove 0.89% in the first 2 in. of motion and an additional 1.0% in the next 2 in. Finally, a 31-cm-thick element would remove 1.21% $\Delta k/k$ for the first 2 in. of travel. From these data a crude estimate can be made of the available control margins for sleeves of 2-, 4-, and 6-in. thicknesses of reflector material as it is removed (along an axial direction) from the core. One such estimate is illustrated in Fig. 4.

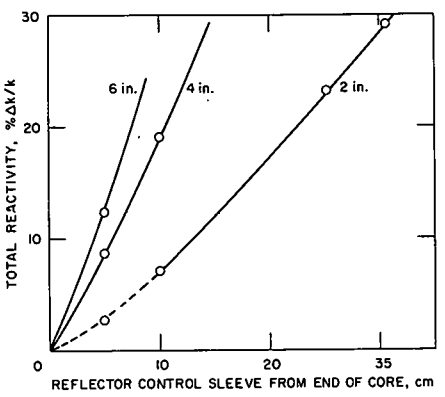


112-7755

Fig. 4. Estimated Integral Worth of Reflector Control Sleeve

## C. Assembly No. 8

Chronologically, Assembly No. 8 was the last assembly studied in the ZPR-9 facility in direct support of the rocket program. Of all the assemblies, it bore the closest relationship to a typical rocket-engine design. It consisted of a simulated $UO_2$-fueled, tungsten-diluted core having approximately 25% porosity. A 10.76-cm-thick sleeve of high-density BeO constituted the radial reflector, and the axial reflector was 35.56 cm of aluminum metal. The radial reflector was surrounded with a 46.3-cm-thick aluminum isolation blanket to prevent backscattering from the matrix, the table bed, and the floor of the assembly room. For safety reasons the BeO reflector was maintained at a nominal 10-cm thickness to limit the thermal power spike at the core-reflector interface, and an aluminum metal axial reflector was used to provide a negative prompt power coefficient.

## 1. Description

The core of Assembly No. 8 was identical in composition to the core of Assembly No. 9 in which materials were loaded to a length of 10 in. and in the following sequence from east to west in both halves of the matrix: WOFWAWOFWAWFOWAWFO. Material identification and weights are given in the appendix. Loading 11 was a reasonably cylindrical and symmetric loading with an excess reactivity of 69.9 Ih. The geometric outline of the stationary half of Loading 11 is shown in Fig. 5. Nonsymmetrical areas of the core and reflector outlined were mirror-imaged in the movable half.

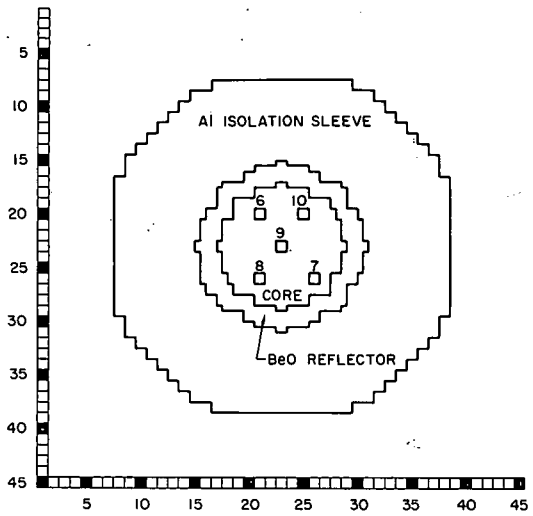


112-7754

Fig. 5. Geometric Outline of Stationary Half, Assembly No. 8, Loading 11.

## 2. Critical Properties

The customary practice has been to make corrections for the excess reactivity, the heterogeneity, the fuel, and the central gap at the core midplane and the irregularity of the outer boundary in terms of edge fuel. Typically, fuel-edge worth will be determined during the process of loading a cylindrical and symmetric core. In this case, however, the replacement of a core drawer by BeO has a larger effect, than can be attributed to the loss of fuel alone. This is a consequence of the high worth of the BeO reflector. In a series of measurements of the worth of the various materials at the core and reflector outer boundaries, replacing the core material by BeO gave a measured reactivity worth that varied from 10 to 21 Ih/kg of $U^{235}$, depending on the peripheral location and plate orientation of the fuel being removed as well as the location of the removed BeO used to compensate for the interchange of core and reflector material.

Figure 5 shows that Loading 11 contained four half-loaded core drawers in each half (at matrix positions 17-23, 23-29, 29-23, and 23-17) with four compensating, half-loaded BeO reflector drawers in each half (positions 15-23, 23-31, 31-23, and 23-15). Replacement of the core material in the drawers at matrix positions S-1923 and M-1923 (removal of 1378.16 g of $U^{235}$) by BeO (addition of 1741.68 g of BeO) accounted for a reactivity loss of 25.2 Ih for a fuel-edge worth of 18.3 Ih/kg of $U^{235}$. This and similar measurements are summarized in Table XI. Table XII summarizes the various material worths at the core-reflector interface and the BeO reflector aluminum isolation blanket interface. The loss of reactivity associated with the removal of peripheral fuel from the core does not linearly add to the gain of reactivity associated with the addition

of BeO in the voided space. In the measurements involving core material, an attempt was made to remove fuel of different orientations and locations on the core surface, so that any single measurement would properly weight the space-dependent variables. At the outer edge of the reflector, on the other hand, Table XI shows that the reactivity lost by the removal of BeO at the reflector-isolation blanket interface very nearly adds in a linear manner to the reactivity lost by the addition of aluminum to the voided space. To establish fuel-edge worth suitable for making various corrections, the reactivity lost by the removal of edge fuel and its replacement by BeO accompanied by the removal of an equivalent amount of BeO from the outer edge of the reflector is used as the edge worth. For all practical purposes, a conservation of reflector volume in this type of measurement is also a conservation of reflector thickness.

The critical parameters for Assembly No. 8 Loading 11 are listed in Table XXXII. Radii listed for the various regions of the core were determined from the size of the circle that had the same cross-sectional area as that physically occupied by the drawers in the matrix. Dimensions given for the core and axial reflector lengths are measured from the core midplane and include half the central gap. Measurements with a dial indicator gave an average drawer-front thickness of 0.406 mm (16 mils). Estimates of the air gap between drawer fronts when the

TABLE XI. Worth of Material near Core Boundary in Assembly No. 8

| Loading No. | Core Material | | BeO Reflector Material | | Reactivity, Ih |
|---|---|---|---|---|---|
| | Removed | Replaced by | Removed | Replaced by | |
| 13 | S-1923, M-1923 (1378.16 g of $U^{235}$) | BeO (1741.68 g) | - | - | -25.2 ± 0.2 |
| 37 | S-1723, S-2317, M-2329, M-2923 (2576.32 g of $U^{235}$) | BeO (3980.32 g) | - | - | -18.6 ± 0.2 |
| 41 | - | - | S-1920, S-2836, M-1926, M-1820 (3780.32 g) | Void | -135.8 ± 0.3 |
| 42 | - | - | S-2730, S-1916, M-2716, M-1930 (3780.32 g) | Void | -83.4 ± 0.2 |
| 43 | - | - | S-2716, S-1523, S-2315, S-3123, S-2331, M-1627, M-1523, M-2317, M-3123, M-2331 (9450.80 g) | Aluminum (8708.40 g) | -42.23 ± 0.2 |
| 45 | S-1919, S-1927, S-2719, S-2727, M-1919, M-1927, M-2719, M-2727 (5512.64 g of $U^{235}$) | BeO (7560.64 g) | - | - | -114.8 ± 0.3 |

two halves of the machine are together range from 1.0 to 2.5 mm, depending on the sag and total weight load in the matrix. An average gap between fuel columns in the two halves is taken as 3 mm and includes the aluminum drawer fronts.

TABLE XII. Worth of Fuel and Reflector Materials at Core Boundary

| Identification | Worth |
|---|---|
| At Core-Reflector Interface | |
| Core Material Relative to BeO | |
| No Change in Outer Boundary of Reflector | +10.66 Ih/kg of $U^{235}$ |
| Reflector Volume Kept Constant | +20.83 Ih/kg of $U^{235}$ |
| Core Material Relative to Void | |
| No Change in Outer Boundary of Reflector | +24.54 Ih/kg of $U^{235}$ |
| BeO Relative to Void | +10.14 Ih/kg of BeO |
| At Reflector-Isolation Blanket Interface | |
| BeO Relative to Void | +6.43 Ih/kg of BeO |
| Aluminum Relative to Void* | -5.39 Ih/kg of Al |

*This value is smaller in magnitude and opposite in sign from results obtained by traversing techniques. An evaluation of the aluminum isolation blanket in previous assemblies would also lead one to expect a positive worth in this case.

Because of the rather large uncertainty in the fuel-edge worth and hence in the correction for the excess reactivity, a larger than normal uncertainty must be associated with the critical mass and critical radius of this assembly.

### 3. Central Worths of Nonhydrogenous Materials

The central worths for several nonhydrogenous materials are listed in Table XIII. For those cases for which errors are shown with the measured worths, the material worth was determined from the change in reactor period associated with sample-in and sample-out conditions. Periods were determined by on-line computer least-squares fit of the d.c. signal from one of the reactor-monitoring instruments to a single exponential. Errors in this period are propagated through the inhour equation to give the rms dispersion due to sampling statistics and do not include systematic or sample placement errors. As with previous assemblies, a standard ±0.3-Ih error is assigned to the remaining measured reactivities.

TABLE XIII. Central Worths of Nonhydrogenous Material in Assembly No. 8

| Sample | Weight, g | Measured Worth, Ih | Sample Worth, Ih/kg |
|---|---|---|---|
| Carbon | 103 | +0.893 ± 0.160 | +8.7 ± 1.6 |
| Boron | 75.2 | -39.8 | -529 ± 4 |
| Beryllium | 114.309 | +5.77 | +50.5 ± 2.7 |
| Lithium | 28.6 | -1.29 | -45 ± 10 |
| $B^{10}$ | 29.2 | -72.5 | -2480 ± 10 |
| $B_4C$ | 59.62 | -15.4 | -257.7 ± 5.0 |
| Al (1100) | 166.9 | -0.46 ± 0.13 | -2.77 ± 0.76 |
| $U^{235}$ | 134.98 | +22.8 | +169 ± 2 |
| $U^{238}$ | 506.956 | -7.49 | -14.8 ± 0.6 |
| Niobium | 481.20 | 8.84 | -18.4 ± 0.8 |
| $Dy_2O_3$ | 104.7 | -2.97 | -28.3 ± 2.9 |
| $WO_2$ | 78.37 | -0.202 | -2.57 ± 3.8 |
| Silver | 642.02 | -38.9 | -60.6 ± 0.5 |
| $Y_2O_3$ | 81.5 | +1.03 | +12.7 ± 3.7 |
| $Eu_2O_3$ | 34.2 | -3.92 | -115 ± 9 |
| $Gd_2O_3$ | 59.2 | -16.8 | -284 ± 5 |
| Tungsten | 1108.0 | -12.8 | -11.6 ± 0.3 |
| Gold | 1183.6 | -27.2 | -23.0 ± 0.3 |
| Gadolinium | 433.6 | -20.7 | -47.8 ± 0.7 |
| Dysprosium | 557.3 | -18.6 | -33.4 ± 0.5 |
| Europium | 304.86 | -52.2 | -171.3 ± 9.8 |
| Rhenium | 1266.9 | -59.9 | 47.2 ± 0.2 |

## 4. Central Worths of Hydrogen

Central worths for a number of polyethylene samples have been determined by the on-line computer technique and are shown in Table XIV. For each polyethylene sample listed in Table XIV, the weights of hydrogen and carbon are listed as well as the correction made to the measured value for the reactivity effect of carbon. Equivalent worth of hydrogen per gram is shown in the last column. Linear extrapolation to zero sample size gives the infinitely dilute hydrogen worth of 4.85 Ih/g.

TABLE XIV. Central Worths of Hydrogen in Assembly No. 8

| Sample | | Constituent Weights, g | | Carbon Correction, Ih | Hydrogen Worth, Ih/g |
|---|---|---|---|---|---|
| Weight, g | Worth, Ih | Hydrogen | Carbon | | |
| 1.9900 | 1.7 ± 0.2 | 0.2845 | 1.7054 | 0.015 | 5.9 ± 0.7 |
| 4.0423 | 2.8 ± 0.2 | 0.5780 | 3.4642 | 0.030 | 4.7 ± 0.3 |
| 8.0300 | 5.6 ± 0.2 | 1.1482 | 6.8817 | 0.060 | 4.85 ± 0.17 |
| 12.0097 | 8.2 ± 0.2 | 1.7173 | 10.2923 | 0.090 | 4.69 ± 0.12 |
| 16.0079 | 10.7 ± 0.2 | 2.2891 | 13.7187 | 0.12 | 4.62 ± 0.09 |
| 20.0039 | 13.2 ± 0.2 | 2.8605 | 17.1433 | 0.15 | 4.56 ± 0.07 |
| 23.973 | 15.98 ± 0.17 | 3.4281 | 20.5448 | 0.18 | 4.609 ± 0.049 |
| 29.075 | 19.01 ± 0.16 | 4.1577 | 24.9172 | 0.22 | 4.519 ± 0.038 |
| 34.029 | 21.90 ± 0.17 | 4.8661 | 29.1628 | 0.25 | 4.449 ± 0.035 |
| 39.051 | 24.65 ± 0.16 | 5.5842 | 33.4667 | 0.29 | 4.362 ± 0.028 |
| 43.857 | 27.15 ± 0.20 | 6.2715 | 37.5854 | 0.33 | 4.276 ± 0.031 |
| 49.116 | 29.08 ± 0.24 | 7.0235 | 42.0924 | 0.37 | 4.088 ± 0.034 |
| 53.918 | 31.05 ± 0.06 | 7.7102 | 46.2077 | 0.40 | 3.975 ± 0.008 |
| 58.9865 | 33.30 ± 0.23 | 8.4350 | 50.5514 | 0.44 | 3.896 ± 0.027 |

## 5. Central Worths of Boron-Lucite Mixtures

Central-worth data for mixtures of boron and Lucite are listed in Table XV. Included in the table are the weights of the individual constituents of the sample. Most of the measured worths listed were determined by the on-line computer techniques and have associated with them an error on the order of 0.005 Ih. Column 7 lists the hydrogen worth per gram appropriate to the weight of hydrogen in each sample. Columns 7 through 9 are the predicted worths of the constituent parts of the sample if they were separately isolated and measured. Oxygen and carbon are assumed to have central worths of 0.0177 and 0.0087 Ih/g, respectively, and to be independent of sample size. Column 10 is the measured worth divided by the sample weight, and column 11 lists the apparent or effective boron worth.

TABLE XV. Central Worths of Boron-Lucite Mixtures

| Identification | Weight, g | | | | Corrections, Ih | | | | Sample Worth, Ih/g | Apparent Boron Worth,[f] Ih/g |
|---|---|---|---|---|---|---|---|---|---|---|
| | Boron | Carbon | Hydrogen | Oxygen | Measured Worth | Hydrogen[c] | Carbon[d] | Oxygen[e] | | |
| 100% B powder[a] | 75.2 | - | - | - | -39.81 | - | - | - | -0.529 | -0.529 |
| 90% B powder | 54.1485 | 3.6099 | 0.4813 | 1.9252 | -42.374 | 2.325 | 0.031 | 0.034 | -0.704 | -0.784 |
| 75.7% B pellet | 14.5913 | 2.8100 | 0.3746 | 1.4986 | -11.641 | 1.813 | 0.024 | 0.027 | -0.603 | -0.926 |
| 60% B powder | 33.8220 | 13.5288 | 1.8038 | 7.2153 | -27.778 | 8.550 | 0.118 | 0.128 | -0.492 | -1.081 |
| 50% B pellet | 9.9274 | 5.9563 | 0.7941 | 3.1767 | -5.760 | 3.819 | 0.052 | 0.056 | -0.290 | -0.976 |
| 40% B pellet | 12.5228 | 11.2705 | 1.5027 | 6.0109 | -7.576 | 7.153 | 0.098 | 0.106 | -0.241 | -0.678 |
| 35% B powder | 16.4465 | 18.3297 | 2.4439 | 9.7758 | -7.788 | 11.533 | 0.159 | 1.173 | -0.165 | -1.195 |
| 20% B pellet | 5.4462 | 13.0709 | 1.7427 | 6.9711 | -2.445 | 8.278 | 0.114 | 0.123 | -0.089 | -1.608 |
| 15% B powder | 6.2556 | 21.2690 | 2.8358 | 11.3434 | -2.735 | 13.680 | 0.185 | 0.201 | -0.065 | -2.686 |
| 0% B[b] | | | | | | | | | +4.85 | |

[a]Crystalline boron taken from Table XIII.
[b]Infinitely dilute hydrogen.
[c]Taken from Table XIV.
[d]From Table XIII, C → 0.0087 Ih/g.
[e]Used calculated value for O → 0.0177 Ih/g.
[f]Defined as $\frac{\rho_S - \rho_C - \rho_H - \rho_O}{\text{weight of boron}}$

## 6. Kinetic Parameters

Rossi-alpha measurements made in Assembly No. 8 gave evidence of the existence of the three modes of decays in the prompt-neutron chain that have been observed in the $Al_2O_3$ reflector assemblies. Results of these measurements, as well as the calculated value for $\beta_{eff}$, and the prompt-neutron lifetime, $\ell$, are listed in Table XVI. From the calculated value of $\beta_{eff}$ (0.00664) and the conventional definition of the prompt-neutron lifetime for the assembly ($\alpha_3 \doteq \beta_{eff}/\ell$) the lifetime inferred from these measurements for this assembly is 5230 x $10^{-9}$ sec.

TABLE XVI. Kinetic Properties of Assembly No. 8

| | | |
|---|---|---|
| Measured Rossi | $\alpha_1$ | (1.27 ± 0.27) x $10^3$ $sec^{-1}$ |
| | $\alpha_2$ | (3.5 ± 0.5) x $10^3$ $sec^{-1}$ |
| | $\alpha_3$ | (5.8 ± 1.7) x $10^4$ $sec^{-1}$ |
| $\beta_{eff}$ (calculated) | | 0.00664 |
| $\ell$ (= $\alpha_3/\beta_{eff}$) | | 5230 x $10^{-9}$ sec |

## 7. Spatially Dependent Fuel Worths

In a series of material-replacement measurements, the spatially dependent worths of columns of $U^{233}$ and $Pu^{239}$ were made and compared to the worth of $U^{235}$. In these measurements, two of the 1/16-in. columns of $U^{235}$ fuel were removed from one of the drawers and replaced by a single, 1/8-in.-thick column of $U^{233}$ (or $Pu^{239}$) of roughly equivalent mass. The worth of the drawer was then mapped out starting at the core center and going out to the core edge. To provide an absolute scale to these measurements, the worth of a 1/8-in.-thick void column was mapped out in the same way. These results are listed in Table XVII. The last two columns show the measured worth of $U^{233}$ and $Pu^{239}$ relative to the worth of $U^{235}$ at each measuring point and averaged over the core. Table XVII also shows the isotopic compositions and the total weights of the fuel columns.

TABLE XVII. Results of Spatially Dependent Fuel-worth Measurements

| | | | | Ratio of Fuel Worth to $U^{235}$ Worth | |
|---|---|---|---|---|---|
| | $U^{233}$ | $U^{235}$ | $Pu^{239}$ | $U^{233}$ | $Pu^{239}$ |
| | | Fuel Worths, Ih/kg | | | |
| Position, cm | | | | | |
| 0 | 209.6 | 112.6 | 188.2 | 1.86 | 1.67 |
| 16.61 | 167.6 | 89.1 | 147.0 | 1.88 | 1.65 |
| 22.14 | 134.3 | 71.1 | 116.7 | 1.89 | 1.64 |
| 27.68 | 108.3 | 57.4 | 88.0 | 1.89 | 1.53 |
| | | | Average: | 1.88 | 1.62 |
| | | Isotopic Weights, g | | | |
| Isotope | | | | | |
| $U^{232}$ | Trace | | | | |
| $U^{233}$ | 711.96 | | | | |
| $U^{234}$ | 17.07 | 7.17 | | | |
| $U^{235}$ | 1.46 | 689.12 | | | |
| $U^{236}$ | 0.15 | 1.77 | | | |
| $U^{238}$ | 2.64 | 41.41 | | | |
| $Pu^{238}$ | | | 0.06 | | |
| $Pu^{239}$ | | | 601.65 | | |
| $Pu^{240}$ | | | 28.36 | | |
| $Pu^{241}$ | | | 2.85 | | |
| $Pu^{242}$ | | | 0.06 | | |
| Cladding | | | | | |
| Aluminum | 26.5 | | 33.9 | | |
| 304 SS | 99.6 | | 99.6 | | |

## 8. The Central Gap

The worth of the central gap at the core midplane has been determined by the on-line computer technique, originally developed for rod-calibration measurements. Figure 6 shows the results of these

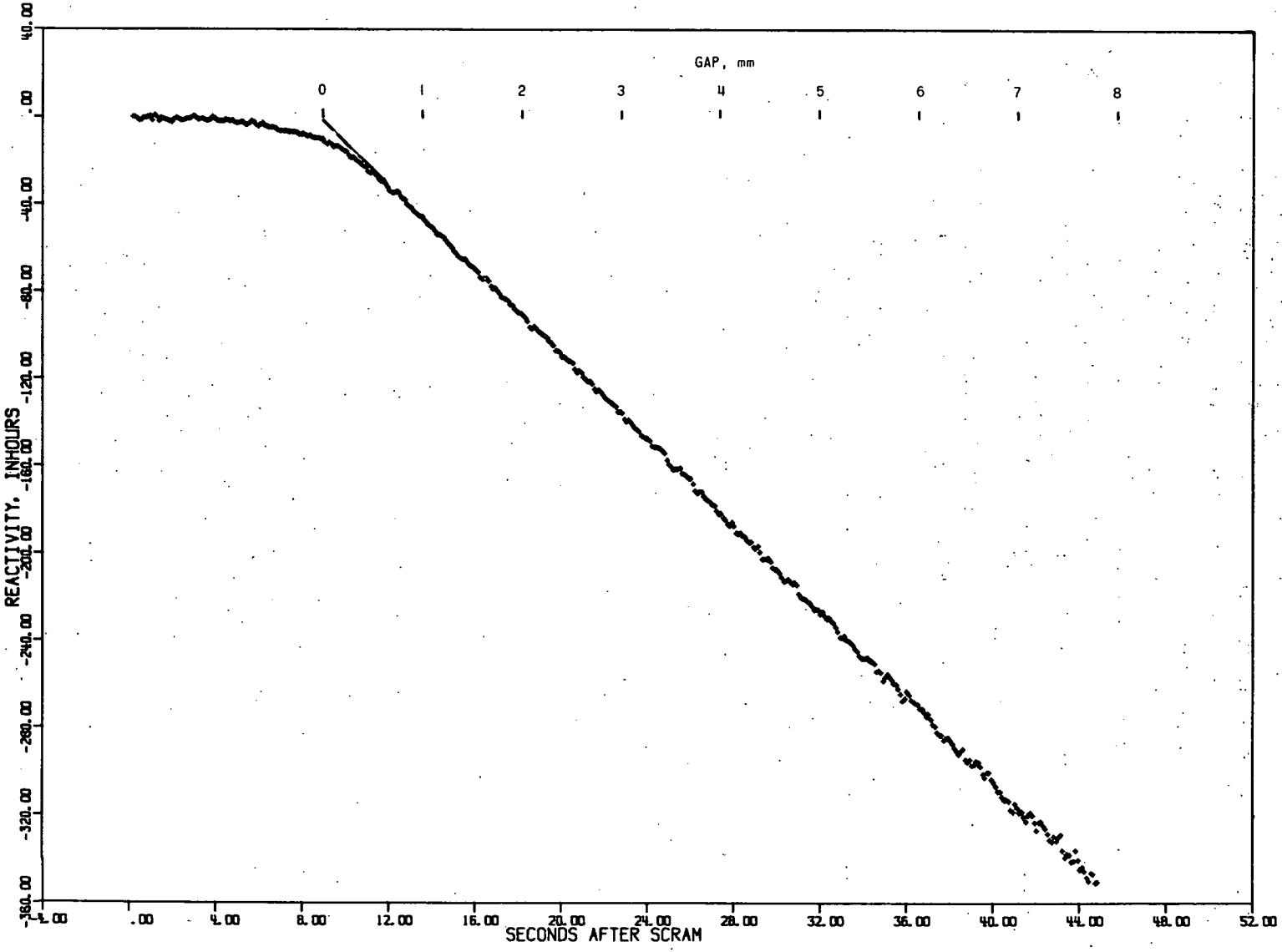


Fig. 6. Gap Worth of Assembly No. 8

measurements. The zero-point reference for these measurements is established by taking data with the reactor just critical and with zero midplane gap. Then as the tables are separated, and the system becomes subcritical, the change of flux is converted to a loss in reactivity on a real-time scale. From a knowledge of the table-separation speed, the real-time scale is converted to millimeters of gap. The curvature in the data between 4 and 12 sec is caused by the nonlinear speed of the table, as it is accelerated from rest to its constant separation speed of 1.3 cm/sec. After the table has attained a constant speed, the reactivity loss is constant with time and hence with gap size. Through the first 8 mm, the gap is 1.05% $\Delta k/k/cm$, very close to the pre-experiment predicted value of 1% $\Delta k/k/cm$.

## 9. Reflector Studies

Measurements were performed to determine the worth of beryllium metal relative to BeO in the reflector region. In the first measurement, the replacement of two drawers of BeO with beryllium metal in each half of the reactor resulted in a reactivity gain of 0.290 ± 0.006 Ih. Table XVIII gives the weight of the replacing material and the solid angle subtended from the core axis. In the subsequent replacement of the oxide for its metal, reactivity was lost from the system. If the last of these measurements is extrapolated to 360°, the substitution of the metal for its oxide in the beryllium reflector region would account for a loss of approximately 0.1% $\Delta k/k$. Although the metal has more than $1\frac{1}{2}$ times the number of beryllium atoms per unit volume than its oxide, it represents a loss in reactivity. Therefore, a substantial gain in reactivity must be attributed to the oxygen.

TABLE XVIII. Worth of Beryllium Metal

| Loading No. | No. of Drawers per Half | Beryllium Metal Weight, kg | Solid Angle, deg | Worth, Ih | Worth/Weight, Ih/kg |
|---|---|---|---|---|---|
| 60 | 2 | 4.814 | 9.16 | 0.291 ± 0.06 | +0.060 |
| 61 | 10 | 24.080 | 41.35 | -2.08 ± 0.06 | -0.086 |
| 62 | 20 | 48.140 | 86.37 | -10.52 ± 0.10 | -0.22 |

# III. CONTROL STUDIES

The present studies of available control margin were limited primarily to the maximum reactivity effect of boron poison in the reflector. A limited number of measurements were made of the reactivity associated with the movement of reflector material away from the core.

The experimental study has been limited, by and large, to measurements of the reactivity worth of boron since it is readily available, it is extensively studied in the thermal-rocket assemblies, and its cross section is simple, well behaved, and moderately well known. The large down-scattering of oxygen in an oxide reflector softens the spectrum at the core edge, resulting in an increase in the boron absorption and a flattening of the power distribution.

In their most reactive state, a series of boron drums (half-moon shaped) is approximated by a sleeve completely surrounding the core. In their least reactive state the boron drums would be far removed from the core. In the critical experiments, the two extreme conditions were simulated by comparing measurements in an assembly without boron to one in which a boron sleeve, made up of 2-in. by 1/8-in.-thick columns extending the full length of the core, completely surrounded the radial core surface. To compensate for the reactivity loss, the fuel density in a central region of the core was increased. In this region, the fuel had its highest worth and produced minimum variation in the composition and geometry near the core boundary and in the vicinity of the boron.

## A. Boron-sleeve Measurements in Assembly No. 6

The reactivity worth of a boron sleeve in Assembly No. 6 was measured both with and without hydrogen in the reflector. Results of measurements without the hydrogen have been reported in ANL-7207. Results of measurements with the hydrogen are reported here.*

Because of the limited supply of boron for these measurements, only 20 in. of the 24-in. core length was covered by boron. In addition, the effective radius of each boron column varies somewhat. These differences in radii are unavoidable owing to the rectangular matrix structure. Results of these measurements are listed in Table XIX and are compared graphically to the same results in Assembly No. 6 in Fig. 7. In Loading 5 of Table XIX, the two columns of fuel previously removed from the central drawers (1.64688 kg $U^{235}$) were inserted for the reactivity gain of 184 Ih. The removal without the boron lost only 110 Ih. A similar fuel addition in Loading 9 (a fifth fuel column added to the central drawers in both halves) added 187 Ih. Although the change in central fuel worth between Loadings 5 and 9 is not as pronounced as that measured before the boron was added, it

*Assembly No. 6 with hydrogen added to the reflector was designated as Assembly No. 6A. Assembly No. 6A with the boron sleeve surrounding the core is referred to as Assembly No. 6C.

does show how the boron shifts the neutron importance towards the center of the core. When the loading was complete (440 cans), the 1.846 kg of $B^{10}$ held up to 1.3% $\Delta k/k$ at a total subtended angle of 268°. This is to be compared to 0.67% in the aluminum reflector of Assembly No. 6 without the hydrogen but with the same amount of boron and the same total solid angle.

TABLE XIX. Results of Boron-sleeve Experiment in Assembly No. 6A.

| Loading No. | Boron | | Reactivity, Ih | | | Accum Solid Angle |
|---|---|---|---|---|---|---|
| | No. of Columns Added | Accum Weight, g | Excess | Diff | Accum | |
| 1 | ← Reference → | | 191.96 | - | 0 | |
| 2 | 6 | 125.7 ± 6.8 | 142.50 | -49.46 | -49.5 | 18.3° |
| 3 | 8 | 293 ± 16 | 80.47 | -62.03 | -110.9 | 42.6° |
| 4 | 8 | 461 ± 25 | 21.93 | -58.54 | -169.5 | 67.0° |
| 5 | ← Fuel added → | | 206.46 | +184.53 | - | |
| 6 | 8 | 629 ± 34 | 145.17 | -61.28 | -230.7 | 91.4° |
| 7 | 8 | 798 ± 43 | 98.74 | -46.43 | -277.2 | 115.7° |
| 8 | 12 | 1048 ± 57 | 23.55 | -75.19 | -352.4 | 152.1° |
| 9 | ← Fuel added → | | 210.47 | +186.92 | - | |
| 10 | 8 | 1215 ± 66 | 149.39 | -61.09 | -413.4 | 176.6° |
| 11 | 8 | 1388 ± 75 | 109.95 | -39.43 | -452.9 | 200.8° |
| 12 | 8 | 1550 ± 84 | 67.78 | -42.18 | -495.1 | 225.6° |
| 13 | 8 | 1718 ± 94 | 35.60 | -32.18 | -528.1 | 249.8° |
| 14 | 6 | 1846 ± 101[a] | 5.01 | -30.59 | -557.8 | 268.0° |

[a]Does not include (361 ± 9) g of $B^{11}$, (229 ± 9) g of other impurities nor (5.31 ± 0.05) kg of cladding.

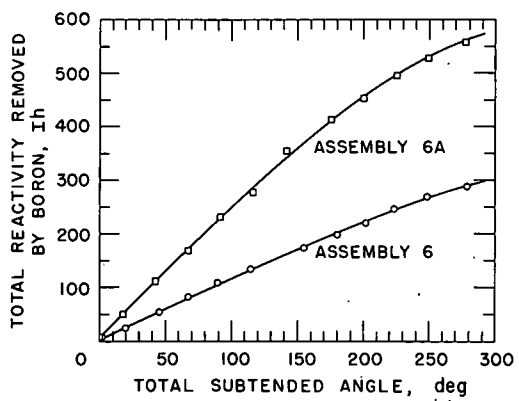


112-5690

Fig. 7. $B^{10}$ Sleeve Worth in Assemblies No. 6 and 6A.

To estimate the effect of extending the 10-in.-long boron columns to the actual core half length (12 in.), an extra 2 x 2 x 1/8-in. can was added to 26 of the 88 boron columns (29.55% of the total). This removed 17.70 Ih reactivity. Extrapolating over the entire core yielded 1.43% $\Delta k/k$, as the reactivity tied up by a complete boron ring. The corresponding number for Assembly No. 6 was 1.01% $\Delta k/k$.

## B. Boron-sleeve Measurements in Assembly No. 7*

Because of the limited supply of boron, it was not possible, in the measurements of the worth of a sleeve of $B^{10}$ surrounding the core in Assemblies No. 6 (reported in ANL-7207) and 6A, to make a sleeve more than 1/8-in. thick, nor to completely surround the core in a radial direction. For the measurements in Assembly No. 7,

*Assembly No. 7 with the boron sleeve is referred to as Assembly No. 7C.

however, additional quantities of boron were available in the form of powdered crystalline (natural) boron, sealed in 1/8 x 2 x 2-in. aluminum cans. There were also available 2500 plates of hot-pressed, high-purity $B_4C$. Variations in empty-can weight, packing densities, boron assay, and plate dimensions lead to an overall error in the mean of about 5% in the total $B^{10}$ weight. Material weights are summarized in Table XX. A major difference between the measurements in Assembly No. 7C and those in other assemblies is the amount of material used in the experiments. The initial plan was to continue to add sufficient boron to the sleeve until a uniform 25% increase in fuel density had been achieved through the core. However, the supply of boron was exhausted before the increased fuel concentration could be completed. In the final loading (No. 118, the first critical loading of Assembly No. 7C; see Tables XXII and XXXII), the $U^{235}$ atom density was 25% higher in all but the central core drawer in each half; these contained only two fuel columns. The fuel density in the edge drawers and in the partially loaded drawers was not changed in Assembly No. 7C. Loading 96 was very nearly equivalent to the boron-sleeve experiments on Assemblies No. 6C and 8C.

TABLE XX. Boron Material Weights

| Material | Weights, g | | |
|---|---|---|---|
| | Enriched $B^{10}$ | Natural Boron | $B_4C$ |
| $B^{10}$ | 4.20 ± 0.12 | 1.20 ± 0.05 | 1.62 ± 0.10 |
| $B^{11}$ | 0.41 ± 0.01 | 4.93 ± 0.18 | 6.67 ± 0.40 |
| Carbon | - | - | 2.44 ± 0.15 |
| Other | 0.26 ± 0.01 | 0.16 ± 0.01 | Trace |
| Aluminum cladding | 6.306 ± 0.052 | 6.295 ± 0.052 | - |

1. Loading of Assembly No. 7C

The measured reactivity effect of a given column of boron varied considerably, depending on whether the boron was added to the east or west side of the core, or to the top or bottom side. A column of boron consisted of five 2 x 2 x 1/8-in.-thick cans, packed with $B^{10}$ and lined end to end in a drawer so that each column was 5.54 cm beyond the outer-core radius and in the $Al_2O_3$ reflector. A series of reproducibility measurements indicated that the measured differences of the boron worth at the different positions were statistically significant. For this reason, an attempt was made to load a perfectly symmetric core (Loading 26). Figure 8 shows an outline of this loading. The worth of a 20-in.-long column of $B^{10}$ was mapped out in the various regions of this loading. These results are also shown in Fig. 8, where the eight radial positions are lettered A through H. Because of the ~12% smaller solid angles subtended by the off-axes boron columns, their worths are expected to be somewhat smaller than those on the 90° axes.

Also, because of symmetry in loading of the individual fuel drawers, two columns of diluent material exist between the last fuel plate in the core and the boron columns to the left of the core; only one column of diluent (that being 45% density aluminum) was between the last fuel column and the boron on the right-hand side of the core as viewed in Fig. 8. For this reason, worths on the right-hand side of Fig. 8 are expected to be somewhat higher than those on the left side. The half-loaded core drawers at the top and bottom had one column of 45% density aluminum between the last fuel plate and the boron column. The asymmetry between positions A and E (top and bottom of the core) therefore cannot be attributed to either the solid angle or the amount or type of material between the last fuel plate and the boron column. One measurement was made in position E to determine the effect of moving the boron 1/8 in. closer to the core. This resulted in a gain of 3.62 Ih, relative to the 102.75 Ih measured for the correct position. Since it was the same column of boron used in all the measurements, differences between them cannot be attributed to uncertainties in the $B^{10}$ content in the columns or to a reactivity change because of the flux depression caused by the boron.

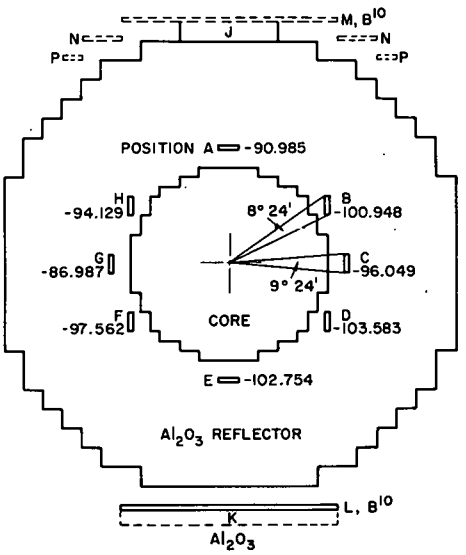


112-7749

Fig. 8. Geometric Outline of Loadings 26-40

A rather lengthy and involved series of measurements was performed to determine the effects of different reflector geometries on the worth of boron in the various locations around the core. Table XXI summarizes the entire series of 65 loadings. For each loading, the excess reactivity and the mass of fuel loaded into the core are entered in columns 2 and 3. Column 4 refers to the figure giving the geometric outline of the core and the reflector. Columns 5 and 6 list the change in reactivity associated with each loading with respect to a particular reference loading. Columns 7 and 8 list the outer radius of the core and the reflector. These correspond to the "as-loaded" radii of circles having the equivalent cross-sectional area as the drawers in the core. Figures 8 through 13 show that changes in the reflector make it impossible to determine a cylindrical cross-sectional area for some of the loadings. The outer radius for these loadings are listed as irregular. Columns 9 through 12 list the differences between the reference figure and the actual loading. Differences in fuel are listed as kg of $U^{235}$, additions or removals of boron and other materials are listed as the number of drawers in which the material was added or removed. For a drawer with boron in it, five of the 2 x 2 x 1/8-in.-thick cans were put end to end down the center of the drawer. Reference to the figures will indicate whether this was a horizontal or a vertical column. The columns headed S-2323 and M-2323 list the contents of a central drawer in

TABLE XXI. Results of Boron Worth Studies in Assembly No. 7

| Loading No. | Excess Reactivity, Ih | Mass of $U^{235}$ in Core, kg | Fig No. Ref | Change in Reactivity, Ih | Rel to Loading No. | Outer Radius, cm | | Fuel Change, kg | No. of Drawers with $B^{10}$ [e] | No. of Drawers with $Al_2O_3$ | No. of Drawers of Other Materials | Contents of | | Description[h] |
|---|---|---|---|---|---|---|---|---|---|---|---|---|---|---|
| | | | | | | Core | Reflector | | | | | S-2323 | M-2323 | |
| 15 | 128.435 | 218.99951 | 9 | | | 27.884 | 65.375 | | 0 | 0 | 0 | SC[b] | 4[c] | Ref.,[d] SC[b] in S-2323 |
| 16 | S[a] | ↓ | ↓ | | | ↓ | ↓ | | 8 | ↓ | ↓ | ↓ | | $B^{10}$ in S/M-A,C,E,G |
| 17 | S[a] | | | | | | | | 4 | | | | | $B^{10}$ in S/M-C,G |
| 18 | 151.219 | 219.13387 | | +22.784 | 15 | | | 0.13436 | 0 | | | 4[c] | | SC[b] and $B^{10}$ removed, Ref.[d] |
| 24 | 147.411 | | | | | | | | 0 | | | | | Repeat of Loading 18 |
| 19 | S[a] | | | | | | | | 4 | | | | | $B^{10}$ in S-A,E and M-G,C |
| 20 | 55.769 | | | -95.450 | 18 | | | | 2 | | | | | $B^{10}$ in S/M-C |
| 25 | 58.540 | | | | | | | | ↓ | | | ↓ | | Repeat of Loading 20 |
| 21 | 156.114 | 219.82295 | | +100.345 | 20 | | | 0.68908 | | | | 6[c] | | 2 col. of fuel added to S-2323, $B^{10}$ in S/M-C |
| 23 | 156.195 | | | | | | | | ↓ | | | | | Repeat of Loading 21 |
| 22 | 79.286 | ↓ | ↓ | | | ↓ | ↓ | | 4 | ↓ | ↓ | ↓ | | $B^{10}$ at S/M-C,G |
| 26 | 184.919 | 217.75571 | 8 | | | 27.708 | | -2.06724 | 0 | | | 4[c] | | Ref.[d] (1/2 dr.of fuel removed from near S-A & M-F) |
| 36 | 184.384 | | | | | | | | | | | | | Repeat of Loading 26 |
| 27 | 88.870 | | | -96.049 | 26 | | | | 2 | | | | | $B^{10}$ at S/M-C |
| 28 | 97.932 | | | -86.987 | | | | | | | | | | $B^{10}$ at S/M-G |
| 29-1 | 78.550 | | | -106.369 | | | | | | | | | | $B^{10}$ at S/M-E but 1/8 in. closer to core |
| 29-2 | 82.161 | | | -102.754 | | | | | | | | | | $B^{10}$ at S/M-E in normal position |
| 30-1 | 92.970 | | | -91.949 | ↓ | | | | | | | | | $B^{10}$ in S/M-A |
| 30-2 | 92.444 | | | -91.940 | 36 | | | | | | | | | Same as Loading 30-1, but probe hole removed |
| 31 | 83.971 | | | -100.413 | | | | | | | | | | $B^{10}$ in S/M-B |
| 32 | 90.790 | | | -93.594 | | | | | | | | | | $B^{10}$ in S/M-H |
| 33 | 87.357 | | | -97.027 | | | | | | | | | | $B^{10}$ in S/M-F |
| 34 | 81.336 | | | -103.048 | ↓ | | ↓ | | | ↓ | | | | $B^{10}$ in S/M-D |
| 35 | 92.720 | | | +11.384 | 34 | | Irr[f] | | ↓ | 10 | | | | 5 dr. of $Al_2O_3$ added S/M-J |
| 37 | 185.206 | | | +1.822 | 36 | | ↓ | | 22 | 22 | | | | Plane of $B^{10}$ in S/M-L, $Al_2O_3$ in S/M-K |
| 38 | 176.829 | | | -7.555 | | | 65.375 | | | 0 | | | | Plane of $B^{10}$ in S/M-L |
| 39 | 181.900 | | | -2.484 | | | Irr[f] | | ↓ | | | | | Plane of $B^{10}$ at S/M-M |
| 40 | 180.166 | ↓ | ↓ | -4.218 | ↓ | ↓ | ↓ | | 34 | | | | | $B^{10}$ at S/M-M,N,P |
| 41 | 164.497 | 217.06663 | 10 | | | 27.619 | | -0.68908 | 0 | | | | | Ref. (1/4 dr. removed from S/M-A) |
| 42 | 70.486 | | ↓ | -94.011 | 41 | | | | 2 | | | | | $B^{10}$ in S/M-B |
| 43 | 106.879 | | 11 | -77.505 | 36 | | 65.375 | | 0 | 0 | | | | Ref. (removed $Al_2O_3$ from S/M-C) |
| 48 | 107.596 | | | | | | | | | | | | | Repeat of Loading 43 |
| 52 | 108.626 | | | | | | | | | | | | | Repeat of Loading 43 |
| 44 | 165.752 | | 10 | +58.873 | 43 | | Irr[f] | | | 0 | | | | Ref. |
| 45 | 70.002 | | | -95.750 | 44 | | | | 2 | | | | | $B^{10}$ in S/M-B |
| 46 | 189.560 | | | +119.557 | 45 | | | | 0 | 50 | | | | $Al_2O_3$ in S/M-D |
| 47 | 91.454 | | | -98.106 | 46 | | | | 2 | 50 | | | | $B^{10}$ in S/M-B, $Al_2O_3$ S/M-D |
| 49 | 127.224 | | 11 | +20.345 | 43 | | | | 0 | 0 | | | | SS[g] in S/M-B |
| | | ↓ | ↓ | | ↓ | ↓ | ↓ | | ↓ | ↓ | ↓ | ↓ | | |

TABLE XXI (Contd.)

| Loading No. | Excess Reactivity, Ih | Mass of $U^{235}$ in Core, kg | Fig No. Ref | Change in Reactivity, Ih | Rel to Loading No. | Outer Radius, cm: Core | Outer Radius, cm: Reflector | Fuel Change, kg | No. of Drawers with $B^{10}$[e] | No. of Drawers with $Al_2O_3$ | No. of Drawers of Other Materials | Contents of: S-2323 | Contents of: M-2323 | Description[h] |
|---|---|---|---|---|---|---|---|---|---|---|---|---|---|---|
| 50 | 192.872 | | | +85.993 | | | | | | | 44 SS[g] | | | SS[g] in S/M-A |
| 51 | 95.055 | | | -97.817 | 50 | | | | 2 | | 44 SS[g] | | | $B^{10}$ in S/M-C, SS[g] in S/M-A,B |
| 53 | 172.324 | 215.68847 | | | | 27.664 | 78.432 | -1.37816 | 0 | 192 | 0 | | | $Al_2O_3$ in S/M-A,B,D, 1/4 dr. fuel removed S/M-E |
| 55 | 172.563 | | | | | | | | | | | | | Repeat of Loading 53 |
| 54 | 173.668 | | | +1.344 | 53 | | | | | | | | | Contents of core dr. S-F rotated 90° |
| 56 | 78.567 | | | -93.757 | 53 | | | | 2 | | | | | $B^{10}$ in S/M-C |
| 57 | 91.782 | 214.99939 | 12 | -96.540 | 58 | 27.620 | | 0.68908 | | 0 | | | | $B^{10}$ in S/M-A |
| 58 | 188.322 | | | | | | | | 0 | | | | | Ref. |
| 60 | 188.272 | | | | | | | | | | | | | Repeat of Loading 58 |
| 59 | 82.390 | | | -105.932 | 58 | | | | 2 | | | | | $B^{10}$ in S/M-B |
| 61 | 216.238 | 216.37755 | | | | 27.796 | | +1.37816 | 0 | | | | | Vert. loaded full dr. S/M-C |
| 62 | 221.445 | | | +33.123 | 58 | | | | | | | | | Horiz. loaded full dr. S/M-C |
| 63 | 233.992 | | | 45.670 | 58 | | | | | | | | | Vert. loaded full dr. at S-D, M-C |
| 64 | 240 | | | 51.678 | 58 | | | | | | | | | Horiz. loaded S-D, Vert. loaded M-C |
| 65 | 211.2 | 215.68847 | | 22.878 | 58 | 27.664 | | -0.68908 | | | | | | Vert. loaded full dr. M-C |
| 66 | 130.882 | | | 41.442 | 53 | | Irr[f] | | | -92 | | | | Vert. full dr. M-C, $Al_2O_3$ removed from S/M-E |
| 67 | 154.341 | 216.37755 | | 23.459 | 66 | 27.796 | | +0.68908 | | | | | | Vert. full dr. S-D, M-C |
| 68 | 181.419 | 212.24307 | | +27.078 | 67 | | 78.432 | -4.13448 | | 0 | | | | Horiz. 1/4 dr. S/M-G,F,H,I |
| 69 | 25.440 | | 13 | | | 27.083 | | | | | | | | Ref. |
| 70 | 33.749 | | | 8.309 | 69 | | Irr[f] | | | | 104 Al | | | Al in S/M-A |
| 71 | 50.876 | | | 25.436 | 69 | | 90.042 | | | | 400 Al | | | Al in S/M-A,B |
| 72 | 74.364 | 213.62123 | | 23.488 | 71 | 27.620 | | +1.37816 | | | | | | 1/4 horiz. fuel dr. S/M-C,D |
| 73 | 97.017 | 214.99939 | | 22.653 | 72 | 27.708 | | +1.37816 | | | | | | 1/4 horiz. fuel dr. S/M-C,D,E,F |
| 74 | 106.221 | 216.37755 | | 9.204 | 73 | 27.796 | | +1.37816 | | | | | | 1/4 horiz. fuel dr. S/M-C,D,E,F, 1/4 vert. dr. S/M-G,H |
| 75 | 132.151 | 217.75571 | | 25.930 | 74 | 27.884 | | +1.37816 | | | | | | 1/4 horiz. fuel dr. S/M-C,D,E,F, 1/4 vert. dr. S/M-G,H,I,J |
| 76 | 39.651 | | | -92.501 | 75 | | | | 2 | | | | | Fuel in S/M-C,D,E,F,G,H,I,J; $B^{10}$ in S/M-K |
| 77 | 40.098 | | | -92.053 | 75 | | | | | | | | | Fuel in S/M-C,D,E,F,G,H,I,J; $B^{10}$ in S/M-L |
| 78 | 35.304 | | | -96.847 | 75 | | | | | | | | | Fuel in S/M-C,D,E,F,G,H,I,J; $B^{10}$ in S/M-M |
| 79 | 47.234 | | | -84.917 | 75 | | | | | | | | | Fuel in S/M-C,D,E,F,G,H,I,J; $B^{10}$ in S/M-N |
| 80 | 48.295 | | | +1.061 | 79 | | | | | | | | | Fuel in S/M-C,D,E,F,G,H,I,J; $B^{10}$ in S/M-N, except fuel in S/M-I,J 1/8 in. closer to core |

[a] S = Subcritical.
[b] SC = Sample Changer.
[c] A numeral designates the number of fuel columns in a drawer.
[d] Ref. = Reference measurement.
[e] Each drawer with a column of $B^{10}$ (five 2 x 2 x 1/8 in. cans) has (21.0015 ± 0.5965) g of $B^{10}$.
[f] Irr = Irregular outer boundary.
[g] SS = Stainless steel.
[h] In hyphenated expressions, letters to left refer to stationary (S) or movable (M) half or both (S/M); letters to right refer to positions in Fig. No. Ref.

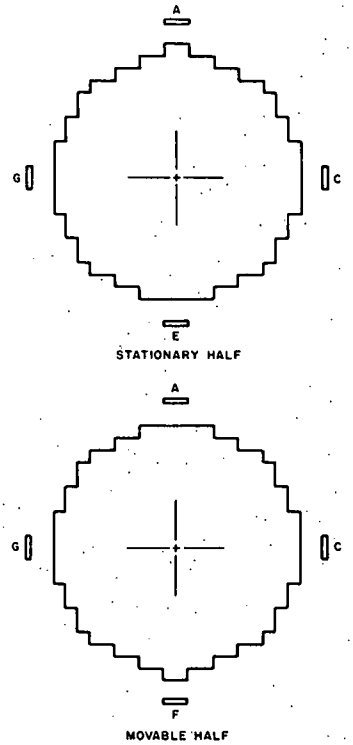


112-7761

Fig. 9. Geometric Outline of Loadings 15-25

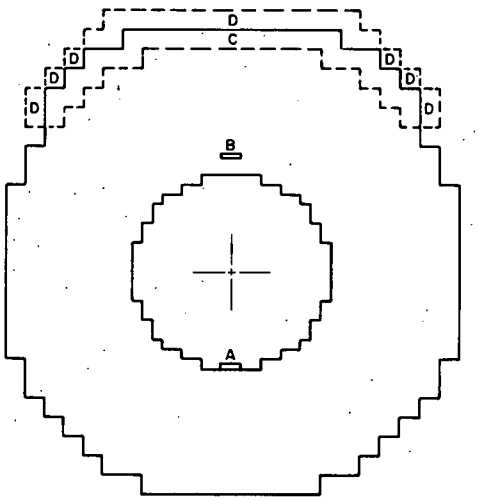


112-7760

Fig. 10. Geometric Outline of Loadings 41-48

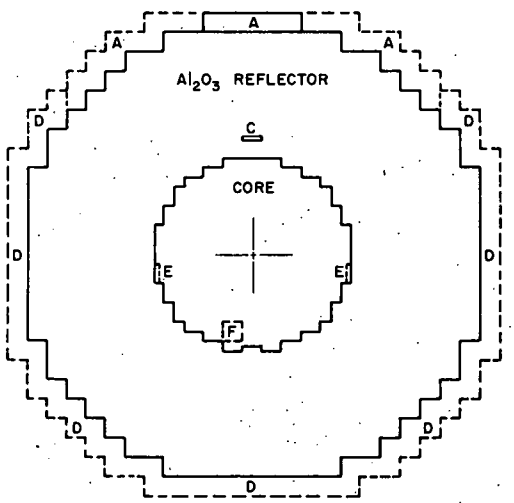


112-7750

Fig. 11. Geometric Outline of Loadings 49-56

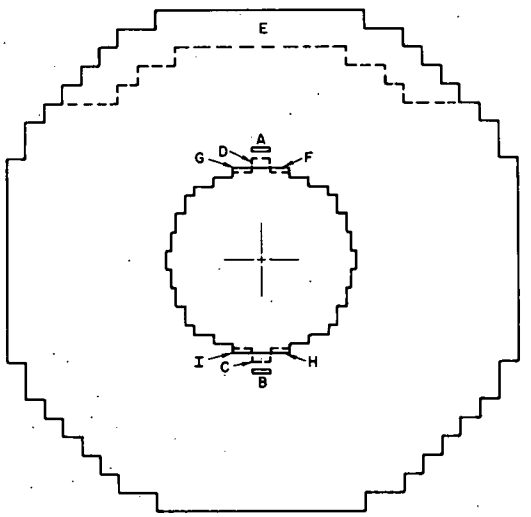


112-7753

Fig. 12. Geometric Outline of Loadings 57-68

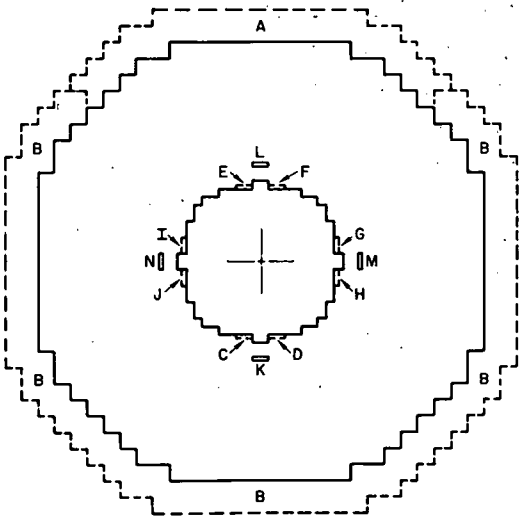


112-7752

Fig. 13. Geometric Outline of Loadings 69-80

each half of the reactor. A numeral indicates the number of fuel columns in the drawer; the letters SC represent Sample Changer. Each loading change is described briefly in the last column of the table. Although all the data available from this table will not be analyzed, the origin of the different worths in Fig. 8 can be seen from the first 15 or so entries. The middle section of the table shows how the addition and/or removal of parts of the reflector affect the boron worth and the fuel worths. The effects of adding a two-drawer-thick aluminum metal isolation blanket around an $Al_2O_3$ reflector can be seen near the end of the table, and the symmetry in the boron worth of an isolated assembly can be seen in the last 10 or so loadings in the table. In Loadings 72 through 75, where fuel was added to the core, there appeared to be a moderate degree of consistency in the fuel-edge worth, varying from 16 to 19 Ih/kg, with an average value of 17.43, very close to the earlier reported value of 17.7, measured with an aluminum metal axial reflector. Fuel at the center of the core (the difference between Loadings 15 and 18) had a measured worth of 169.57 Ih/kg.

The worth of a single column of fuel in the stationary half at the center of the core was 145.62 Ih/kg. In general, repeated measurements in various parts of the table showed the reproducibility of the data to be within ±1 Ih. There were slight differences between the reactivity associated with horizontally loaded fuel plates in the edge drawers and vertically loaded fuel plates. From the symmetry in $B^{10}$ worths in Loadings 67 to 80, we concluded that Loading 71 with a two-drawer-thick aluminum metal isolation blanket completely surrounding the $Al_2O_3$ reflector was indeed an isolated assembly.

Table XXII gives the sequence of loadings in going from the reference core (Loading 87) to the final measurements of the boron ring (Loading 118). The fourth column lists the number of drawers in each half in which five columns of fuel were loaded in place of the original four columns. Although no attempt was made to load these drawers in the circular cross-section pattern, an equivalent zone radius (column 5) was determined from a circle that had the same cross-sectional area as that occupied by the drawers. The sequence of materials in a drawer containing five fuel columns and going from east to west was: WAFAWAFWAFWAWF-AWAFW, where the various materials are identified in the appendix. The 1/16-in.-thick column of aluminum metal (a) together with the added

1/16-in.-thick fuel column replaced one of the 1/8-in.-thick 45% density aluminum columns. The next three columns in Table XXII list the number of columns of the boron-containing materials loaded into the reflector. Each column consisted of five cans or plates (each 1/8 in. thick and 2 x 2 in. sq) loaded end to end in the reflector drawer so that the inner radius of the boron sleeve was exactly one matrix position (5.543 cm) out from the last fuel column in the core. Thus, for example, the 32 boron columns in each half of Loading 96 correspond to a 20-in.-long, 1/8-in.-thick sleeve surrounding the core. Figure 14 shows the cross section of this loading. Each boron column is labeled with a letter, and each quadrant of the loading is symmetric. For the upper right quadrant, Fig. 15 shows

TABLE XXII. Results of Thick Boron-sleeve Experiment in Assembly No. 7

| Loading No. | Excess Reactivity, Ih | Mass of $U^{235}$ Loaded in Core, kg | No. of Drawers in Central Zone | Zone Radius, cm | No. of Columns per Half | | | No. of Fuel Columns in S/M-2323 | Outer $B^{10}$ Radius,[a] cm | Avg Sleeve Thickness, cm | Description[b] |
|---|---|---|---|---|---|---|---|---|---|---|---|
| | | | | | $B^{10}$ | Nat B | $B_4C$ | | | | |
| 87 | 200.005 | 212.47562 | 0 | 0 | 0 | 0 | 0 | 4 | 0 | 0 | Ref.[c] |
| 96 | 90.51 | 229.01108 | 24 | 15.6 | 32 | | | 4 | 32.984 | 0.345 | $B^{10}$ added to S/M A-FF |
| 97 | 213.5 | 229.70036 | 25 | | 32 | | | 5 | | | 5th fuel col. added to S/M-2323 |
| 98 | 103.5 | | | | 36 | | | 5 | 33.027 | 0.388 | 1/8 in. $B^{10}$ added to S/M-$A_1$, $I_1$, $Q_1$, $Y_1$ |
| 99 | | 232.45668 | 29 | 16.8 | 36 | | | | | | Fuel added to central zone |
| 100 | 184.5 | | | | 44 | | | | 33.113 | 0.474 | 1/8 in. $B^{10}$ added to S/M-D,F,L, N,S,V,BB,DD |
| 101 | Subcrit. | | | | | 40 | | | 33.975 | 1.336 | 800 cans of Nat B added to S/M-B,C,E,G,H,J,K,M,O,P,R,S,U,W, X,Z,AA,CC,EE,FF |
| 102 | Subcrit. | 235.21300 | 33 | 17.9 | | | | | | | Fuel added to central zone |
| 103 | 96.0 | 237.96932 | 37 | 19.0 | | | | | | | Fuel added to central zone |
| 104 | 32.0 | | | | | 46 | | | 34.105 | 1.466 | 1/8 Nat B added S/M-B,E,H,J,M, P,R,U,X,Z,CC,FF |
| 105 | 269.0 | 240.73564 | 41 | 20.0 | | | | | | | Fuel added to central zone |
| 106 | Subcrit. | | | | | | 36 | | 34.881 | 2.242 | $B_4C$ added to all B drs. |
| 107 | 58.0 | 243.48196 | 45 | 20.9 | | | | | | | Fuel added to central zone |
| 108 | 257.0 | 246.23828 | 49 | 21.9 | | | | | | | Fuel added to central zone |
| 109 | Subcrit. (-34.5) | | | | | | 68 | | 35.570 | 2.932 | 2 col. of $B_4C$ added to each B dr. |
| 110 | 150.0 | 248.99460 | 53 | 22.7 | | | | | | | Fuel added to central zone |
| 111 | Subcrit. | | | | | | 100 | | 36.26 | 3.622 | 2 col. of $B_4C$ added to each B dr. |
| 112 | 96.0 | 251.75092 | 57 | 23.6 | | | | | | | Fuel added to central zone |
| 113 | Subcrit. | | | | | | 122 | | 36.735 | 4.096 | $B_4C$ added |
| 114 | 69.2 | 254.50724 | 61 | 24.4 | | | | | | | Fuel added to central zone |
| 115 | Subcrit. | 251.06184 | | | | | | 0 | | | Fuel removed from S/M-2323 |
| 116 | Subcrit. | 253.81816 | 65 | 25.2 | | | | | | | Fuel added to central zone |
| 117 | Subcrit. | 256.57268 | 69 | 26.0 | | | | | | | Fuel added to central zone |
| 118 | 82.038 | 247.95264 | | | | | | 2 | | | 2 col. of fuel added to S/M-2323 |

[a] Inner $B^{10}$ sleeve radius = 32.639 cm.
[b] In hyphenated expressions, letters to left refer to stationary (S) or movable (M) half or both (S/M); letters to right refer to positions in Fig. No. Ref.
[c] Ref. = reference measurement.

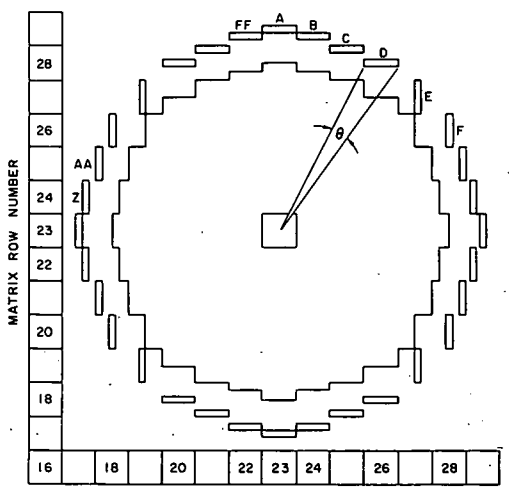


Figure 14

Geometric Outline of Loading 96

112-7508

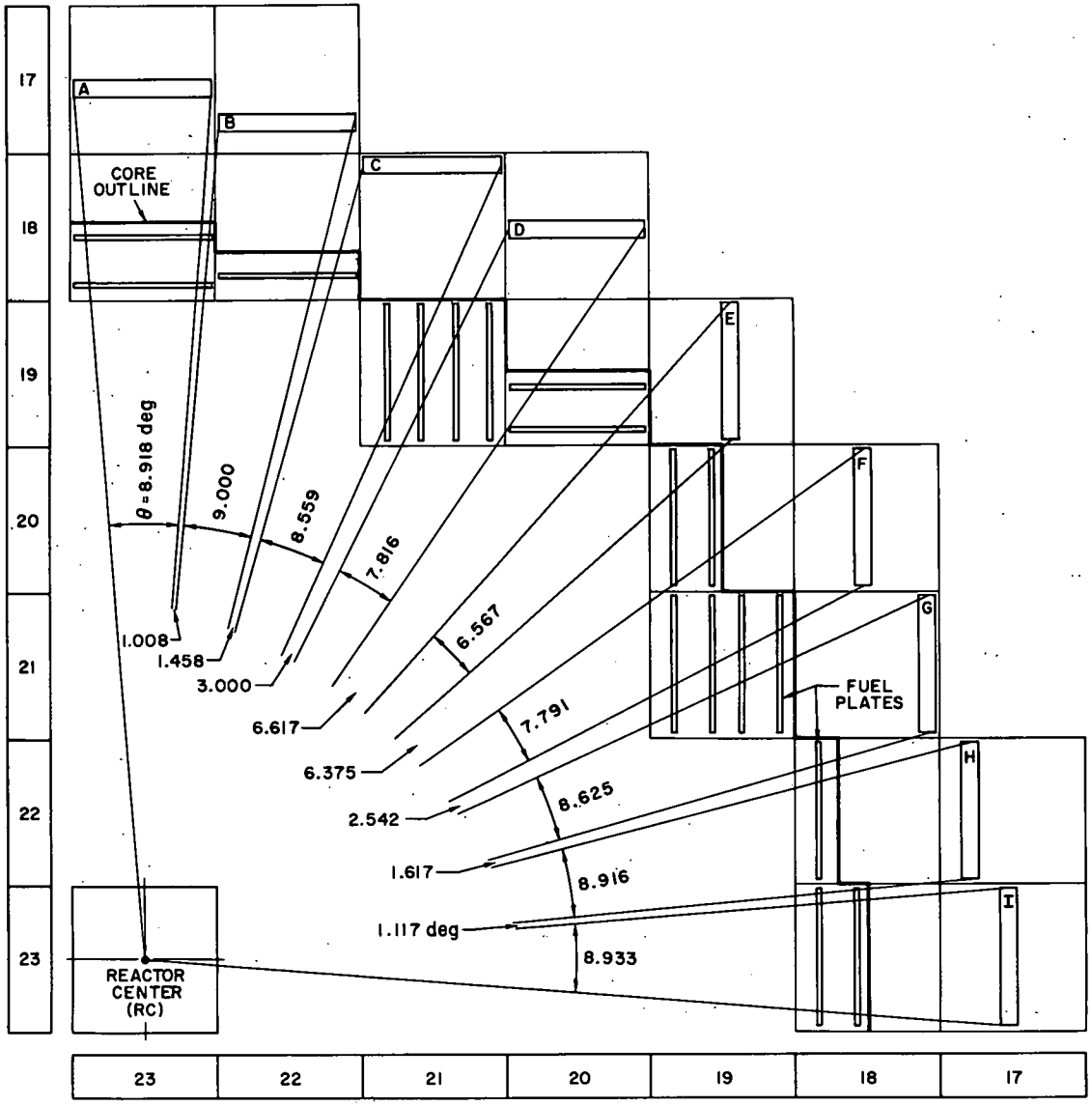


DIMENSIONS GIVEN IN CORE AS MEASURED FROM THE REACTOR CENTER LINE

MODEL

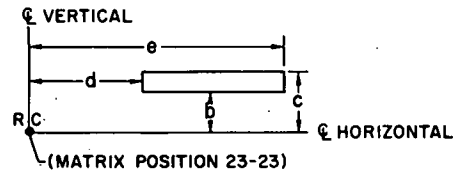


| | LOADING POSITION | | | |
|---|---|---|---|---|
| | A | B | C | D |
| $\bar{r}$* | 32.629 | 31.843 | 31.909 | 31.762 |
| b | 32.575 | 31.295 | 29.898 | 29.040 |
| c | 33.210 | 31.932 | 30.215 | 27.675 |
| d | -2.540 | 2.995 | 8.530 | 14.065 |
| e | 2.540 | 8.075 | 13.610 | 19.145 |

MODEL

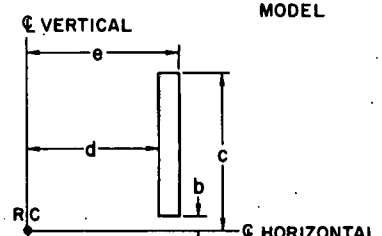


| | LOADING POSITION | | | | |
|---|---|---|---|---|---|
| | E | F | G | H | I |
| $\bar{r}$* | 31.311 | 31.862 | 31.636 | 31.746 | 32.785 |
| b | 19.600 | 14.065 | 8.530 | 2.995 | -2.540 |
| c | 24.680 | 19.145 | 13.610 | 8.075 | 2.540 |
| d | 22.240 | 27.198 | 29.580 | 31.095 | 32.733 |
| e | 22.775 | 27.833 | 30.215 | 31.930 | 33.368 |

*$\bar{r}$ IS THE ROOT MEAN SQUARE DISTANCE OF THE BORON COLUMN FROM REACTOR CENTER

112-7745 Rev. 1

Fig. 15. Details of $B^{10}$ Sleeve in Loadings 7-96

details of the X-Y coordinate positions and the angle $\theta$ subtended by the boron columns and the gap, $\phi$, between plates as measured from the core axis. The other three quadrants were minor images of the one illustrated. In the octant of Loading 96 shown in Fig. 15, the boron sleeve subtended a solid angle of slightly less than 66.2° or 73.5% of a 90° solid angle. The inner and outer radii of the boron sleeve, as well as the thickness of the sleeve, were determined in the same manner as the zone radius by equivalent cross-sectional areas. The last column of Table XXII briefly describes the loadings.

Figure 16 shows the geometric outline of the final loading of Assembly No. 7 (Loading 118), which becomes the first loading of Assembly No. 7C. As will be noted from the figure, the fuel-plate spacing in the outer drawers has not been changed, but those in the inner regions of the core have been changed. Figure 14 shows the physical location of the boron, $B_4C$, and natural boron for each loading. The 32 columns of $B^{10}$ in Loading 96 as indicated in Table XXII are shown in Fig. 16 at positions A-96 through I-96 for the upper right-hand quadrant of Fig. 14. In Loading 100, positions B and F had one column of $B^{10}$ added and are shown in Fig. 16 as B-101 and F-100.

Wherever the plane of the boron column was parallel to the plane of the outer fuel plate, there existed one column of aluminum or tungsten (belonging to the core) and the equivalent of 15 columns of $Al_2O_3$ (belonging to the reflector). Each matrix position is 5.551 x 5.535 cm for an average of 5.543 cm. Between the core edge (27.442 cm) and the first $B^{10}$ can, there is an average of 5.197 cm of $Al_2O_3$. Therefore, the inner radius of the boron sleeve is 5.19 cm beyond the outer edge of the core or 32.639 cm from the core axis. An inventory of the type and amount of boron in each of the loadings is shown in Table XXIII. The Boron Position columns give the number of columns of the various materials at each position. The last column lists the sum of all the $B^{10}$ in each loading and includes the uncertainty mentioned earlier in boron weights.

## 2. Critical Properties of Assembly No. 7C

Table XXIV shows the size of the zones and the atom densities of the various materials in the initial loading (87), the intermediate-stage loading (96), and the final loading (118) of Assembly No. 7C. Loading 96 with one column of enriched $B^{10}$ in each of the matrix positions surrounding the core, is the same geometry as the sleeve experiments in the other assemblies. The radii given for the various regions of the core and reflector were determined from equivalent cross-sectional areas. The thickness of the inner $Al_2O_3$ reflector (between the boron sleeve and the outer edge of the core) was fixed at 5.197 cm. The thickness of the boron sleeve is determined from the radius of a circle whose area was the sum of the areas inside the sleeve plus the actual physical area occupied by the boron materials. Thus, the experiment is represented by a homogenized sleeve

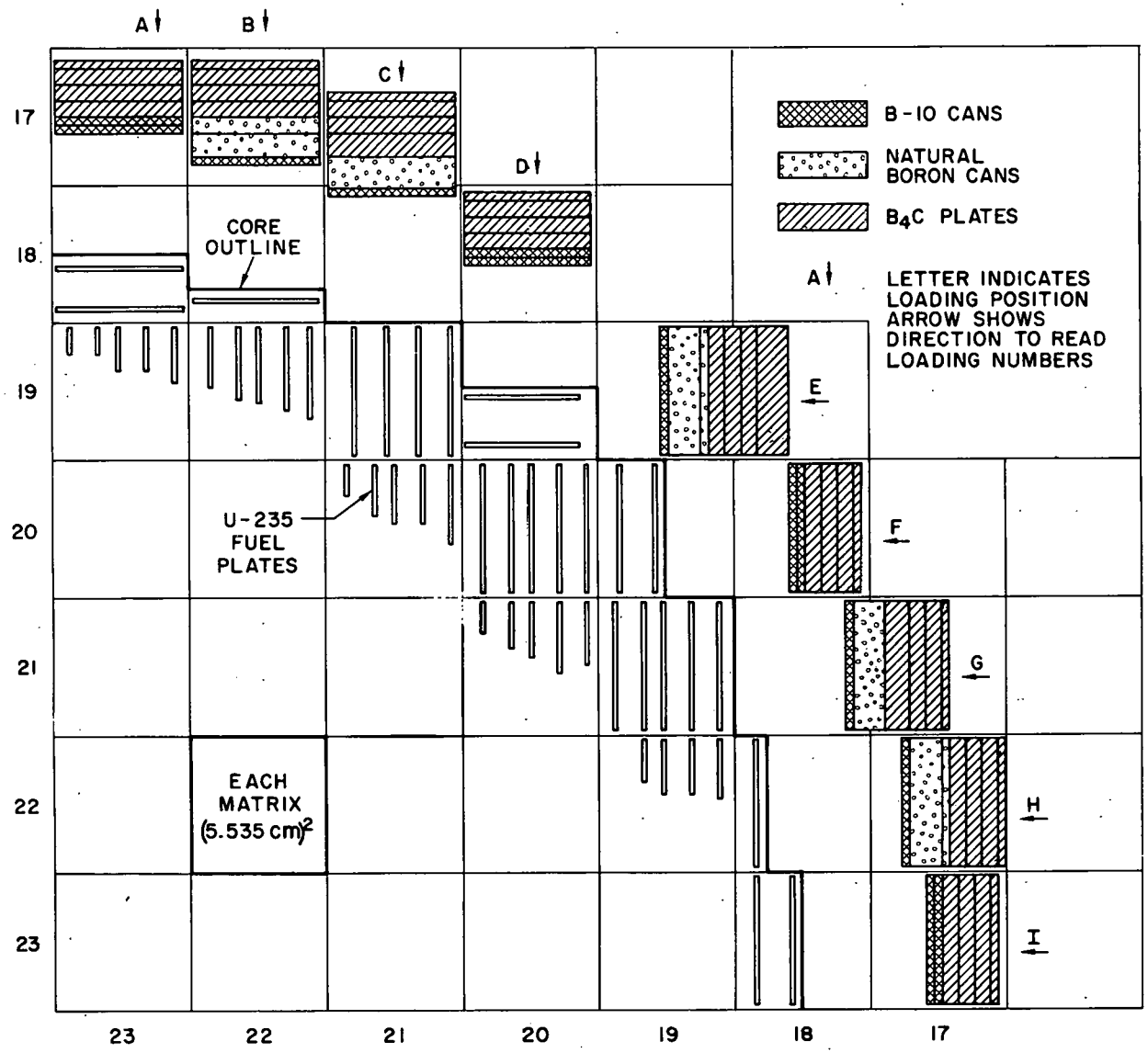


LOADING NUMBERS AND POSITIONS

| A | D | G |
|---|---|---|
| 113 | 113 | 113 |
| 111 | 111 | 111 |
| 109 | 109 | 109 |
| 106 | 106 | 106 |
| 98 | 100 | 101 |
| 96 | 96 | 96 |

| B | E | H |
|---|---|---|
| 113 | 113 | 113 |
| 111 | 111 | 111 |
| 109 | 109 | 109 |
| 106 | 106 | 106 |
| 104 | 104 | 104 |
| 101 | 101 | 101 |
| 96 | 96 | 96 |

| C | F | I |
|---|---|---|
| 113 | 113 | 113 |
| 111 | 111 | 111 |
| 109 | 109 | 109 |
| 106 | 106 | 106 |
| 101 | 100 | 98 |
| 96 | 96 | 96 |

Fig. 16. Geometric Outline of Loadings 7-118

TABLE XXIII. Boron Inventory in the Boron-sleeve Experiment of Assembly No. 7

| Loading No. | Material | Boron Position A | B | C | D | E | F | G | H | I | Total Cans (Plates) in Reflector | $B^{10}$ Weight, g | Total $B^{10}$ in Reflector, g |
|---|---|---|---|---|---|---|---|---|---|---|---|---|---|
| | | No. of Columns of Boron | | | | | | | | | | | |
| 98 | $B^{10}$ | 2 | 1 | 1 | 1 | 1 | 1 | 1 | 1 | 2 | 360 | 1512 ± 43 | |
| | Nat B | 0 | 0 | 0 | 0 | 0 | 0 | 0 | 0 | 0 | 0 | 0 | |
| | $B_4C$ | 0 | 0 | 0 | 0 | 0 | 0 | 0 | 0 | 0 | 0 | 0 | |
| | | | | | | | | | | | | | 1512 ± 43 |
| 100 | $B^{10}$ | 2 | 1 | 1 | 2 | 1 | 2 | 1 | 1 | 2 | 440 | 1846 ± 52 | |
| | Nat B | 0 | 0 | 0 | 0 | 0 | 0 | 0 | 0 | 0 | 0 | 0 | |
| | $B_4C$ | 0 | 0 | 0 | 0 | 0 | 0 | 0 | 0 | 0 | 0 | 0 | |
| | | | | | | | | | | | | | 1846 ± 52 |
| 101 | $B^{10}$ | 2 | 1 | 1 | 2 | 1 | 2 | 1 | 1 | 2 | 440 | 1846 ± 52 | |
| | Nat B | 0 | 4 | 4 | 0 | 4 | 0 | 4 | 4 | 0 | 800 | 960 ± 36 | |
| | $B_4C$ | 0 | 0 | 0 | 0 | 0 | 0 | 0 | 0 | 0 | 0 | 0 | |
| | | | | | | | | | | | | | 2806 ± 64 |
| 104 | $B^{10}$ | 2 | 1 | 1 | 2 | 1 | 2 | 1 | 1 | 2 | 440 | 1846 ± 52 | |
| | Nat B | 0 | 5 | 4 | 0 | 5 | 0 | 4 | 5 | 0 | 900 | 1104 ± 41 | |
| | $B_4C$ | 0 | 0 | 0 | 0 | 0 | 0 | 0 | 0 | 0 | 0 | 0 | |
| | | | | | | | | | | | | | 2950 ± 66 |
| 106 | $B^{10}$ | 2 | 1 | 1 | 2 | 1 | 2 | 1 | 1 | 2 | 440 | 1846 ± 52 | |
| | Nat B | 0 | 5 | 4 | 0 | 5 | 0 | 4 | 5 | 0 | 920 | 1104 ± 41 | |
| | $B_4C$ | 2 | 2 | 3 | 2 | 2 | 2 | 3 | 2 | 2 | 720 | 1168 ± 71 | |
| | | | | | | | | | | | | | 4118 ± 97 |
| 109 | $B^{10}$ | 2 | 1 | 1 | 2 | 1 | 2 | 1 | 1 | 2 | 440 | 1846 ± 52 | |
| | Nat B | 0 | 5 | 4 | 0 | 5 | 0 | 4 | 5 | 0 | 920 | 1104 ± 41 | |
| | $B_4C$ | 4 | 4 | 5 | 4 | 4 | 4 | 5 | 4 | 4 | 1360 | 2206 ± 134 | |
| | | | | | | | | | | | | | 5156 ± 149 |
| 111 | $B^{10}$ | 2 | 1 | 1 | 2 | 1 | 2 | 1 | 1 | 2 | 440 | 1846 ± 52 | |
| | Nat B | 0 | 5 | 4 | 0 | 5 | 0 | 4 | 5 | 0 | 920 | 1104 ± 41 | |
| | $B_4C$ | 6 | 6 | 7 | 6 | 6 | 6 | 7 | 6 | 6 | 2000 | 3244 ± 196 | |
| | | | | | | | | | | | | | 6194 ± 207 |
| 113 | $B^{10}$ | 2 | 1 | 1 | 2 | 1 | 2 | 1 | 1 | 2 | 440 | 1846 ± 52 | |
| | Nat B | 0 | 5 | 4 | 0 | 5 | 0 | 4 | 5 | 0 | 920 | 1104 ± 41 | |
| | $B_4C$ | 7 | 7 | 8 | 7 | 10 | 7 | 8 | 7 | 7 | 2440 | 3958 ± 240 | |
| | | | | | | | | | | | | | 6908 ± 249 |

TABLE XXIV. Composition and Critical Properties of Assembly No. 7, Loadings 87, 96, and 118

| Assembly Regions | Outer Radius, cm | Atom Density (in units of $10^{24}$ atoms/cm$^3$) $U^{235}$ | $U^{238}$ | Aluminum | Iron | Tungsten | $B^{10}$ | Oxygen | Total Fuel Mass, kg $U^{235}$ | Excess Reactivity, Ih | Total $B^{10}$ Weight, g |
|---|---|---|---|---|---|---|---|---|---|---|---|
| Loading 87 | | | | | | | | | | | |
| Core | 27.442 | 0.004498 | 0.000325 | 0.01594 | 0.000312 | 0.02111 | | | 212.47562 | 200.005 | 0 |
| Reflector | 77.175 | | | 0.04324 | | | | 0.05469 | | | |
| Isolation Blanket | 88.949 | | | 0.05658 | | | | | | | |
| Loading 96 | | | | | | | | | | | |
| Central Driver | 3.127 | 0.004498 | 0.000325 | 0.01594 | - | 0.02111 | | | 229.01108 | 90.51 | 2688 ± 36 |
| High Fuel-density Zone | 15.34 | 0.005622 | 0.000406 | 0.009402 | 0.000312 | 0.02111 | | | | | |
| Core | 27.442 | 0.004498 | 0.000325 | 0.01594 | - | 0.02111 | | | | | |
| Inner Reflector | 32.638 | | | 0.04324 | | | | 0.05468 | | | |
| Boron Sleeve | 32.936 | | | | | | 0.0615 | | | | |
| Loading 118 (Assembly No. 7C Loading 1) | | | | | | | | | | | |
| Central Driver | 3.127 | 0.002249 | 0.000163 | 0.01594 | - | 0.02444 | | | 247.95264 | 82.038 | 8758 ± 265 |
| High Fuel-density Zone | 25.977 | 0.005622 | 0.000406 | 0.01594 | 0.000312 | 0.02111 | | | | | |
| Core | 27.442 | 0.004498 | 0.000325 | 0.01594 | | 0.02111 | | | | | |
| Inner Reflector | 32.638 | | | 0.04324 | | | | 0.05468 | | | |
| Inner $B^{10}$ Sleeve | 33.047 | | | | | | 0.05165 | | | | |
| Outer $B^{10}$ Sleeve | 34.566 | | | | | | 0.01853 | | | | |

completely surrounding the core but having a slightly smaller thickness than was actually present in the experiment. The $B^{10}$ atom density was determined from the total boron content in the sleeve, divided by the total volume occupied by the boron materials, and again is a homogenization of all the boron in the sleeve. The sleeve is broken into an inner section and an outer

section. The inner section contains the high-density $B^{10}$ in the enriched-boron cans; the outer section has the much lower density of $B^{10}$ characteristic of the natural boron and the $B_4C$ plates. The outer radii of $Al_2O_3$ reflector, as well as of the aluminum metal isolation sleeve, were the same for all three loadings, and hence are listed only for the reference assembly. In place of the two columns of fuel removed from the central drawers in Loading 118 (see Table XXII), 1/16-in. columns of tungsten were used to maintain roughly equivalent scattering and absorption cross sections. This accounts for the higher tungsten density in the central drawer of Loading 118.

TABLE XXV. Central Worths of Material in Assembly No. 7C

| Sample | Weight, g | Sample Worth, Ih/kg |
|---|---|---|
| Polyethylene | 2.019 | 430 ± 20 |
| | 0.288 | 3000 ± 50 |
| $B^{10}$ | 0.775 | -2990 ± 50 |
| $U^{235}$ | 6.4 | 200 ± 10 |

### 3. Central Worths

A limited number of spatially dependent reactivity and reaction-rate traverses were made in this assembly with the automated procedure-computer operated system described in Refs. 7-9. Table XXV lists central worths extracted from these data. The samples used in these measurements are considerably smaller than most of the samples normally used for central-worth measurements. For this reason, a correction had to be made for the background effect of the probe resulting in larger errors.

### 4. Kinetics Measurements

Rossi-alpha measurements were made with pairs of counters, one in each half. We tried to determine if the value of $\alpha_3$ or the relative magnitudes of the three components observed in the previous measurements changed as a function of position. In the first measurement, the detecting chambers were in matrix positions 23-23 (one in each half of the reactor). In the second measurement, the chambers were moved out into the reflector beyond the boron ring to matrix positions 23-31 in both halves. The counting statistics of the second measurement were very poor, but within the error the three alpha values were the same as measured at the core center. Results of measurements at the core center are given in Table XXVI. As with other assemblies, the prompt-neutron lifetime is inferred from the value of $\alpha_3$.

TABLE XXVI. Kinetic Parameters, Assembly No. 7C

| Measured Rossi-alpha, $sec^{-1}$ | | | $\beta_{eff}$, | Prompt-neutron Lifetime, $10^{-9}$ sec | |
|---|---|---|---|---|---|
| $\alpha_1$ | $\alpha_2$ | $\alpha_3$ | Calculated | Measured | Calculated |
| $(5.55 \pm 0.52)$ $10^4$ | $(1.57 \pm 0.07)$ $10^4$ | $(3.65 \pm 0.01)$ $10^3$ | 0.00657 | 1800 | 94.7 |

### 5. Reflector Studies

The radial reflector worths were measured just before the disassembly of Assembly No. 7C. In these measurements, one quadrant of the reflector in the stationary half was removed to determine its worth. Removal was done in increments, starting with a 90° sector of the two-drawer-thick aluminum isolation blanket. Extrapolating the 90° measurements to 360° and over both halves of the core gave an estimated worth of the isolation blanket of 16 Ih. The removal of a 39° pie-shaped section of the radial $Al_2O_3$ reflector of the stationary half resulted in the loss of 74 Ih. Removal of the reflector material from an additional 15° sector lost another 98 Ih. Finally, the removal of all the reflector material in a 90° sector lost a total of 398 Ih. In the process of determining the reactivity loss, fuel was added to the central region to maintain criticality. In this region, a fuel column the full length of the core had a measured worth of 171.24 Ih/kg. Assuming linear extrapolation is justified, the reflector worth measurements through the remaining seven octants indicate that the part of the reflector beyond the boron ring had a total worth of approximately 7.3% $\Delta k/k$.

## C. Assembly No. 8

Of all the assemblies studied, Assembly No. 8 bore the closest relationship to a practical engine design and provided the severest test of the analytical methods and cross-section sets employed in this study. Because of time limitations, we could not study this assembly in as complete a manner as some of its predecessors. However, sufficient basic data were measured so that reliable extrapolations could be made. For this reason, we placed more emphasis on the spatial dependence of perturbing quantities of boron and hydrogen than on the actual worth of a thick or thin boron sleeve. In addition to absorption type of control, a limited number of measurements were made to evaluate the relative merits of leakage control by reflector movement.

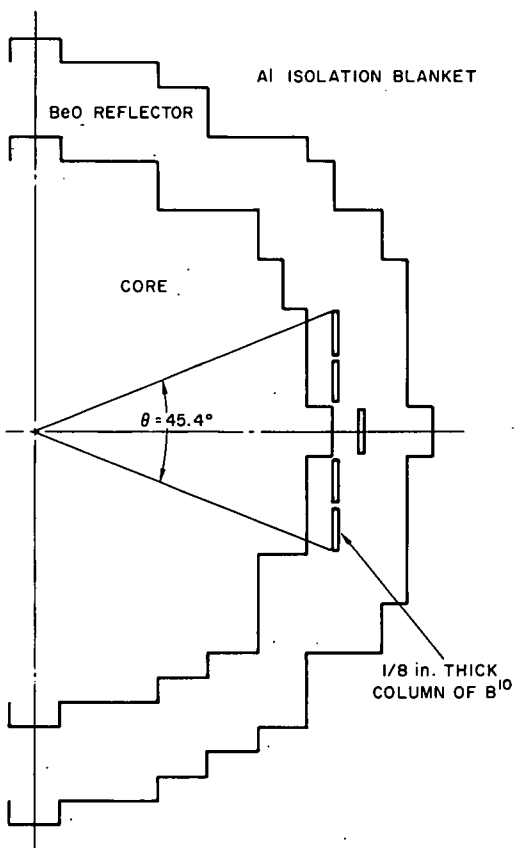


112-7756

Fig. 17. Geometry of Boron Ring Experiment

### 1. Boron-sleeve Measurements on Assembly No. 8

Because of the limited time available for doing experiments on this assembly, we could not do the complete boron-sleeve experiment as had been done on the other assemblies. Figure 17 shows the geometry of the experiment performed. Five columns of $B^{10}$, each 1/8 in. thick and

10 in. long, were loaded into the stationary half in the geometry shown in Fig. 17. This removed 156.8 Ih. A fifth column of fuel was added to the drawer on either side of the central drawer in both halves of the assembly to compensate for this loss. The addition of the same amount of boron in the same geometric location on the movable half removed 111.0 Ih. Calculations of the boron worth in the reflector indicated that these measurements should be quite sensitive to the position of the boron relative to the core edge. For this reason, each boron column is located exactly 2.77 cm beyond the last piece of core material, and 2.54 cm of this space was occupied by BeO. The remaining space (0.17 cm) is occupied by the thickness of the drawer sides and the clearance space between drawers as well as the matrix material. Extrapolating these data to a 360° sleeve gives a total estimated worth of 5.3% $\Delta k/k$ for a sleeve that would contain 1.66 kg of $B^{10}$. The ten columns of $B^{10}$ used in this experiment (each column made up of five 2 x 2-in. cans each 1/8 in. thick) contained a total of 210.0 ± 5.9 g of $B^{10}$. The quoted error includes the dispersion in empty-can weights, boron enrichment, nonboron content, and packing density within the cans.

### 2. Spatial Dependence of Boron Worth in the Reflector

Because of the potentially large thermal-neutron power spike in the BeO reflector, the worth of boron as well as its spatial sensitivity in this region is expected to be quite large. Several spot measurements both in the core and in the reflector were made with a 4.0-g sample of $B^{10}$ to test the sensitivity as a function of position. In these measurements, the worth of a simple 2 x 2 x 1/8-in. can containing 4.20 ± 0.12 g of $B^{10}$ was mapped out in several positions in the reflector. The results of these measurements are summarized in Table XXVII. A correction was applied to the measured worth to account for the effect of removing the BeO. The magnitude of this correction was estimated from a logarithmic extrapolation between the two measured end points listed in Table XII. The gain in reactivity associated with Loading 57 remains unexplained and is felt to be greater than can be accounted for by errors in the measurement. The last column in Table XXVII gives the corrected worth per gram of $B^{10}$.

TABLE XXVII. Worth of Boron in Reflector, Assembly No. 8

| Loading No. | Mean Distance from Core Axis, cm | Total Reactivity Lost Relative to Reflector, Ih | Worth of Removal BeO, Ih | Corrected Worth of $B^{10}$, Ih | $B^{10}$ Worth/Weight, Ih/g |
|---|---|---|---|---|---|
| 53 | Reference | 0 | | | |
| 54 | 30.670 | -14.782 | 0.225 | -15.007 | -0.514 |
| 55 | 33.210 | -14.222 | 0.224 | -14.446 | -0.495 |
| 56 | 38.745 | -2.572 | 0.149 | -2.741 | -0.094 |
| 57 | 41.286 | 1.386 | 0.148 | 1.238 | 0.295 |
| Central worth | 0 | | | | -2.481 |

### 3. Reflector Removal Control Studies in Assembly No. 8

With the high worth of the BeO reflector, it is of interest to determine the magnitude of control margin available by changing the leakage through the removal of reflector material. Two series of reflector-worth determinations relative to a void were made for gaps in the reflector region at the core midplane. In the first, the worth of a 4-in. void at the core midplane was determined for different azimuthal angles. In the second measurement, we determined the worth of a fixed void in the reflector (1.121 ± 0.005 cm) extending completely around the core. Table XXVIII lists the results of both sets of measurements. The z-coordinate in the table is along the axial length of the reactor and is zero at the core midplane. In Loading 63, a 2-in. void was put on either side of the core midplane; in Loadings 64 and 65, the void was restricted to the stationary half only. Small variations in the radial position of the void were caused by the irregular boundary of the approximately cylindrical edge of the core. In the first three measurements listed in Table XXVIII, the voids were created by removing material from the reflector drawers. In the last measurement, however, the void was created by removing the spring in the back of the reflector drawer and moving all the material back from the core midplane. In this case, the depth of the void was determined from about 200 dial-indicator measurements. The 0.56-cm void in Loading 68 does not include the 0.8-cm space taken up by the aluminum drawer fronts in common to the entire core midplane. The last column in Table XXVIII is an extrapolation through the measured angle to 360° and is expressed in reflector void worth per cm. The large voids associated with Loadings 63, 64, and 65 are worth about 1/2% $\Delta k/k/cm$ of void; the small void in Loading 68 is worth about half that amount.

TABLE XXVIII. Results of Reflector Voiding Worth Measurements in Assembly No. 8

| Loading No. | Gap Definition | Reactivity Lost, Ih | Gap Worth/Length, % $\Delta k/k/cm$ |
|---|---|---|---|
| 63 | $-5.63 \leq z \leq +5.63$ cm<br>$30.442 \leq r \leq 41.512$ cm<br>$0 \leq \theta \leq 9.16°$ | 63.77 | 0.51 |
| 64 | $0 \leq z \leq 5.63$ cm<br>$30.58 \leq r \leq 41.62$ cm<br>$0 \leq \theta \leq 18.85°$ | 61.60 | 0.46 |
| 65 | $0 \leq z \leq 5.63$ cm<br>$31.55 \leq r \leq 40.96$ cm<br>$0 \leq \theta \leq 54.55°$ | 203.9 | 0.55 |
| 68 | $-0.561 \leq z \leq +0.561$ cm<br>$31.74 \leq r \leq 42.88$ cm<br>$\theta = 360°$ | 137.6 | 0.284 |

# IV. PROPELLANT STUDIES

The introduction of hydrogen as a propellant in these systems affects the reactivity. In Assembly No. 4B, as reported in ANL-7207, the homogeneous addition of hydrogen to the core removed reactivity; in the present oxide-reflected assemblies, hydrogen increases reactivity in amounts that at least partially compensate for loss of reactivity resulting from a thermal expansion of the core. Although these studies were not directed toward the determination of the control margin that might be available through the controlled pumping of liquid hydrogen through the core, the success of this method of control in the restart studies of the KIWI 4B experiments indicates the potential application of this scheme in fast-reactor propulsion systems.

## A. Assembly No. 6A

After the basic studies in Assembly No. 6 were complete, hydrogen in the form of polyethylene sheets was uniformly added to the reflector. Table XXIX summarizes this sequence of measurements. The polyethylene used in these experiments had a density of 0.9616 g/cm$^3$, and an average hydrogen weight fraction of 14.3%. Each drawer was loaded with 20-mil-thick sheets on the bottom of the drawer and extending the full 24-in. length of the drawer. Attempts to insert a second 20-mil sheet of polyethylene on the sides of the drawer were generally unsuccessful because of the limited clearances and consequent binding of the drawers in the matrix. For this reason, all drawers starting with Loading 56 had a 5-mil thickness of polyethylene added to the east side of each drawer. This pattern was

TABLE XXIX. Reactivity Worth of Hydrogen in Reflector of Assembly No. 6

| Loading No. | No. of Drawers | | Weight of Polyethylene, g | | Weight of Hydrogen, g | | Excess Reactivity, Ih | | Worth of Accumulated Polyethylene, Ih | Worth/Weight of Hydrogen, Ih/g | |
|---|---|---|---|---|---|---|---|---|---|---|---|
| | Added | Accum | Added | Accum | Added | Accum | Added | Accum | | Added | Accum |
| 50 | Reference | | 0 | | 0 | | | 79.75 | 0 | | |
| 53 | 8[a] | 8 | 241.331 | 241.331 | 34.510 | 34.510 | 3.52 | 83.26 | 3.52 | 0.101 | 0.101 |
| 54 | 2[b] | 10 | -63.121 | 178.210 | -9.026 | 25.484 | -0.79 | 82.48 | 2.73 | 0.087 | 0.107 |
| 55 | -2[c] | 8 | -30.161 | 148.049 | -4.313 | 21.171 | -0.91 | 81.57 | 1.82 | 0.201 | 0.085 |
| 56 | 24 | 32 | 444.111 | 592.160 | 63.507 | 84.678 | 14.83 | 96.39 | 16.64 | 0.233 | 0.196 |
| 57[d] | 0 | 32 | Fission chambers removed from reflector | | | | 21.28 | 117.67 | 16.64 | New reference | |
| 58 | 25[e] | 57 | 576.055 | 1168.215 | 82.375 | 167.053 | 9.02 | 126.69 | 25.66 | 0.109 | 0.153 |
| 59 | 24[f] | 81 | 586.663 | 1754.878 | 83.982 | 251.035 | 10.03 | 136.72 | 35.69 | 0.119 | 0.142 |
| 60 | 123 | 204 | 2276.115 | 4030.993 | 325.484 | 576.519 | 65.70 | 202.42 | 101.39 | 0.201 | 0.175 |
| 61 | Two columns of fuel removed from M-2323 and S-2323 | | | | | | -187.50 | 14.92 | | | |
| 62 | 101 | 305 | 1869.005 | 5899.998 | 267.267 | 843.786 | 47.46 | 62.37 | 148.85 | 0.177 | 0.176 |
| 63 | 110 | 415 | 2035.550 | 7935.548 | 291.083 | 1143.869 | 42.32 | 104.69 | 191.16 | 0.145 | 0.168 |
| 64 | 150 | 565 | 2775.750 | 10711.298 | 396.932 | 1531.801 | 33.49 | 138.18 | 224.65 | 0.084 | 0.146 |
| 65 | 166 | 731 | 3099.100 | 13810.398 | 443.171 | 1974.972 | 33.28 | 171.46 | 257.93 | 0.075 | 0.130 |
| 66[g] | 155 | 886 | 2893.895 | 16704.293 | 413.826 | 2388.798 | 16.55 | 188.01 | 274.48 | 0.039 | 0.114 |

[a]All eight drawers had 0.020-in. polyethylene on a side.
[b]Two of the former eight drawers had 0.020-in. polyethylene on a side; remaining six plus two added drawers, had 0.005-in. polyethylene on the side.
[c]Two drawers from Assembly No. 6 Loading 54 with 0.020-in. polyethylene on a side were removed.
[d]Flux probe tube was removed from core, and fission chambers were removed from core-reflector interface.
[e]Nineteen half drawers at core edge and their back drawers in movable half, plus 15 full drawers added.
[f]Nineteen half drawers at core edge and their back drawers in stationary half, plus 15 full drawers added.
[g]Assembly No. 6A Loading 1.

repeated for the entire reflector, including the half-loaded drawers at the core-reflector interface and the axial reflector drawers behind them. To limit the maximum excess reactivity available to the operator, in Loading 61 two columns of fuel were removed from the central drawers in the stationary and movable halves. This resulted in the loss of 183.24 Ih, giving an average central fuel worth of 110.58 Ih/kg of $U^{235}$ on the core axis. In Loading 66, all the reflector drawers contained the prescribed amount of hydrogen. This loading was labeled Assembly No. 6A, Loading 1, where the A designates a completely hydrogenated reflector.

## B. Assemblies No. 8A and 8B

Hydrogen was homogeneously added to both the core and the reflector of Assembly No. 8 in much the same manner as in Assembly No. 6. Polyethylene sheets 20 mils thick were added first to the bottom of each core drawer and then to the bottom of each BeO reflector drawer. Table XXX summarizes the results of these measurements. In the first loading, polyethylene was added to the central 3 x 3 array in both halves of the machine to form a zone with a mean radius of 9.38 cm. The loading accounted for 16.17 g of hydrogen and 96.95 g of carbon and added 31.85 Ih reactivity. In terms of hydrogen worth, this amounts to 1.97 Ih/g of hydrogen. No correction has been made for the effect of carbon. In subsequent loadings, the size of the central zone was increased, and the worth of hydrogen added with each loading is recorded in the next to last column of the

TABLE XXX. Worth of Hydrogen Added Homogeneously to Assembly No. 8

| Loading No. | Effective Radius of Loaded Region, cm | Hydrogen Weight, g | | Carbon Weight, g | | Excess Reactivity in Reactor, Ih | Hydrogen Worth | |
|---|---|---|---|---|---|---|---|---|
| | | Added | Total in Reactor | Added | Total in Reactor | | Added Ih/g | Total Ih |
| 37 | Reference | | | | | 131.41 | | |
| 38 | 9.38 | 16.17 | | 96.95 | | 163.26 | 1.97 | 31.85 |
| 39 | 15.63 | 28.76 | 44.93 | 172.44 | 269.30 | 226.12 | 2.19 | 97.71 |
| 40-43 | Fuel and BeO reflector material removed | | | | | 100.69 | | |
| 44 | 20.02 | 29.66 | 74.59 | 177.73 | 447.03 | 154.28 | 1.81 | 148.29 |
| 45 | Fuel and BeO reflector material removed | | | | | 39.43 | | |
| 46 | 23.61 | 21.57 | 96.16 | 129.26 | 576.29 | 74.72 | 1.64 | 185.58 |
| 47 | 25.97 | 20.67 | 116.83 | 123.88 | 700.17 | 101.07 | 1.27 | 209.93 |
| 48 | 28.49 | 25.16 | 141.99 | 150.81 | 850.97 | 124.57 | 0.93 | 233.42 |
| 49 | 31.43 | 30.56 | 172.55 | 183.12 | 1034.09 | 152.86 | 0.92 | 261.72 |
| | Hydrogen Added to Reflector | | | | | | | |
| 50 | 32.68 | 14.38 | 186.93 | 86.17 | 1120.27 | 159.90 | 0.49 | 268.76 |
| 51 | 34.40 | 21.57 | 208.50 | 129.26 | 1249.53 | 170.75 | 0.50 | 279.61 |
| 52 | 37.65 | 43.14 | 251.64 | 258.52 | 1508.05 | 187.51 | 0.39 | 296.37 |
| 53 | 42.77 | 75.49 | 327.13 | 452.42 | 1960.47 | 200.67 | 0.17 | 309.53 |

table. The last column accumulates the total reactivity added. In Loading 49, all the core drawers except the ten dual-purpose rods had hydrogen added to them. Because of the limited clearances in the dual-purpose rod drawers, these were not loaded with polyethylene sheets. Accumulated excess reactivity amounts to 0.607% $\Delta k/k$ for a fully hydrogenated core. During loading, the excess reactivity introduced with the addition of hydrogen was compensated for by removing fuel from the edge of the core. Correcting the excess reactivity for Loading 49 in terms of edge-fuel removal, the critical radius for the loading was 30.69 cm.

The subsequent addition of polyethylene to each BeO reflector drawer added a total of 0.1% $\Delta k/k$.

## C. Assembly No. 9A

Essentially the same experiment done on Assemblies No. 6 and 8 was repeated on Assembly No. 9. Twenty-mil-thick strips of polyethylene were loaded into the bottom of each core drawer. This sequence of measurements is listed in Table XXXI. The second column represents the equivalent cross-sectional area of the zone having the hydrogen added. In Loading 31, two polyethylene strips (one in each half of the assembly) weigh 12.7 g and contain 1.80 g of hydrogen. When loaded into the central drawer of each half, this amount of hydrogen added 5.42 Ih reactivity. The cross-sectional area of any single matrix position is the same as a circle having a radius of 3.13 cm. To limit the excess reactivity, two columns of fuel were removed from the central drawer in Loading 34. From the loss in reactivity, fuel at the core center was worth 150.4 Ih/kg of $U^{235}$. Again, because of the limited clearances, polyethylene was not added to the dual-purpose rods. Loading 33 had four of the five dual-purpose rods in the hydrogen-loaded zone. In this loading, the addition of 25.16 g of hydrogen in the form of polyethylene sheets added 73.20 Ih, for an average of 2.91 Ih/g of hydrogen added. From this, it is estimated that 7.19 g of hydrogen added to the eight dual-purpose rods would have added 20.91 Ih reactivity, and a completely hydrogenated core would add 221.19 Ih or 0.514% $\Delta k/k$.

TABLE XXXI. Worth of Hydrogen Added Homogeneously to Assembly No. 9

| Loading No. | Effective Radius of Loaded Region, cm | Accumulated Weight, g | | Excess Reactivity in Core, Ih | Reactivity Gained, Ih | Worth/Weight, Ih/g of Hydrogen |
|---|---|---|---|---|---|---|
| | | Polyethylene | Hydrogen | | | |
| 30 | Reference | | | 156.0 | | |
| 31 | 3.13 | 12.57 | 1.80 | 161.4 | 5.42 | 3.02 |
| 32 | 9.38 | 113.12 | 16.18 | 187.9 | 26.45 | 1.97 |
| 33 | 16.25 | 289.09 | 41.34 | 261.1 | 73.20 | 2.54 |
| 34 | Two columns of fuel removed | | | 63.8 | | |
| 35 | 21.09 | 521.62 | 74.59 | 126.3 | 62.50 | 2.24 |
| 36 | 25.35 | 842.14 | 120.43 | 159.4 | 33.10 | 1.66 |

# V. REACTION-RATE TRAVERSES

Perhaps the most fundamental calculation that can be made in these assemblies is the energy distribution of the flux at any point in the reactor. The one-dimensional, multigroup diffusion code, MACH-1,[10] has been used extensively in reactor calculations, principally because of its versatility. MACH-1 provides the group-wise flux, reaction rate, and reactivity distributions along the direction of calculations. A comparison of the reaction rate so calculated to the spatial distribution of the measured reaction rates, provides a significant tool for evaluating both cross sections and calculational techniques.

The data in this section were determined by several methods and are presented as a series of computer-generated graphs. Activation measurements were made with fission foils in some cases; miniature counting chambers were used in others. Two types of counters were used. The boron reaction rates were determined from a standard miniaturized $BF_3$ counter. The $U^{238}$ and $U^{235}$ fission rates were determined using either gas-filled counting chambers or small solid-state counters. The solid-state counters were used for all the fissionable species. In several cases, the $U^{235}$ fission distribution was determined by all three methods. In all cases where more than one type of measurement was made, the agreement between methods was excellent. In some cases, the calculated distribution is shown along with the experimental values. Where two calculated curves are shown, they correspond to two different cross-section sets, as will be discussed in Section VII. Except for the fission ratios, all data have been normalized to unity at the core center.

During these measurements, the reactor flux was maintained at a constant level by an on-line computer technique described by Cohn.[7-9] Counters were introduced into the assembly through a 1.290-cm-diam voided aluminum tube at the core midplane.

## A. Reaction Rates in Assembly No. 7

The $U^{238}$ and $U^{235}$ fission-rate distribution for Assembly No. 7 is shown in Figs. 18 and 19, respectively, and their ratio in Fig. 20. Foils (results shown as small squares in the figures) were 5 mils thick, with from 1/2 to 10 $cm^2$ cross-sectional area, and were arranged in an east-west direction at the core midplane. After activation, the $Mo^{99}$ was chemically separated and absolutely counted. Typical of all foils, the pair at the center weighed 0.1454 g (depleted uranium) and 0.4467 g (enriched foil) and had $1.38 \times 10^{10}$ and $2.47 \times 10^{11}$ fissions/g, respectively, for a fission ratio of 0.05125. Estimated errors range from 3 to 10%.

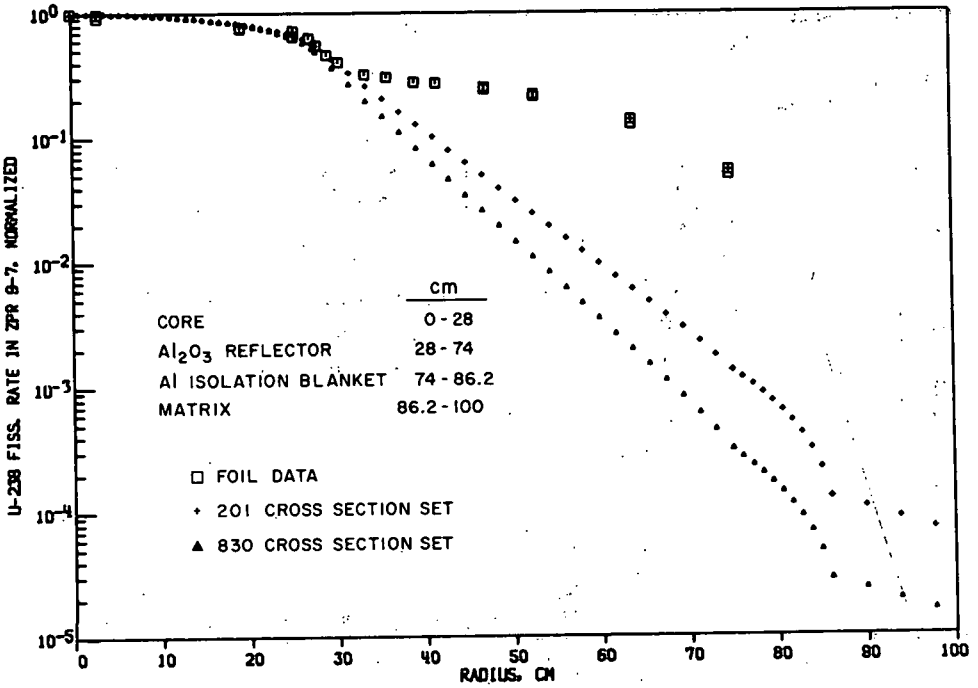


112-7802

Fig. 18. $U^{238}$ Reaction-rate Traverse in Assembly No. 7

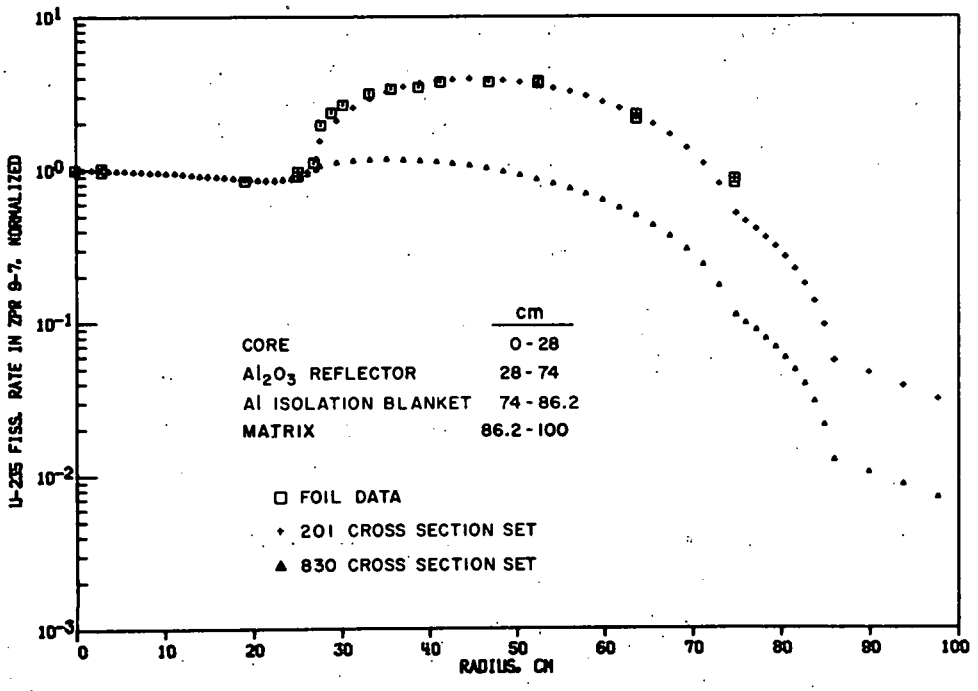


112-7806

Fig. 19. $U^{235}$ Reaction-rate Traverse in Assembly No. 7

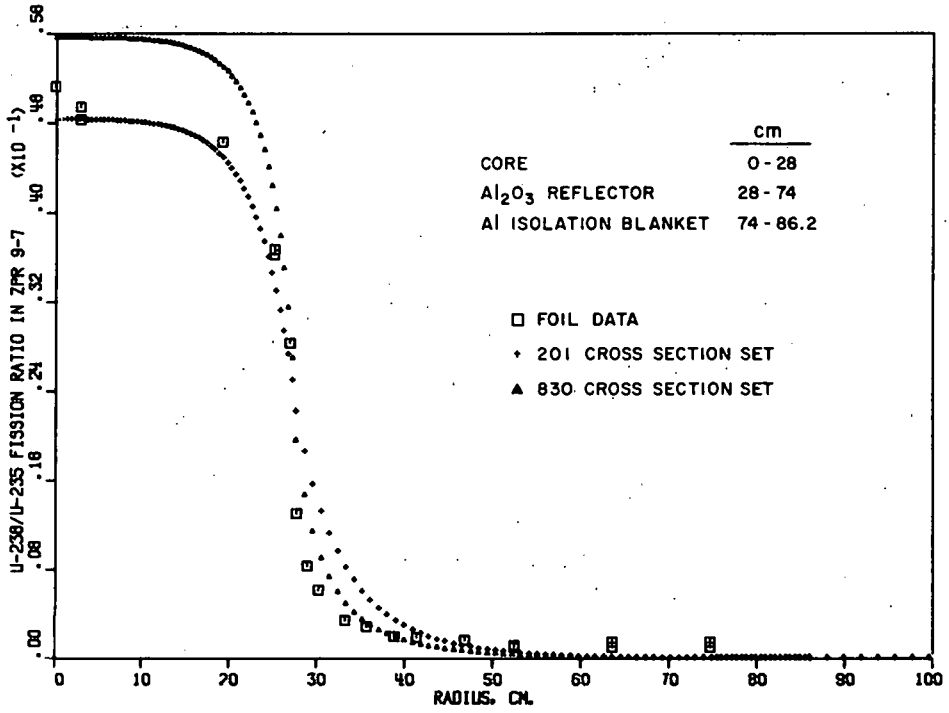


Fig. 20. $U^{238}/U^{235}$ Fission Ratio in Assembly No. 7

The solid-state counters (results shown as squares in the figures) were traversed through the void tube located vertically at the core midplane. The measured and calculated distributions for $U^{233}$, $U^{234}$, and $U^{236}$, as well as for $Np^{237}$, $Pu^{239}$, and $B^{10}$, are shown in Figs. 21 through 26, respectively. The regions in the core, the type of detector used for the measurements, and the cross-section set used in the calculations are indicated on each figure.

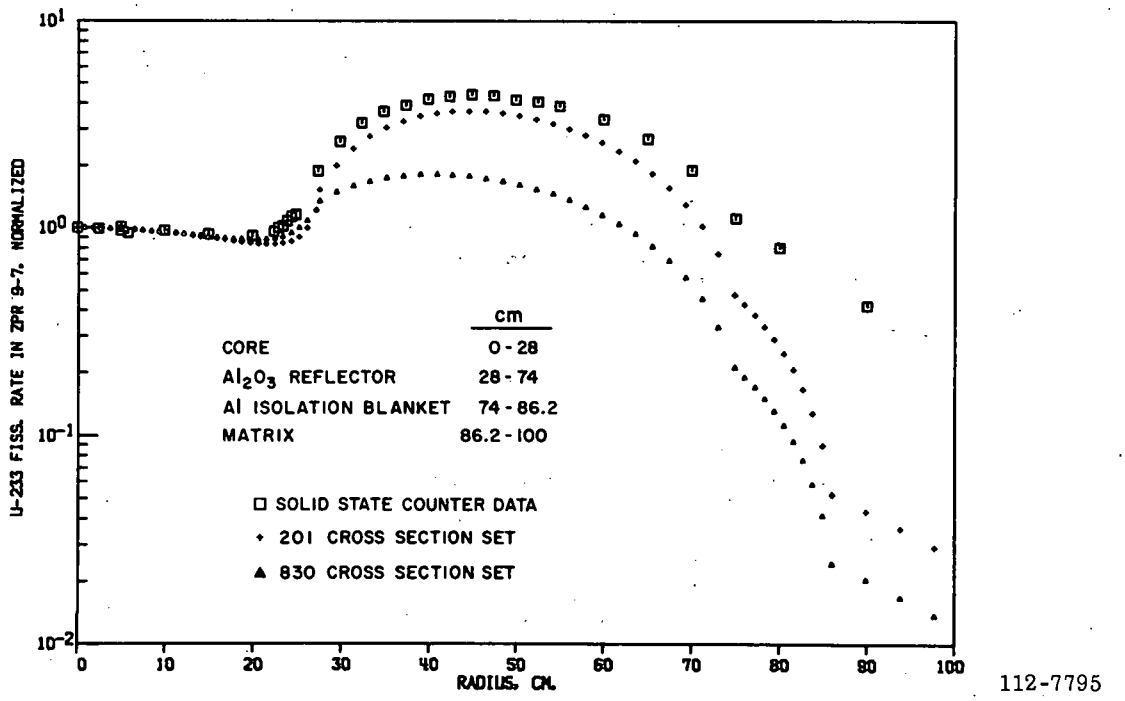


Fig. 21. $U^{233}$ Reaction-rate Traverse in Assembly No. 7

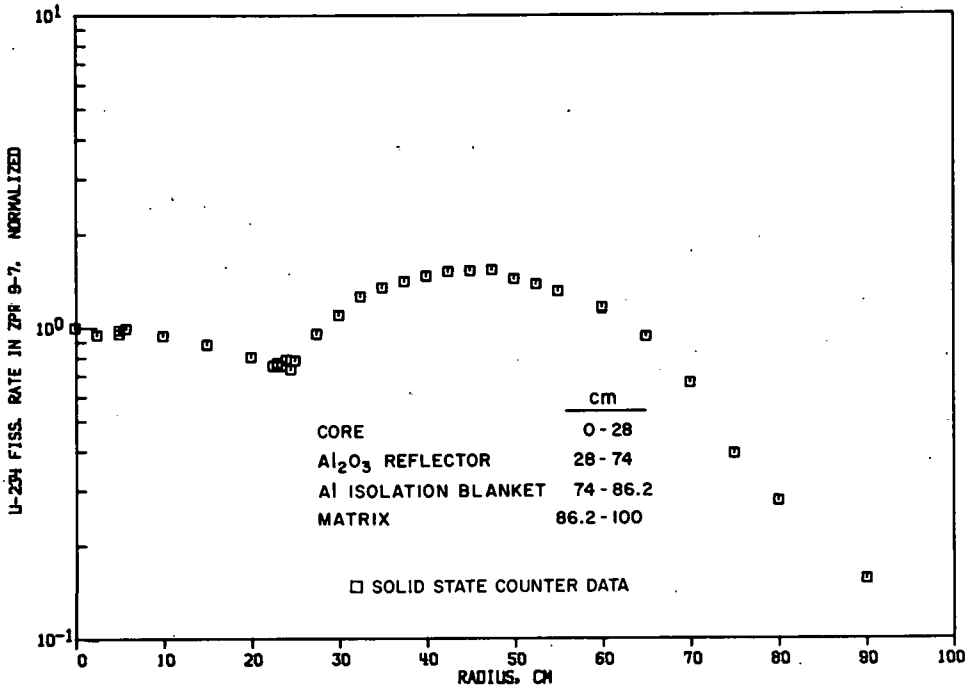


112-7797

Fig. 22. $U^{234}$ Reaction-rate Traverse in Assembly No. 7

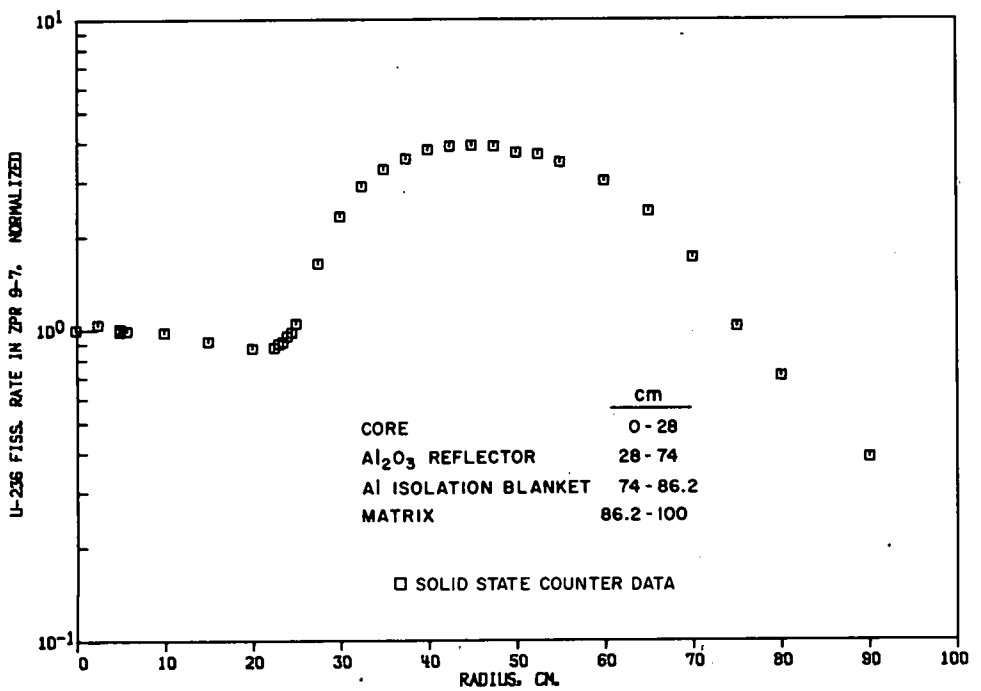


112-7801

Fig. 23. $U^{236}$ Reaction-rate Traverse in Assembly No. 7

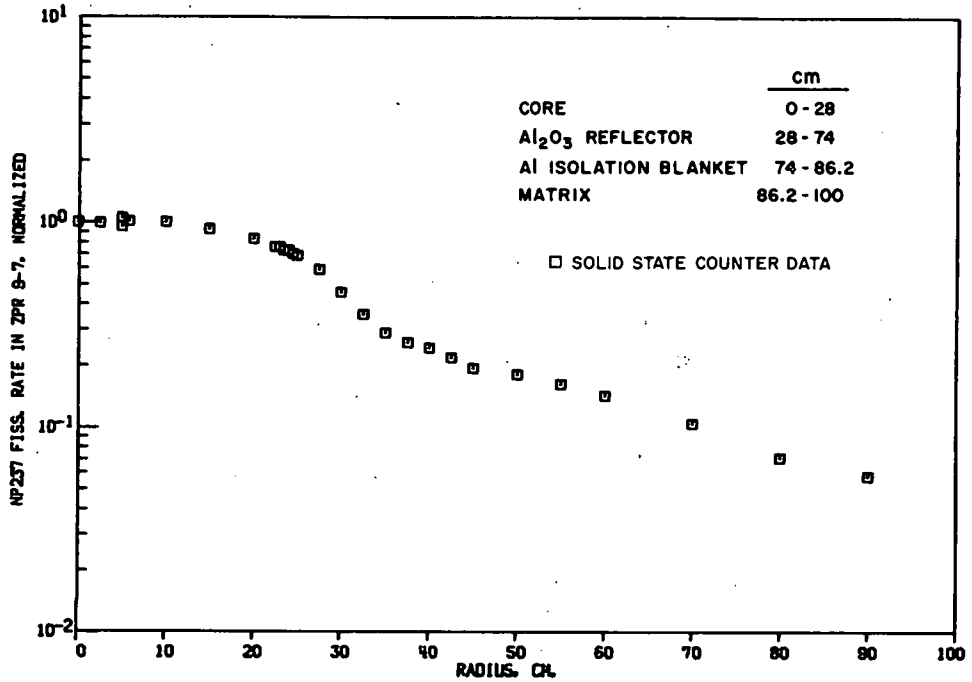


112-7799

Fig. 24. $Np^{237}$ Reaction-rate Traverse in Assembly No. 7

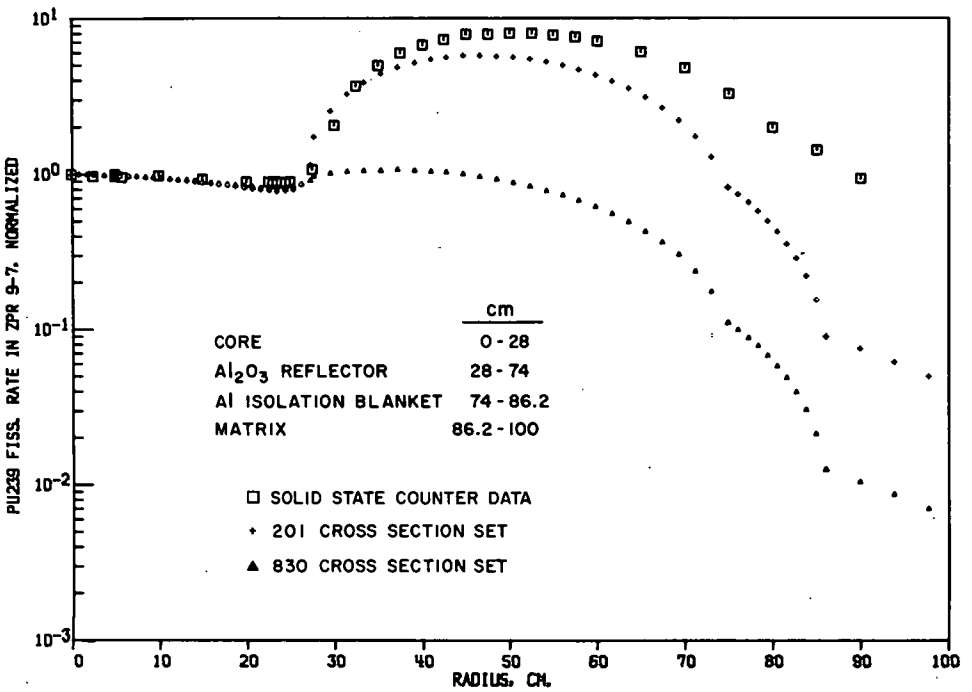


112-7790

Fig. 25. $Pu^{239}$ Reaction-rate Traverse in Assembly No. 7

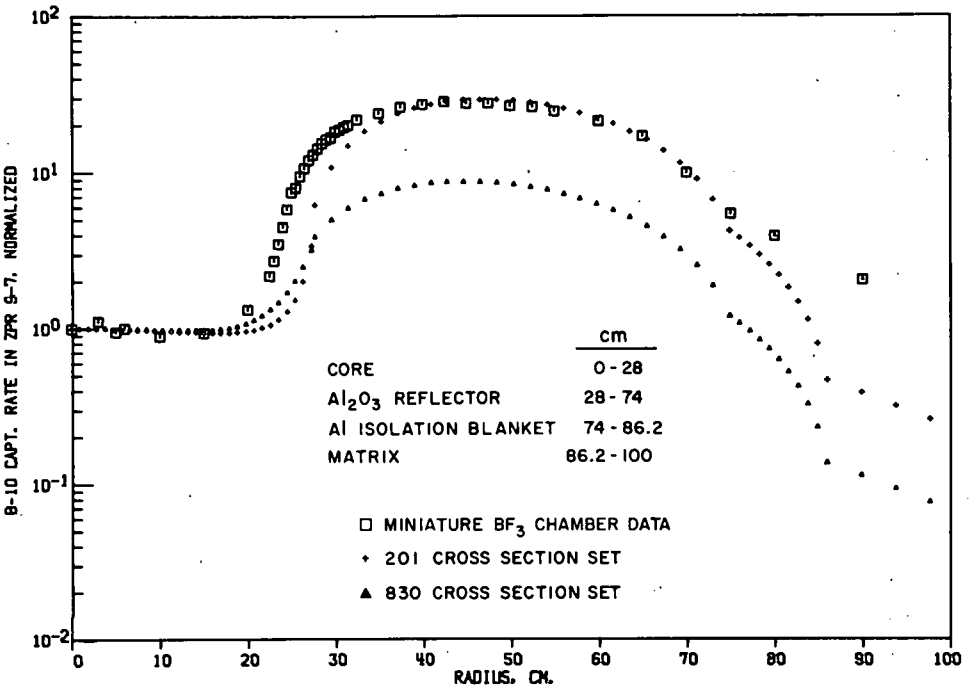


Fig. 26. $B^{10}$ Reaction-rate Traverse in Assembly No. 7

## B. Assembly No. 7C

Figures 27 and 28 show the $U^{238}$ and $U^{235}$ fission reaction rates as determined for Assembly No. 7C by the solid-state counters. Since no foils were irradiated in this assembly, the fission ratio was not determined. Figures 29-33 show other uranium isotopes as well as $Np^{237}$ and $Pu^{239}$ fission distributions. Figure 34 shows the $B^{10}$ distribution.

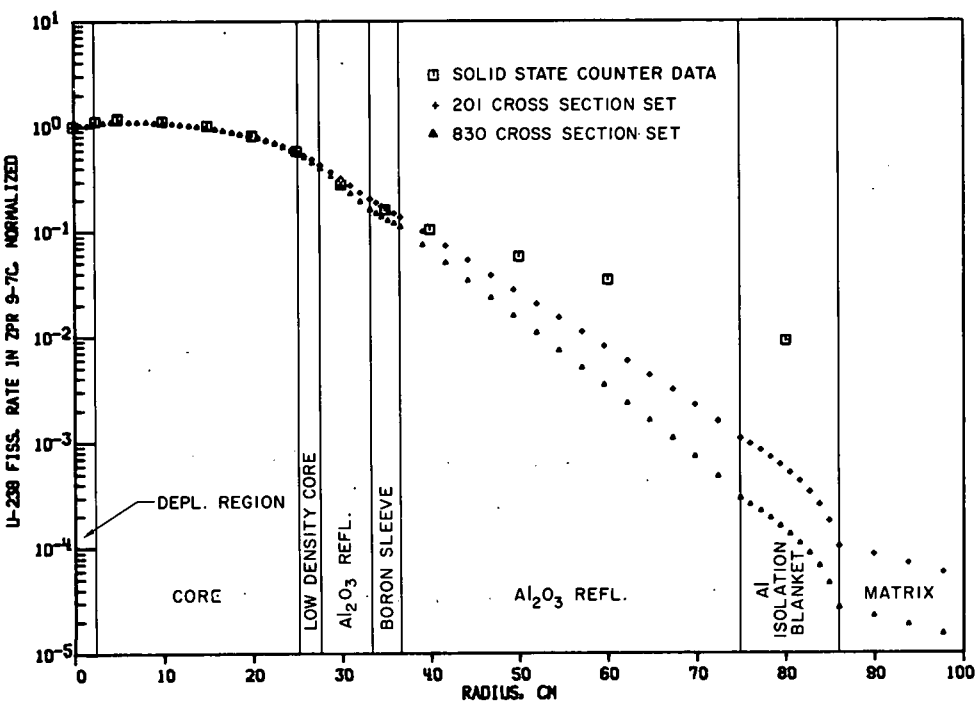


Fig. 27. $U^{238}$ Fission Ratio in Assembly No. 7C

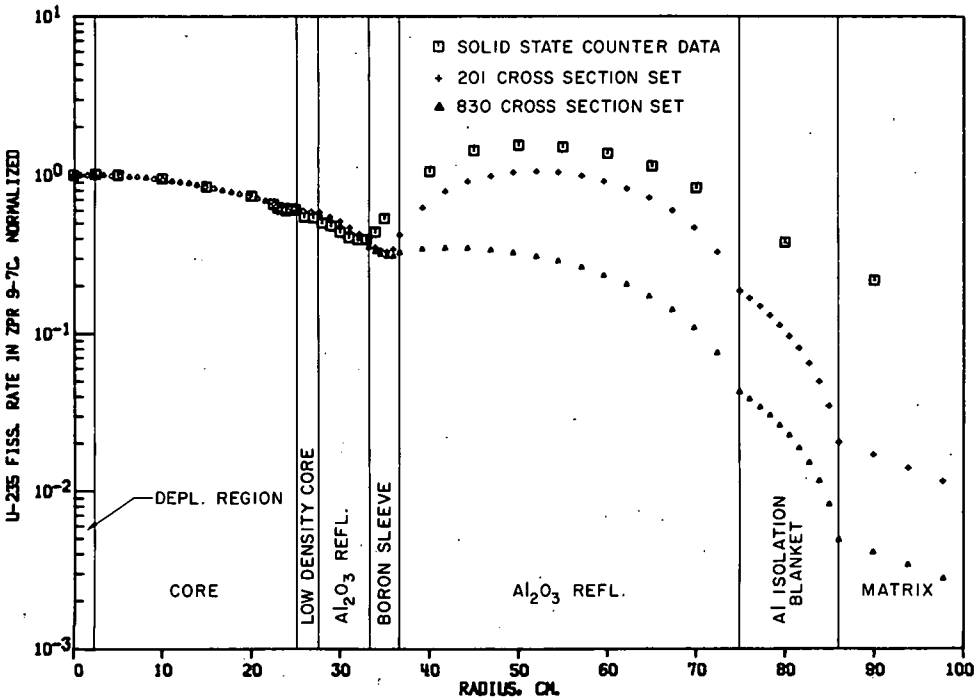


112-7935

Fig. 28. $U^{235}$ Reaction-rate Traverse in Assembly No. 7C

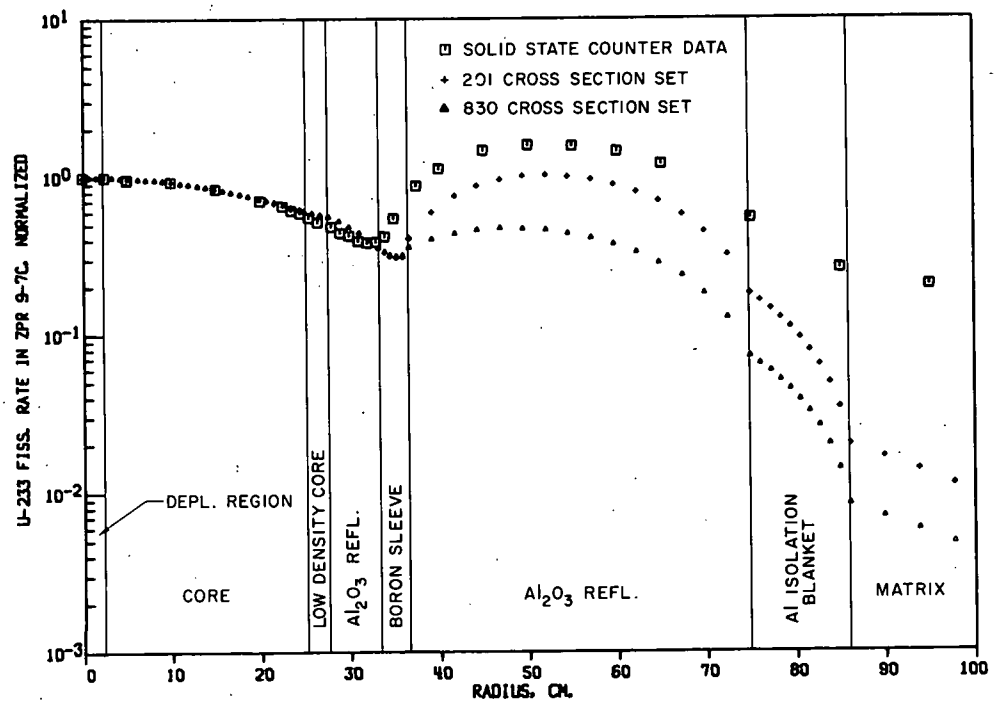


112-7930

Fig. 29. $U^{233}$ Reaction-rate Traverse in Assembly No. 7C

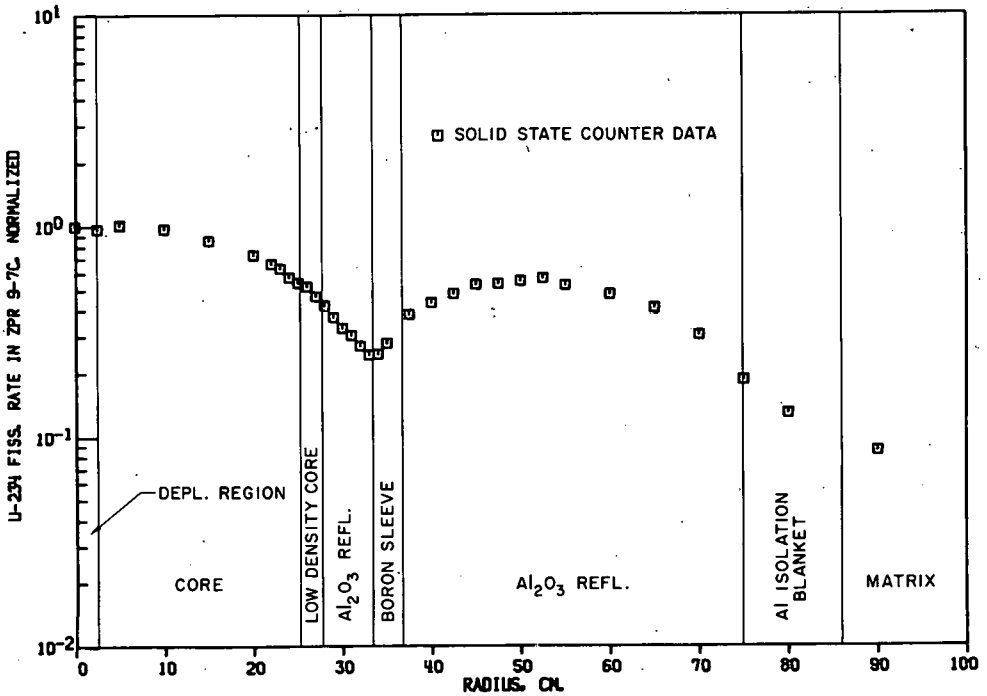


Fig. 30. $U^{234}$ Reaction-rate Traverse in Assembly No. 7C

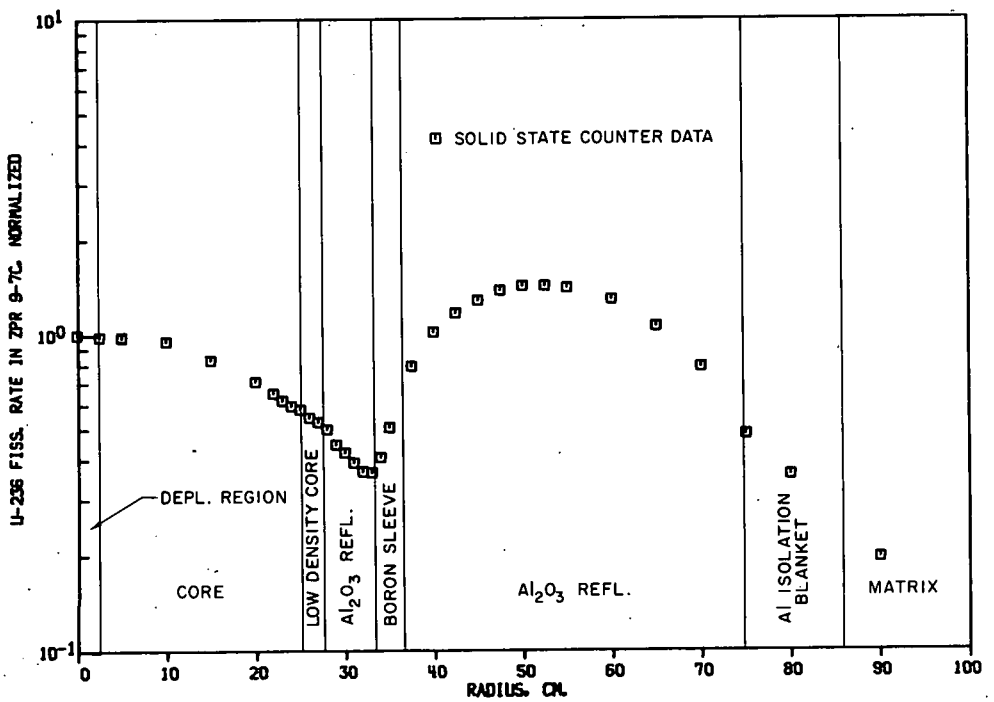


Fig. 31. $U^{236}$ Reaction-rate Traverse in Assembly No. 7C

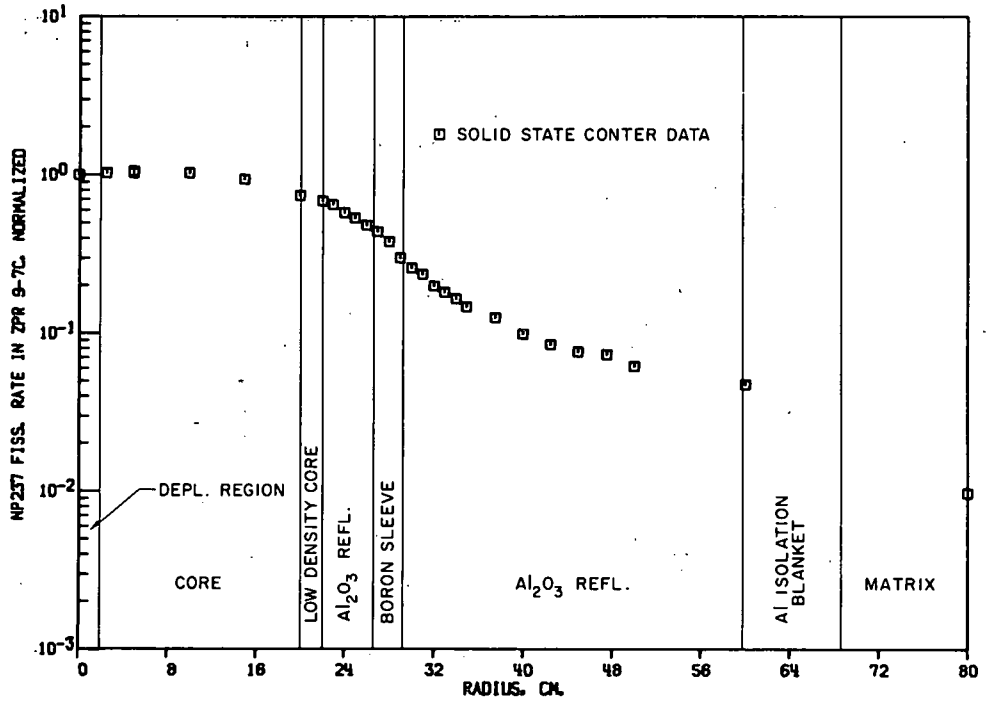


112-7933

Fig. 32. $Np^{237}$ Reaction-rate Traverse in Assembly No. 7C

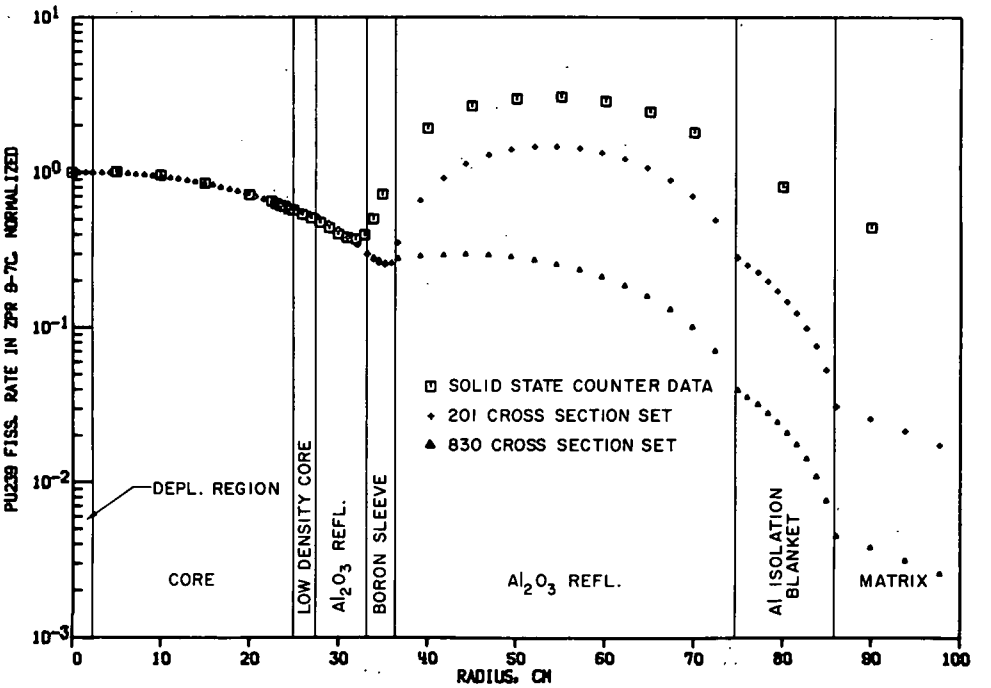


112-7937

Fig. 33. $Pu^{239}$ Reaction-rate Traverse in Assembly No. 7C

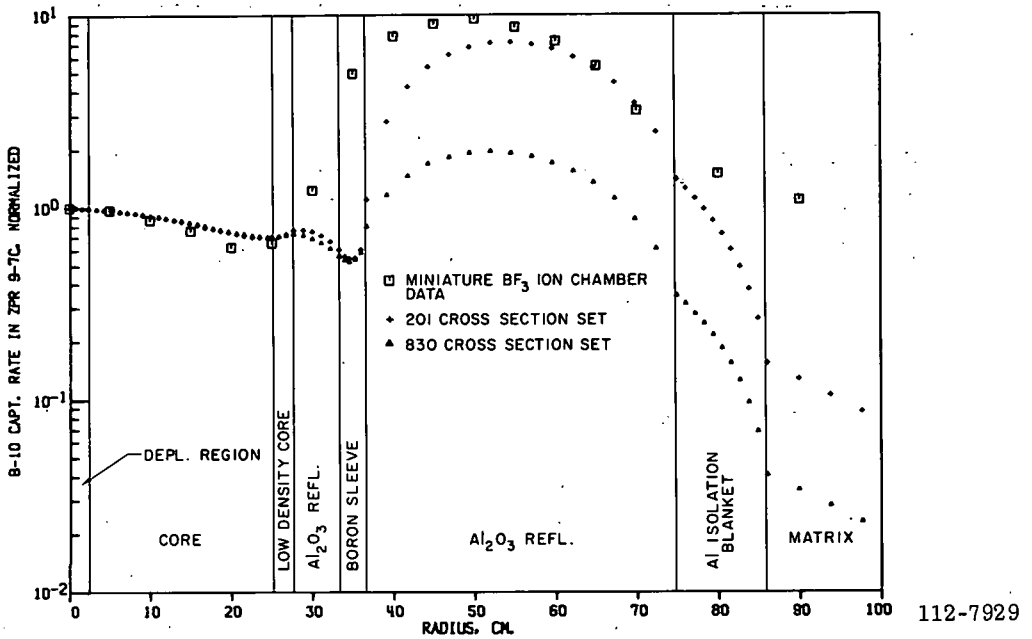


Fig. 34. $B^{10}$ Reaction-rate Traverse in Assembly No. 7C

## C. Assembly No. 8

Because of time limitations in the Assembly No. 8 studies, only the $U^{238}$, $U^{235}$, and $B^{10}$ reaction-rate distributions were determined. These are shown in Figs. 35-37, respectively. The $U^{238}$-to-$U^{235}$ fission ratio is shown in Fig. 38. Only the solid-state counter data are shown in Fig. 36; two sets of foil data (set 1 traversed in a vertical direction, set 2 horizontally) are shown for the $U^{238}$ distributions.

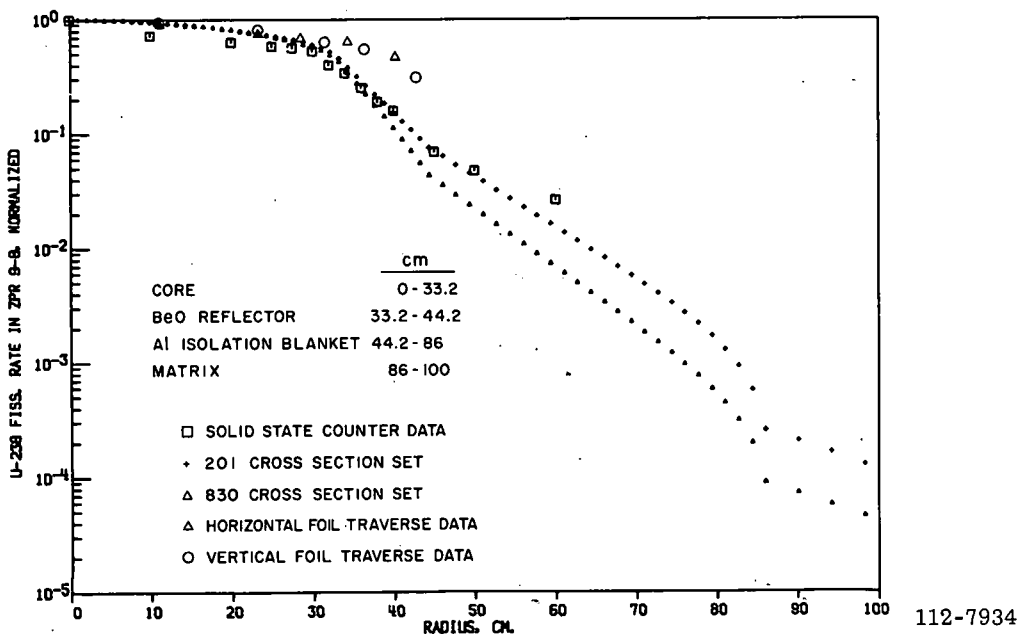


Fig. 35. $U^{238}$ Reaction-rate Traverse in Assembly No. 8

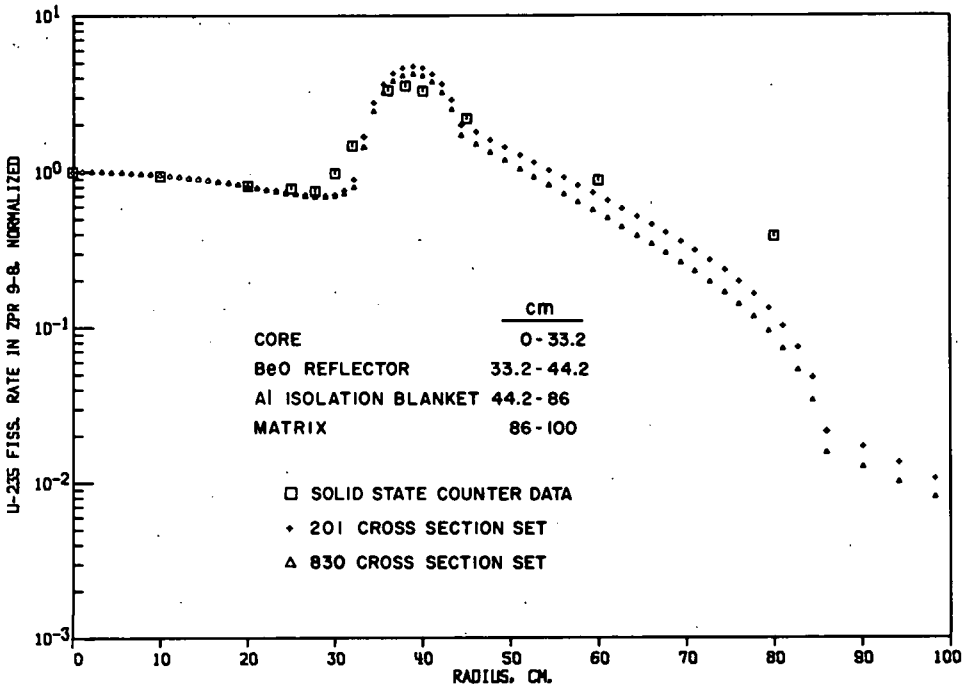


112-7792

Fig. 36. $U^{235}$ Reaction-rate Traverse in Assembly No. 8

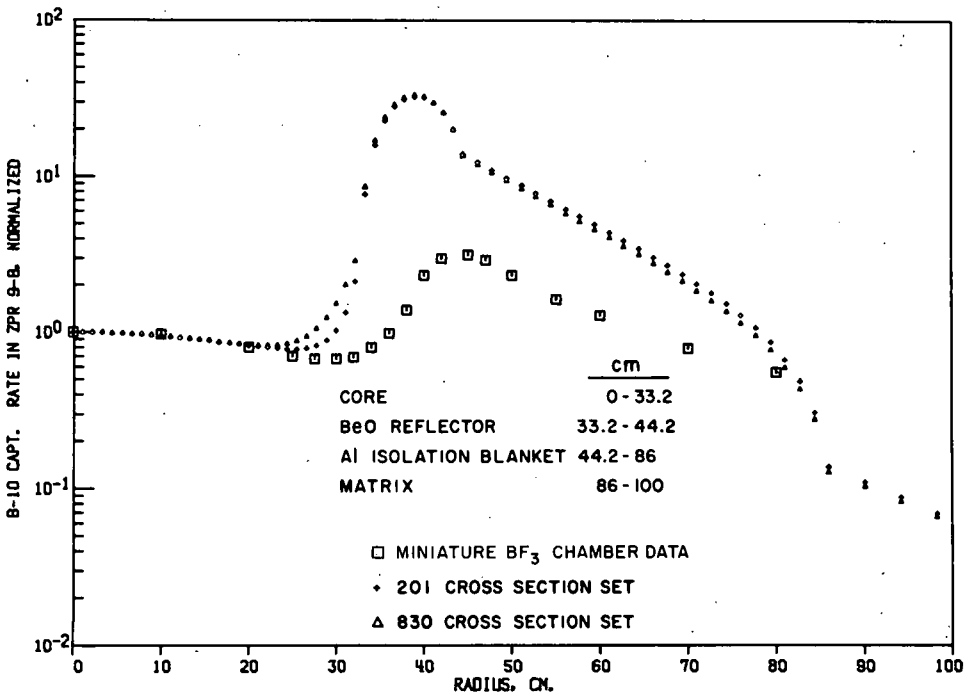


112-7787

Fig. 37. $B^{10}$ Capture Rate in Assembly No. 8

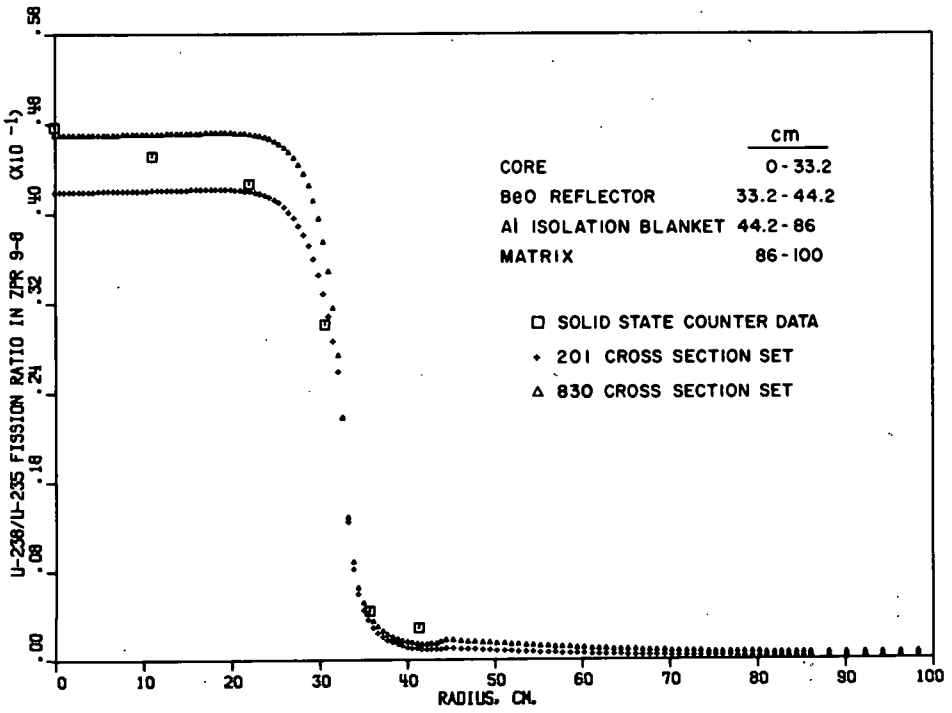


Fig. 38. $U^{238}/U^{235}$ Fission Ratio in Assembly No. 8

## D. Assembly No. 9

Figures 39 and 40 show the distribution for the $U^{238}$ and $U^{235}$ fission rates in Assembly No. 9, and Figs. 41-45 show the measured fission rates for the other uranium isotopes as well as $Np^{237}$ and $Pu^{239}$. Figure 46 gives the measured $B^{10}$ reaction rate.

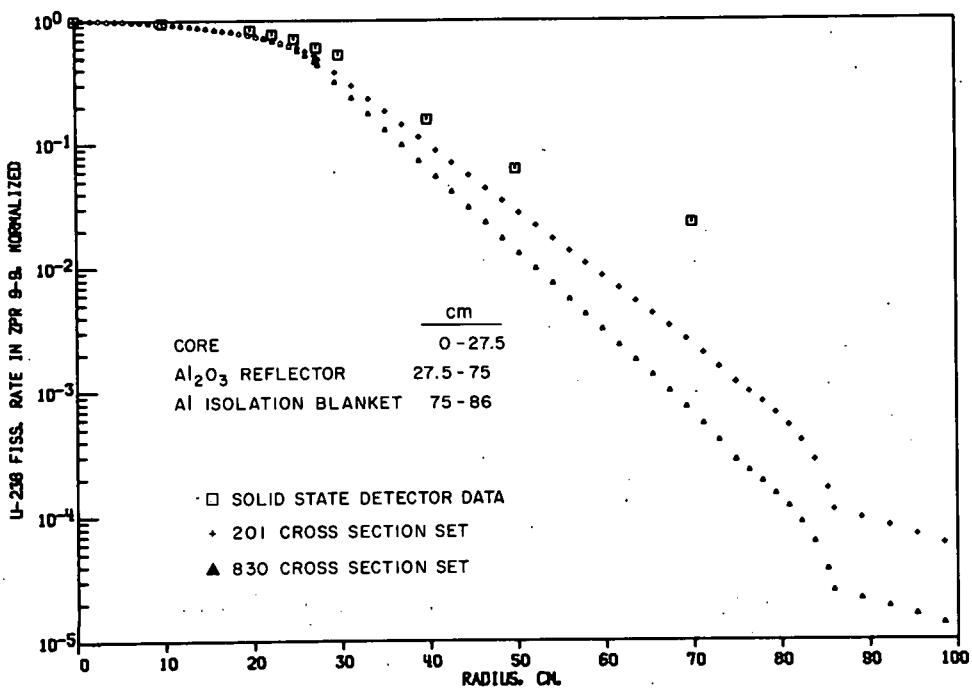


Fig. 39. $U^{238}$ Reaction-rate Traverse in Assembly No. 9

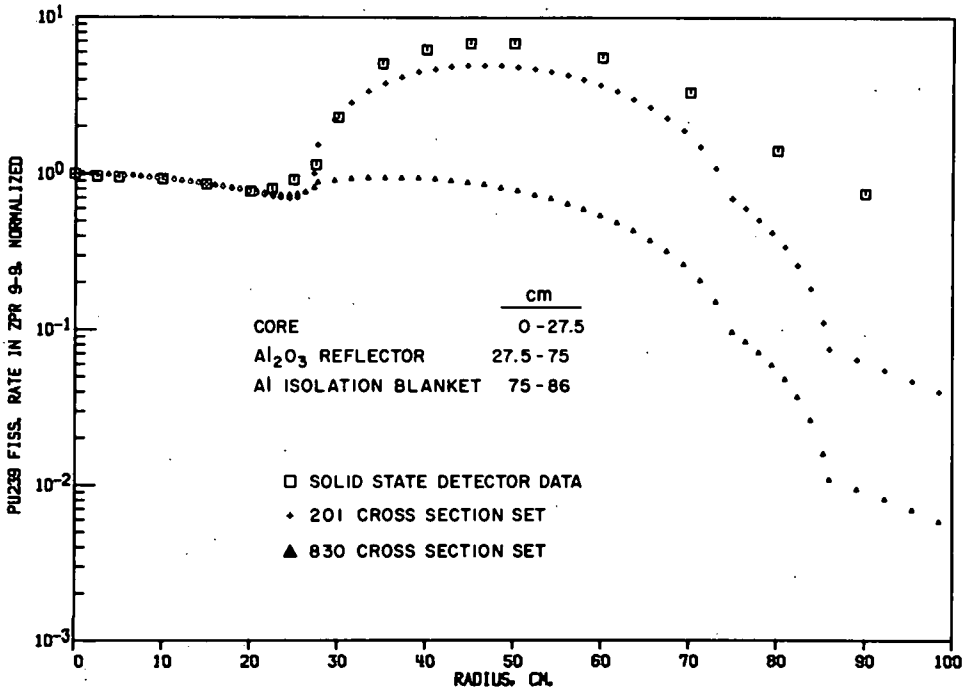


112-7788

Fig. 40. $U^{235}$ Reaction-rate Traverse in Assembly No. 9

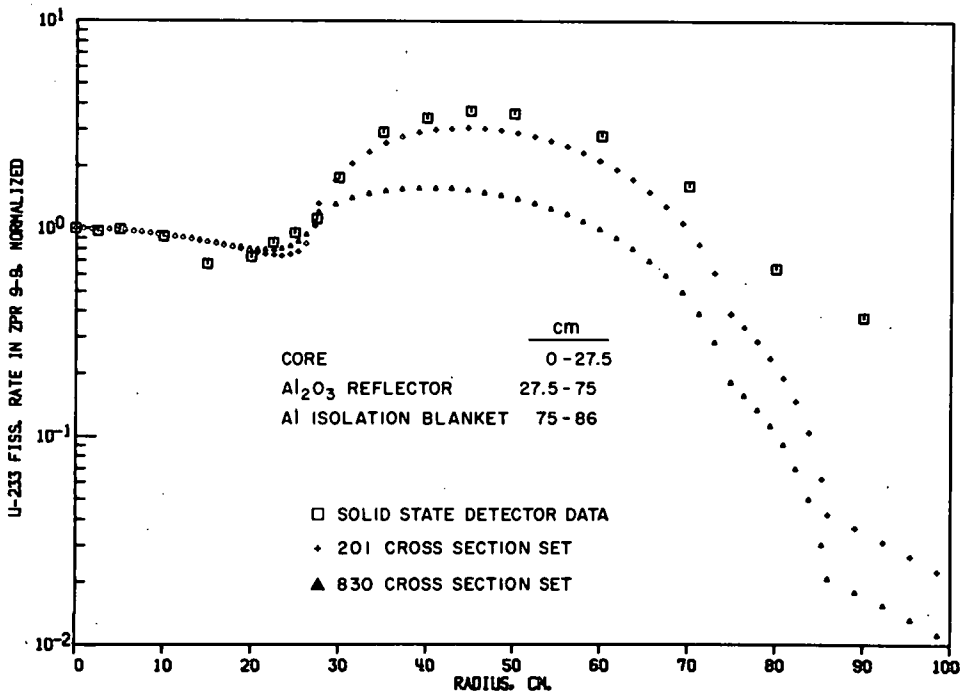


112-7798

Fig. 41. $U^{233}$ Reaction-rate Traverse in Assembly No. 9

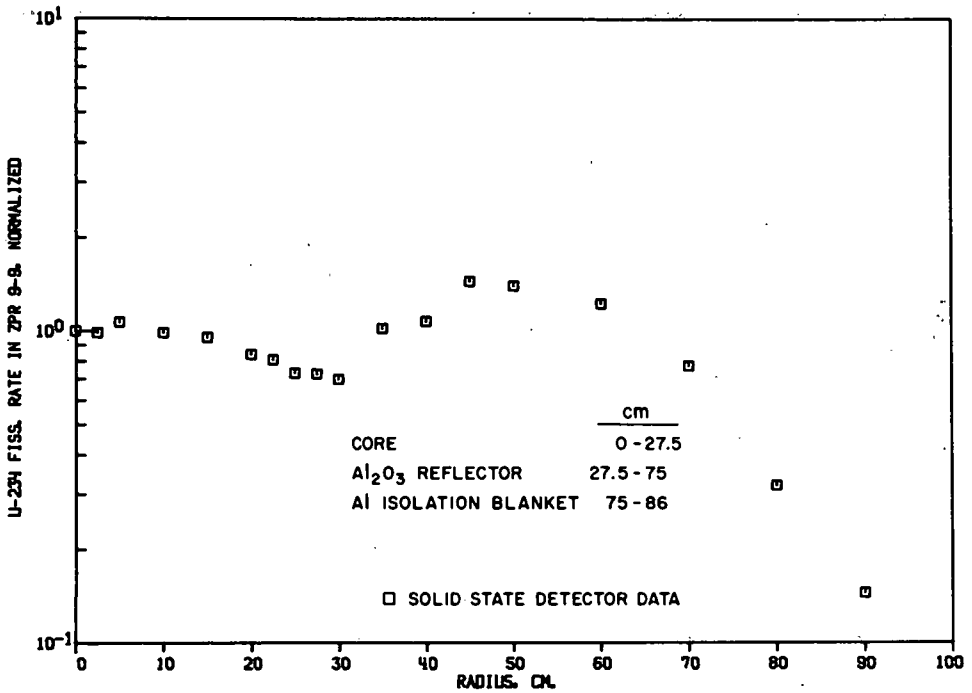


112-7796

Fig. 42. $U^{234}$ Reaction-rate Traverse in Assembly No. 9

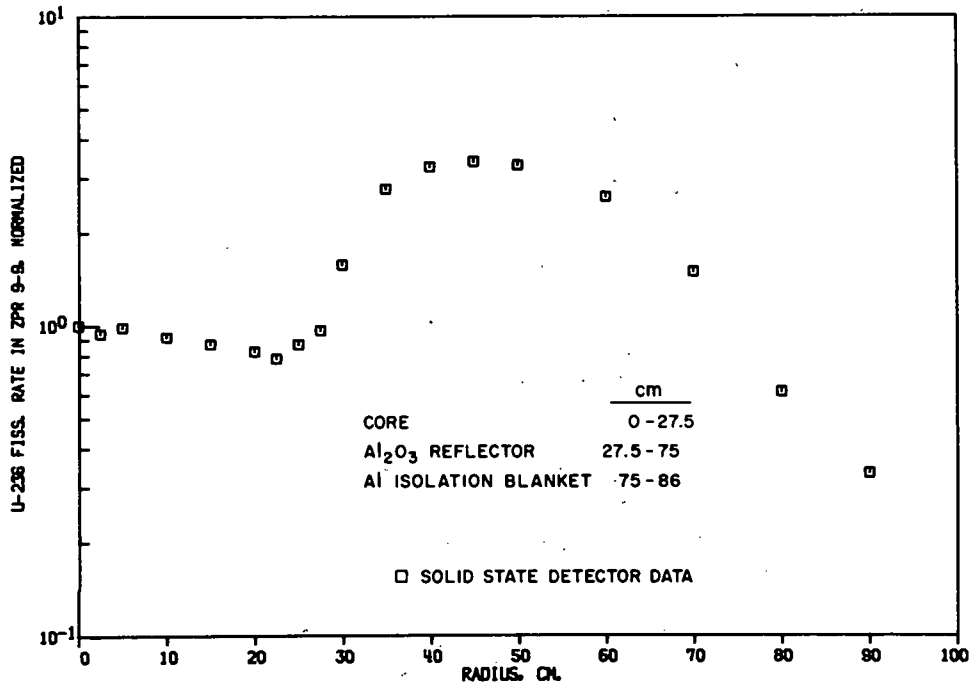


112-7804

Fig. 43. $U^{236}$ Reaction-rate Traverse in Assembly No. 9

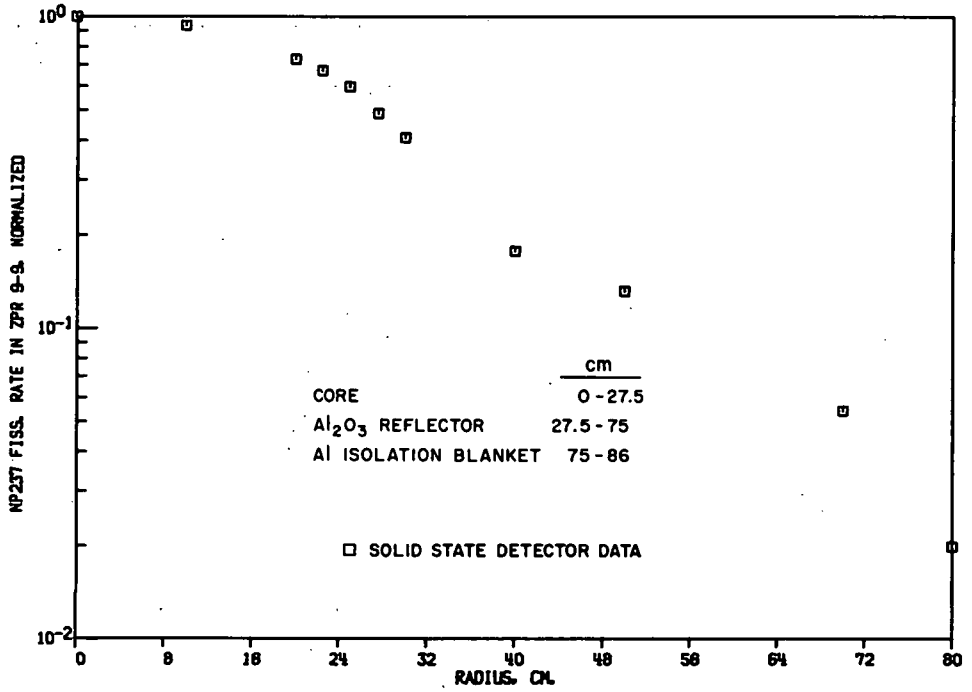


112-7805

Fig. 44. $Np^{237}$ Reaction-rate Traverse in Assembly No. 9

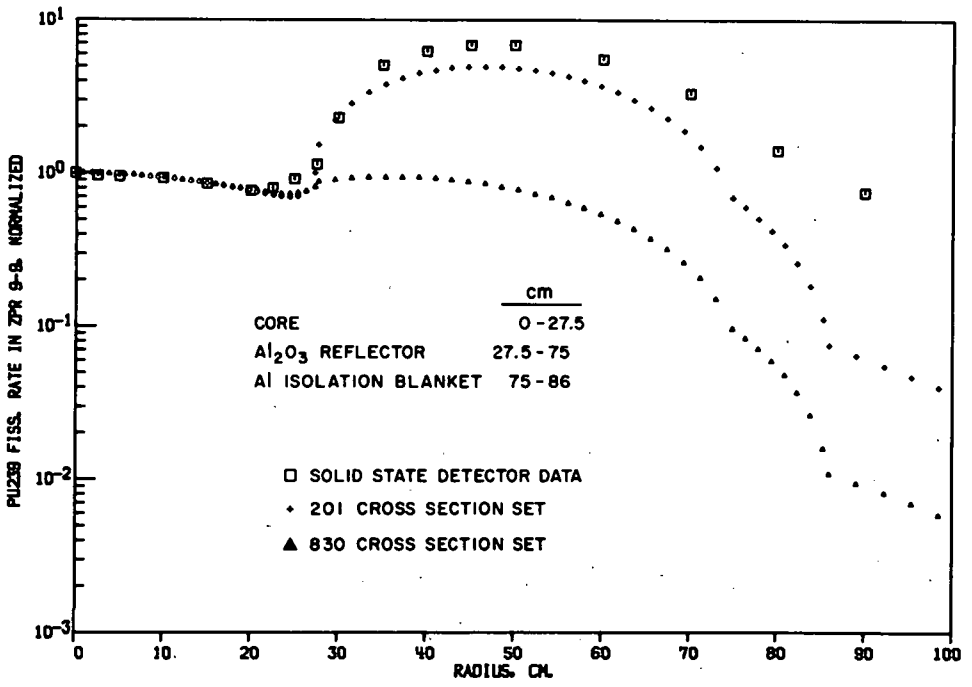


112-7791

Fig. 45. $Pu^{239}$ Reaction-rate Traverse in Assembly No. 9

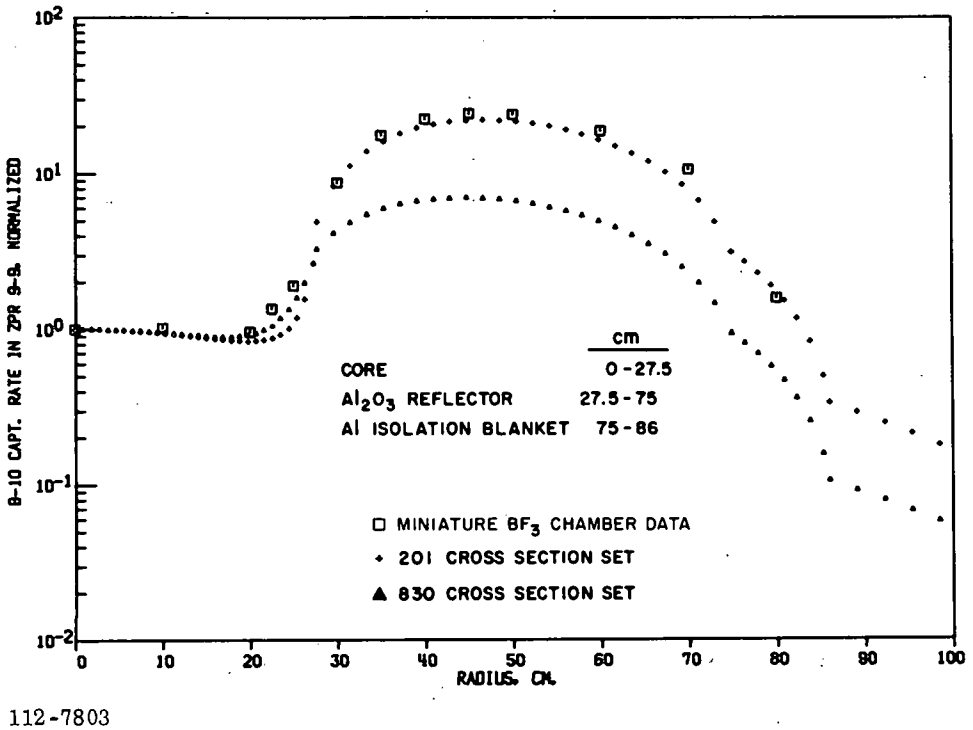


Fig. 46. $B^{10}$ Reaction-rate Traverse in Assembly No. 9

## E. Flux Distributions through an Outer Fuel Plate in Assembly No. 8

Although moderating reflector materials such as BeO have advantages in terms of increased control margin, they can also produce a serious power spike at the core edge. An optimum thickness would trade off control margin for a flat power distribution across the core.

The 11-cm thickness of BeO as the reflector on Assembly No. 8 was thicker than optimum and provided an opportunity to test the ability to calculate the power distribution in the core-reflector interface region.

The fission rate was measured through the outer fuel plate of the core by replacing a 1/2-in.-sq section of the fuel plate by a 1/2-in.-sq stack of twelve 0.005-in.-thick $U^{235}$ foils wrapped in aluminum foil. Two such measurements were made. In the first, shown in Fig. 47, there was a 1/8-in.-thick column of 45% density aluminum plus a 1/8-in.-thick column of $Al_2O_3$ between the last fuel plate and the BeO. In the second measurement, shown in Fig. 48, tungsten replaced the $Al_2O_3$ column. Since the scales to make these plots were selected by the computer, the magnitude of the differences between the two conditions is not immediately obvious. The full-scale drawing at the top of each figure shows the relative locations of the various materials.

The calculated values are the results of a one-dimensional transport calculation using shielded (lowest calculated values) and non-self-shielded cross sections for the $U^{235}$. The 20% difference between measurement and theory is somewhat larger than was expected.

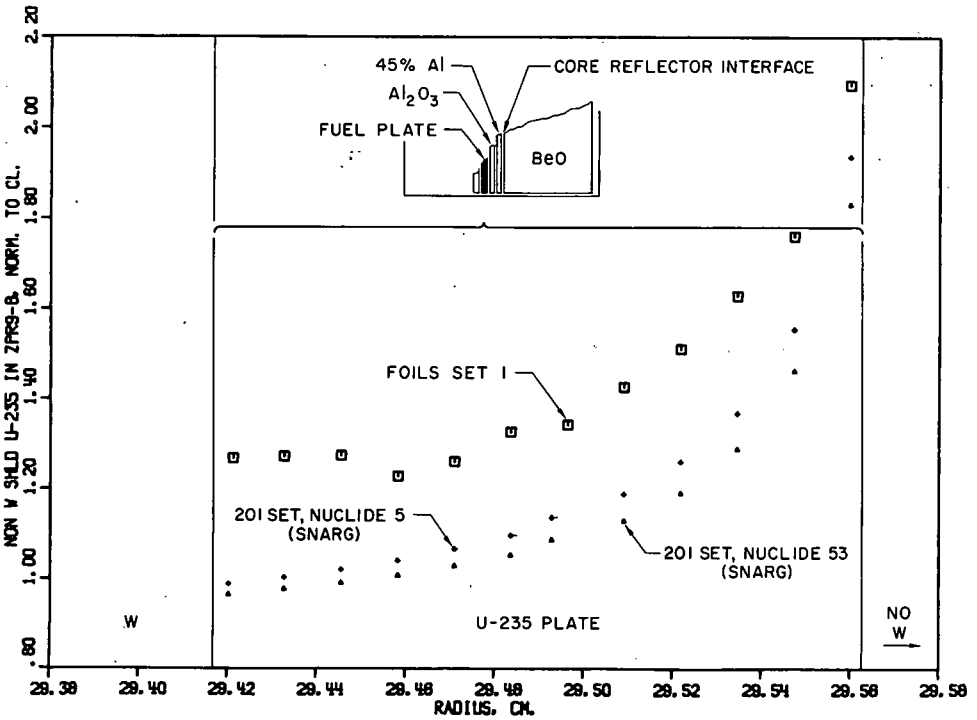


112-7714 Rev. 1

Fig. 47. Microscopic $U^{235}$ Reaction-rate Traverse without Tungsten

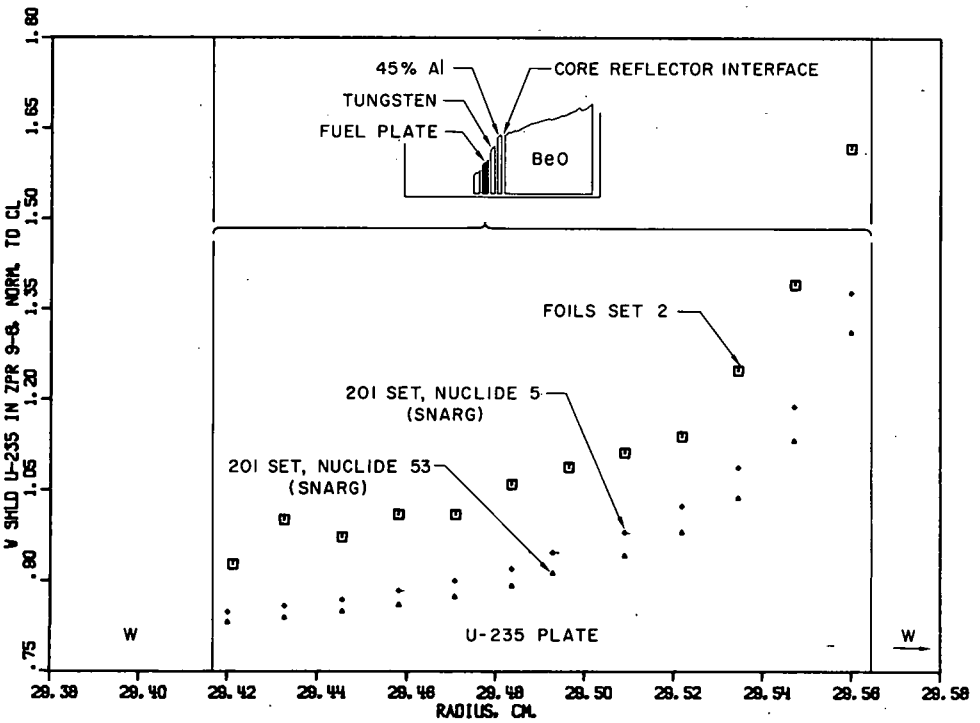


112-7715 Rev. 1

Fig. 48. Microscopic $U^{235}$ Reaction-rate Traverse with Tungsten

# VI. THE SPATIALLY DEPENDENT REACTIVITY TRAVERSES

A comparison of the measured and calculated reaction rates at the positions inside the reactor can be useful in evaluating the accuracy with which the real flux spectrum can be calculated. Although not as straightforward, the comparison between the calculated and the measured reactivity effects at the various space points in the reactor can provide some useful information on the accuracy with which the adjoint spectrum can be calculated. However, the comparison is straightforward only in the center of the core, where the flux gradient is zero.

Small, but finite, reactivity effects were measured with the sampleless probe. This background effect was subtracted from each measurement with the sample. All measurements were made by the on-line computer technique discussed in more detail in Refs. 7-9.

The samples used in these measurements are described in the appendix.

Three mechanisms were used to move the sample through the core. Two used a "Slo-Syn" stepping motor and a gear train. Initial studies were made with the sample mounted on the end of a small aluminum rod, which was driven by the stepping motor. Since the background correction made necessary by the reactivity effect of the rod in the absence of a sample was large, this was replaced in later measurements by an aluminum bead chain. To eliminate reactivity effects due to the chain, it was made long enough to run through the entire diameter of the assembly, and the sample was attached to its midsection.

The third mechanism, designed to manipulate the heavy lead rods, consisted of a large d.c. motor used to unwind steel cable from a drum.

## A. Reactivity Distributions in Assembly No. 7

Figures 49-52 show the spatial distribution for the reactivity effects of small samples of $U^{235}$, polyethylene, $B^{10}$, and borated polyethylene, respectively, in Assembly No. 7. If the worth of carbon in the measurements with the polyethylene is assumed to be negligible, the data in Fig. 50 can be scaled up by a factor of about 7 (polyethylene consists of 14.3 w/o hydrogen) to obtain what would amount to the reactivity worths for pure hydrogen.

## B. Reactivity Distributions in Assembly No. 7C

Figures 53-56 show the measured reactivity distributions for $U^{235}$, polyethylene, $B^{10}$, and borated polyethylene, respectively, for Assembly No. 7C. These are the same samples used previously and are described in the appendix.

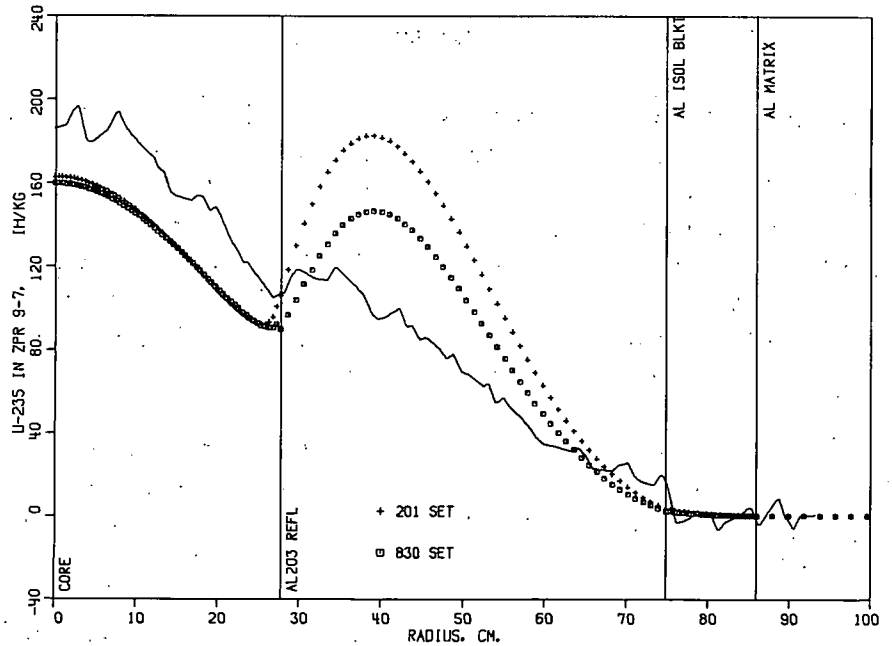


112-7724

Fig. 49. $U^{235}$ Reactivity Traverse in Assembly No. 7

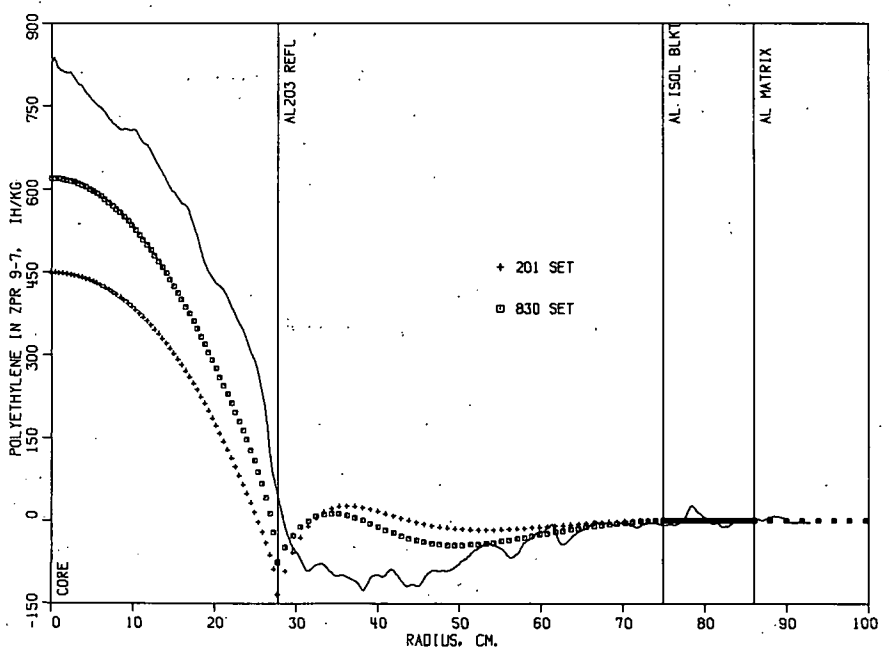


112-7713

Fig. 50. Polyethylene Reactivity Traverse in Assembly No. 7

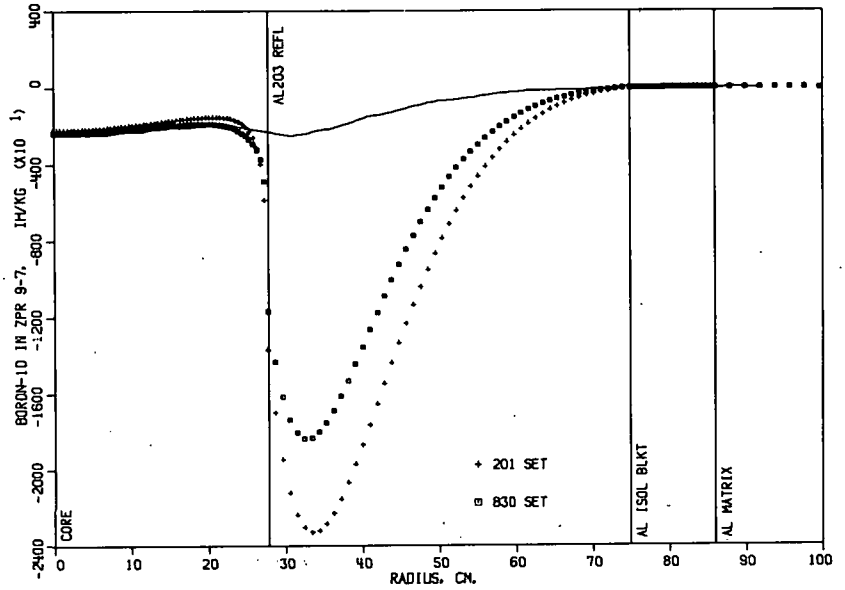


Fig. 51
$B^{10}$ Reactivity Traverse in Assembly No. 7

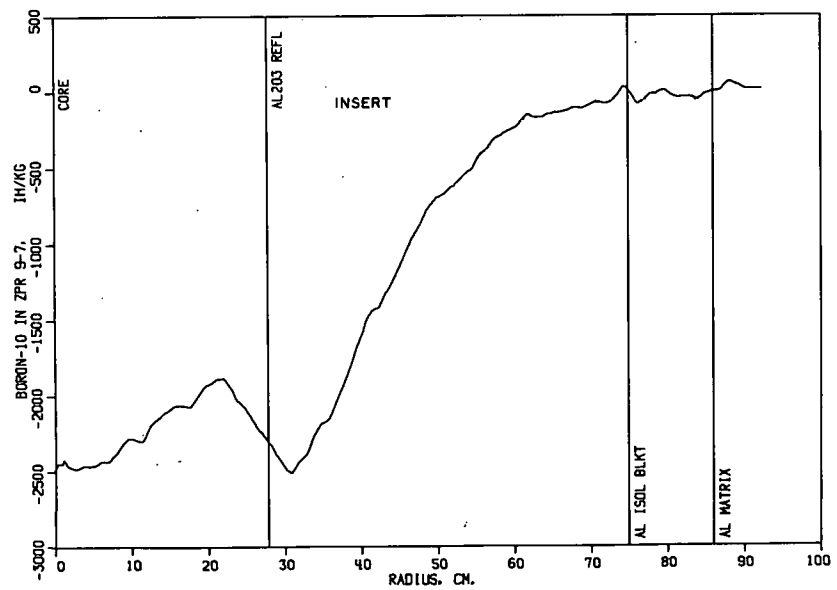


112-7925

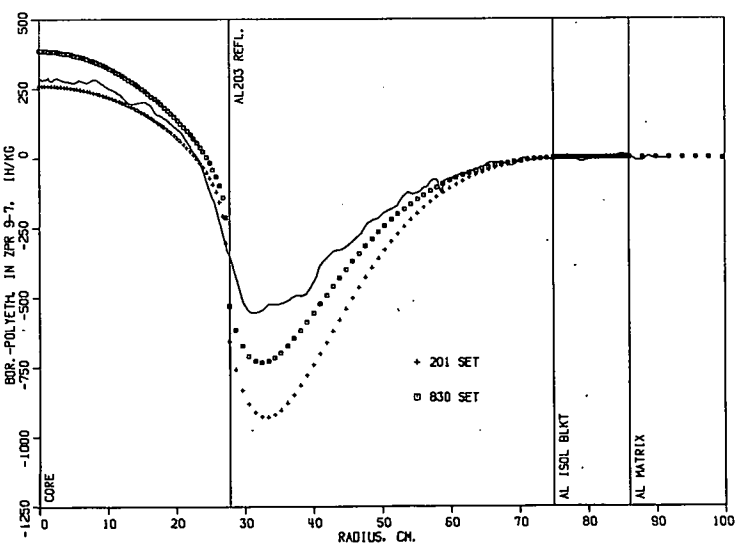


Fig. 52
Borated Polyethylene Reactivity Traverse in Assembly No. 7

112-7347

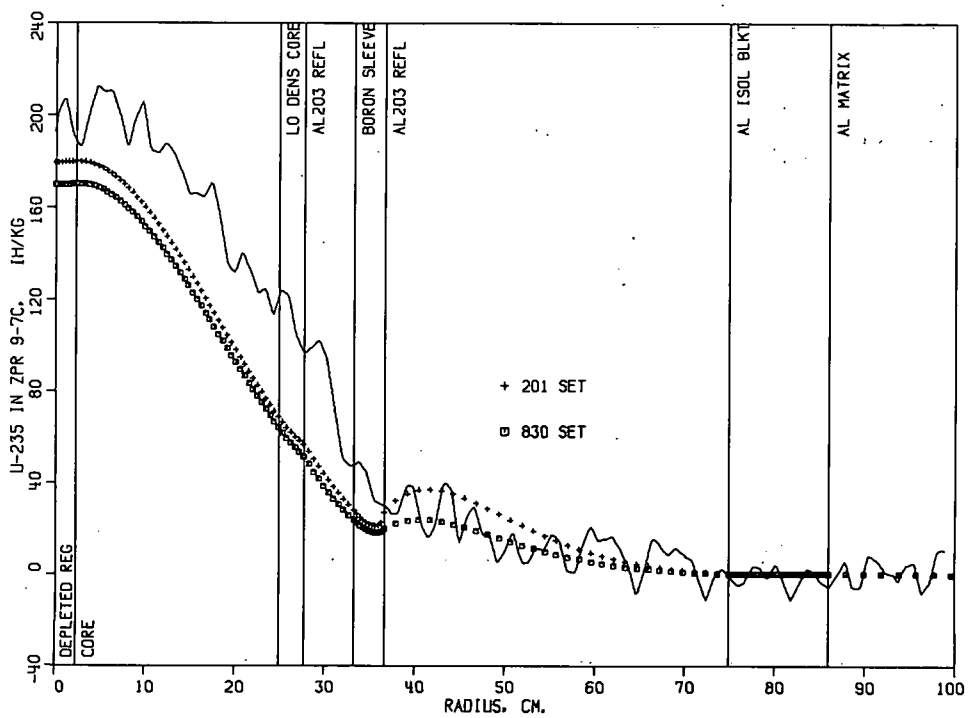


112-7720

Fig. 53. $U^{235}$ Reactivity Traverse in Assembly No. 7C

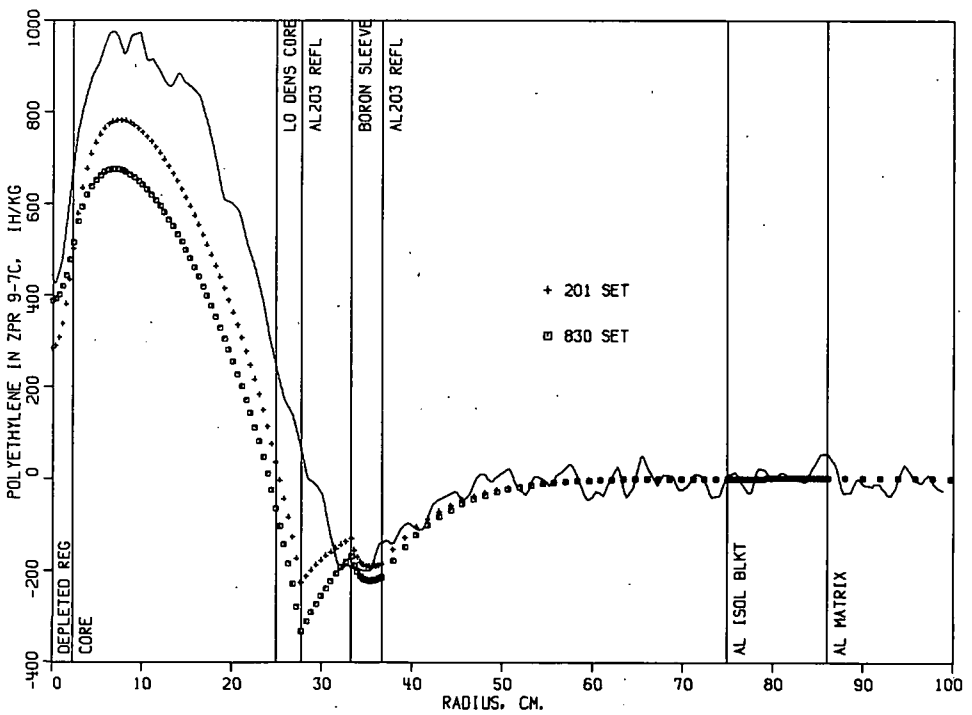


112-7706

Fig. 54. Polyethylene Reactivity Traverse in Assembly No. 7C

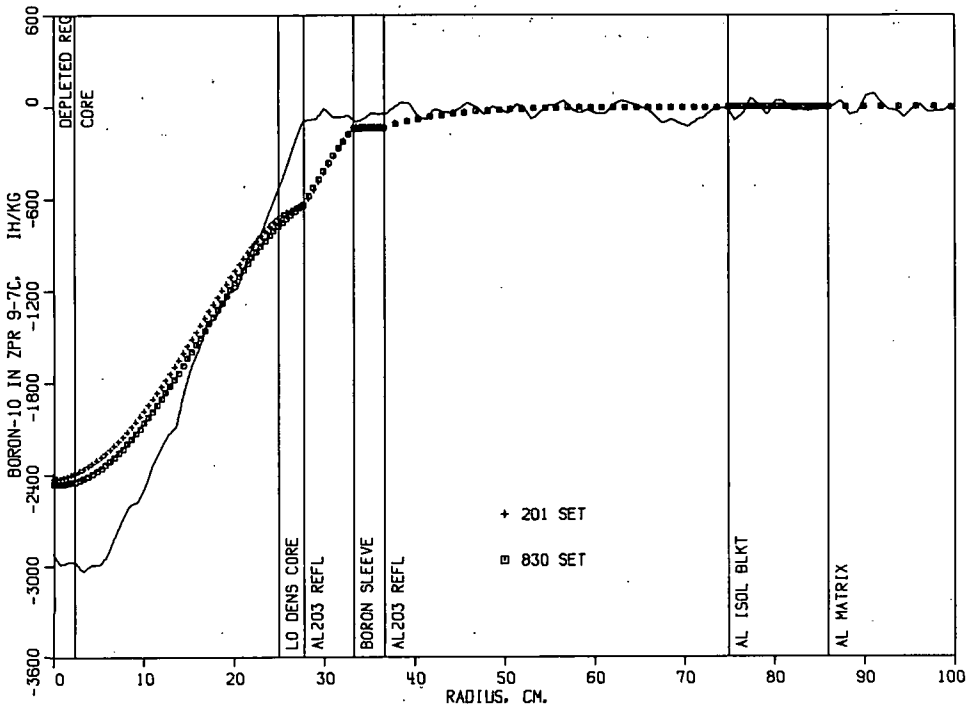


112-7726

Fig. 55. $B^{10}$ Reactivity Traverse in Assembly No. 7C

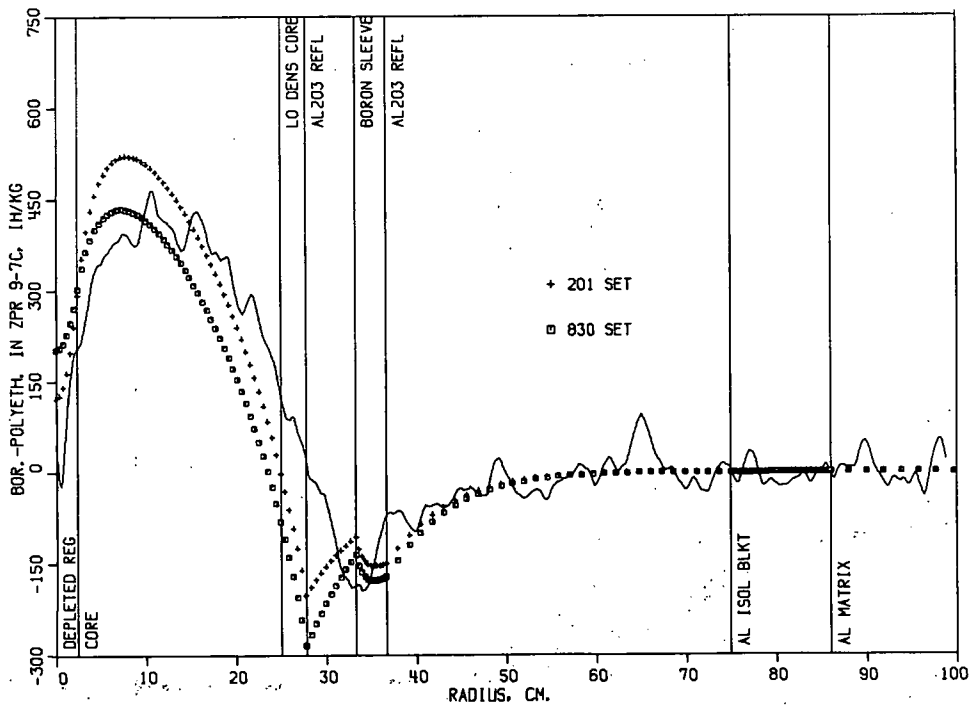


112-7348

Fig. 56. Borated Polyethylene Reactivity Traverse in Assembly No. 7C

## C. Reactivity Distributions in Assembly No. 8

Figures 57 and 58 show the measured spatial distributions for the reactivity effects of $U^{235}$ and polyethylene, respectively, for Assembly No. 8.

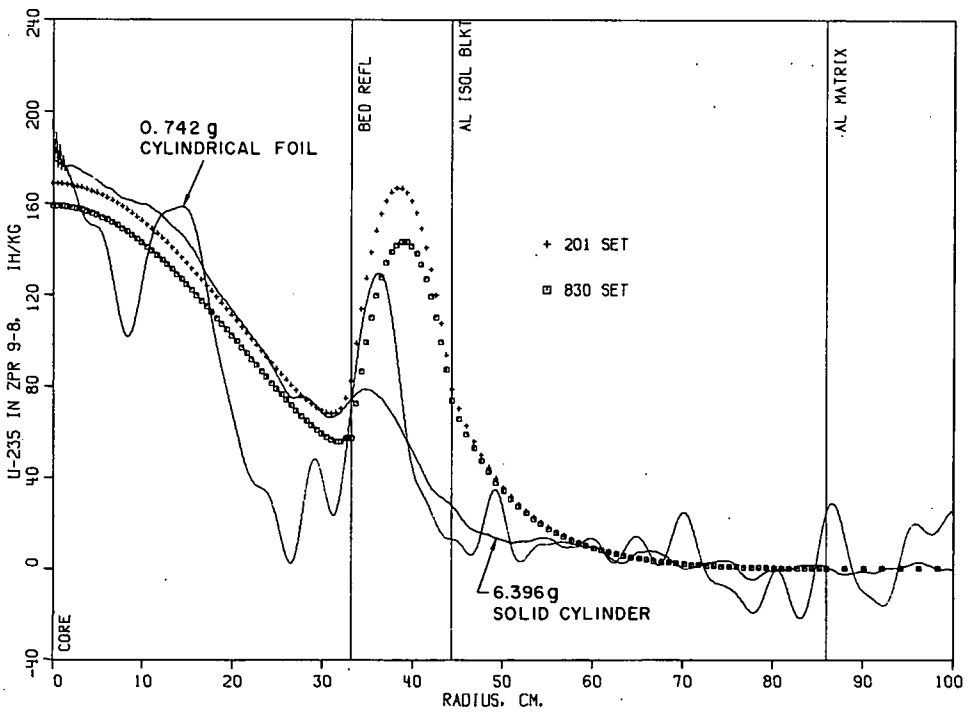


112-7729

Fig. 57. $U^{235}$ Reactivity Traverse in Assembly No. 8

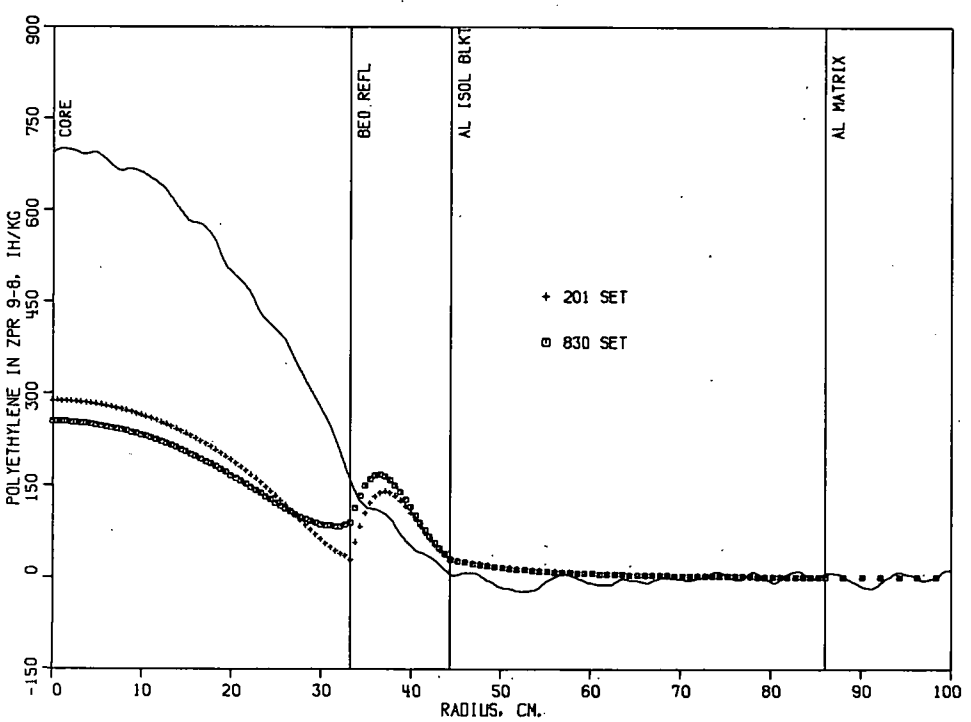


112-7730

Fig. 58. Polyethylene Reactivity Traverse in Assembly No. 8

Two different samples were used for the boron traverses. These are shown in Fig. 59, where significant sample-size effects can be observed. In addition to the traverses, the worth of a single can of $B^{10}$ (4.2 g of $B^{10}$) was mapped through the BeO reflector. These results, shown as the squares in Fig. 59, show a spatial dependence that is noticeably different than that

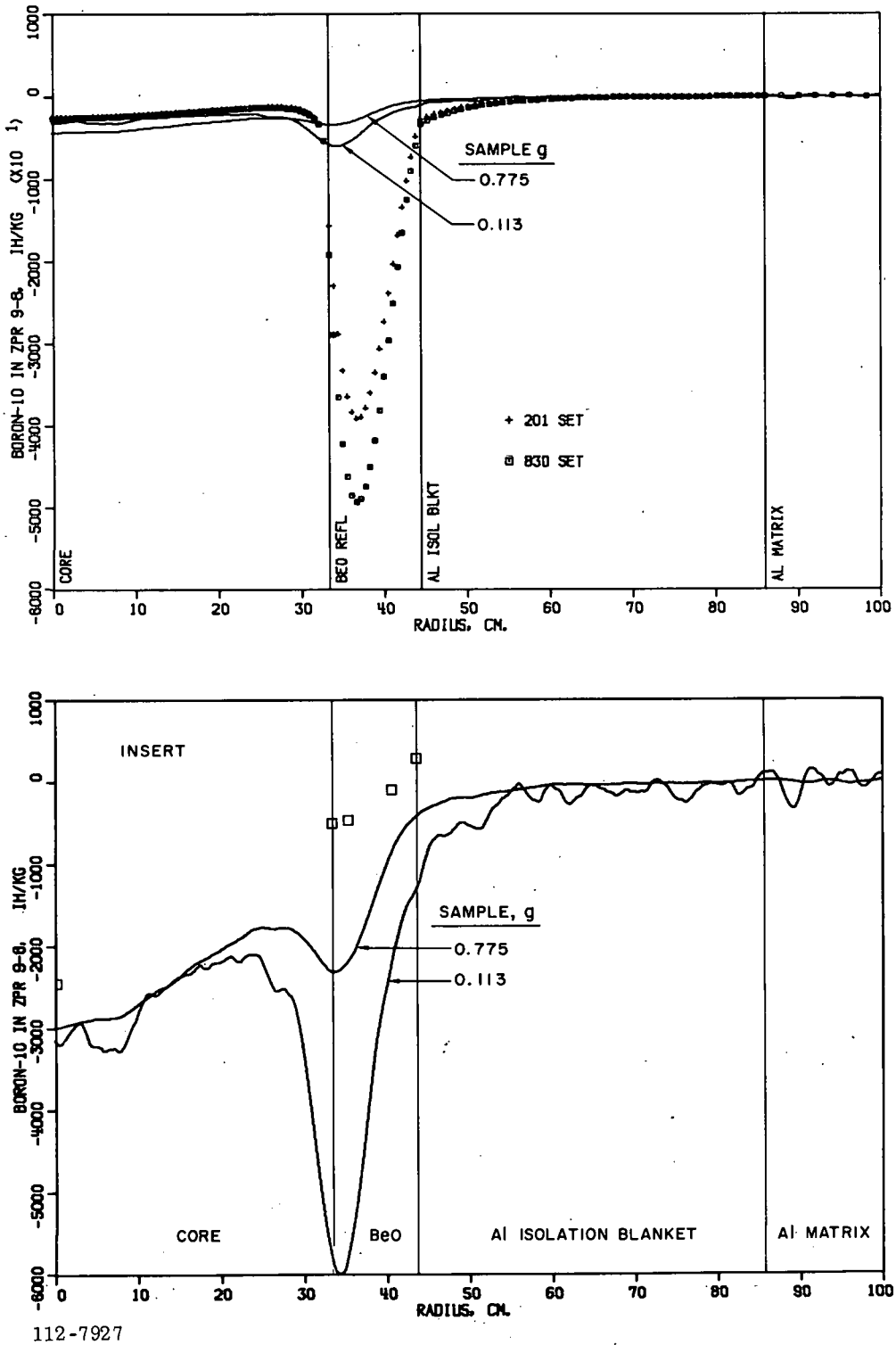


Fig. 59. $B^{10}$ Reactivity Traverses in Assembly No. 8

determined with the smaller traverse samples. At the outer edge of the BeO reflector, the can of $B^{10}$ had a measured positive worth (+1.238 Ih/ 4.2 g of $B^{10}$). In all cases, a small correction (~2% for the two inner points and ~10% for the two outer points) was made for the effect of the displaced BeO. A similar disagreement is noted for the central $B^{10}$ worth determined by the two methods.

Figures 60 and 61 show the spatial distributions of the worth of tungsten and rhenium, respectively, in Assembly No. 8.

## D. Reactivity Distributions in Assembly No. 8B

The $U^{235}$ reactivity distributions in Assembly No. 8B were measured with three different shapes of samples. These are described in the appendix and identified in Fig. 62. Through the core region, the dips and peaks in the three different samples are at approximately the same spots. The valleys in these measurements correspond to the spacing between the drawers in the assembly shown in the figure as short vertical lines on the zero-worth axis. Thus some microstructure is evident from the measurements, although this tends to be masked by the statistical uncertainty in the measurements. Similar sample-size effects were measured for $B^{10}$, as shown in Fig. 63. Measurements made with polyethylene and borated polyethylene as shown in Figs. 64 and 65, respectively. Figures 66-71 show the measured reactivity responses to tungsten, rhenium, gadolinium, europium, dysprosium, and aluminum, respectively.

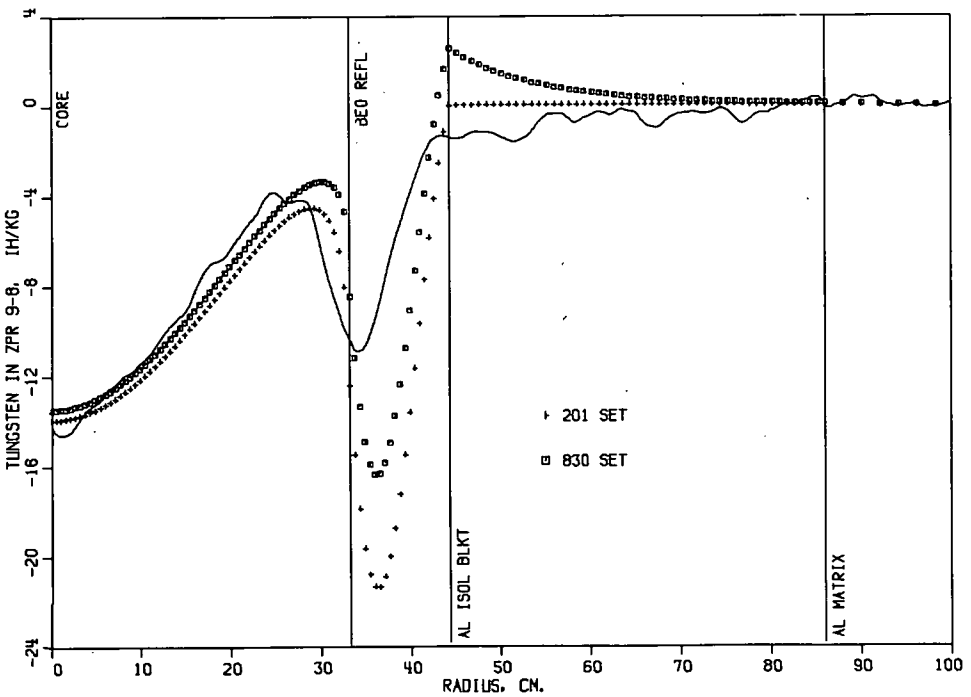


112-7731

Fig. 60. Tungsten Reactivity Traverse in Assembly No. 8

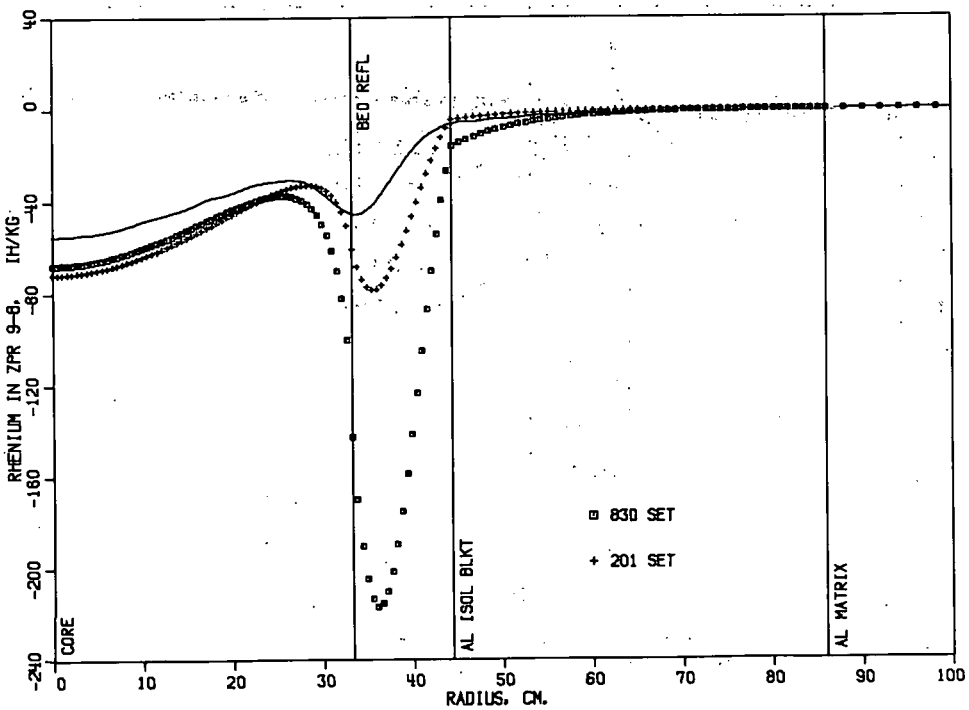


112-7728

Fig. 61. Rhenium Reactivity Traverse in Assembly No. 8

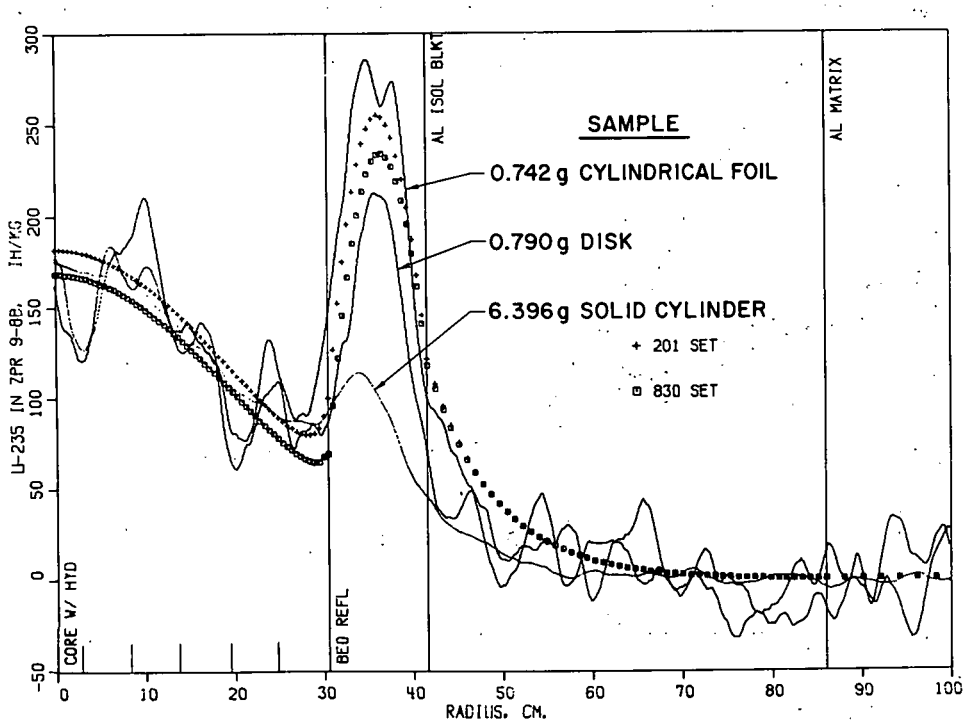


112-7340 Rev. 1

Fig. 62. $U^{235}$ Reactivity Traverse in Assembly No. 8B

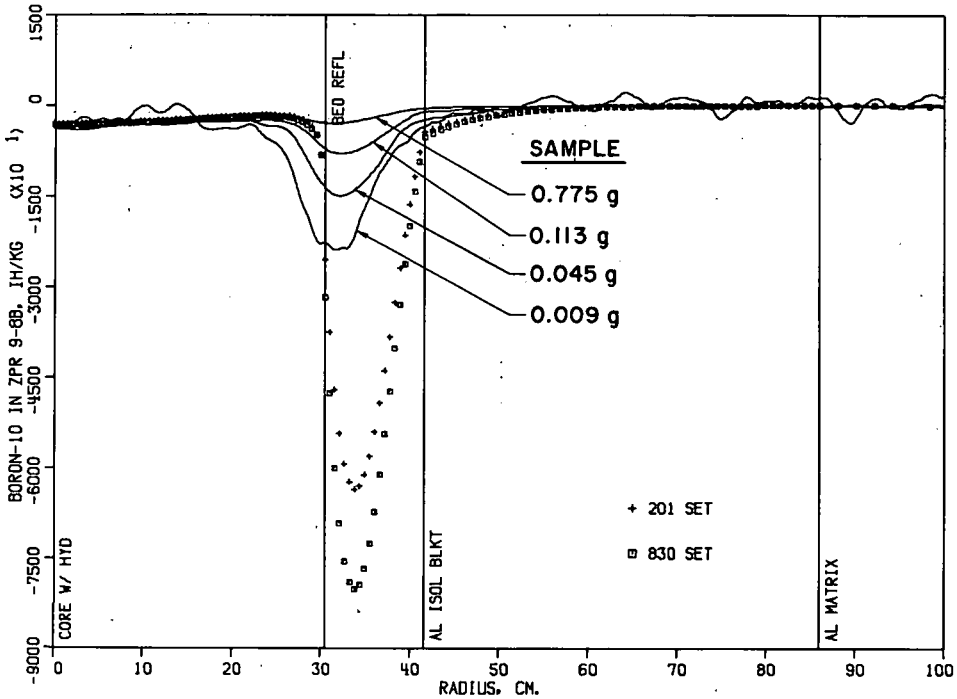


112-7342

Fig. 63. $B^{10}$ Reactivity Traverse in Assembly No. 8B

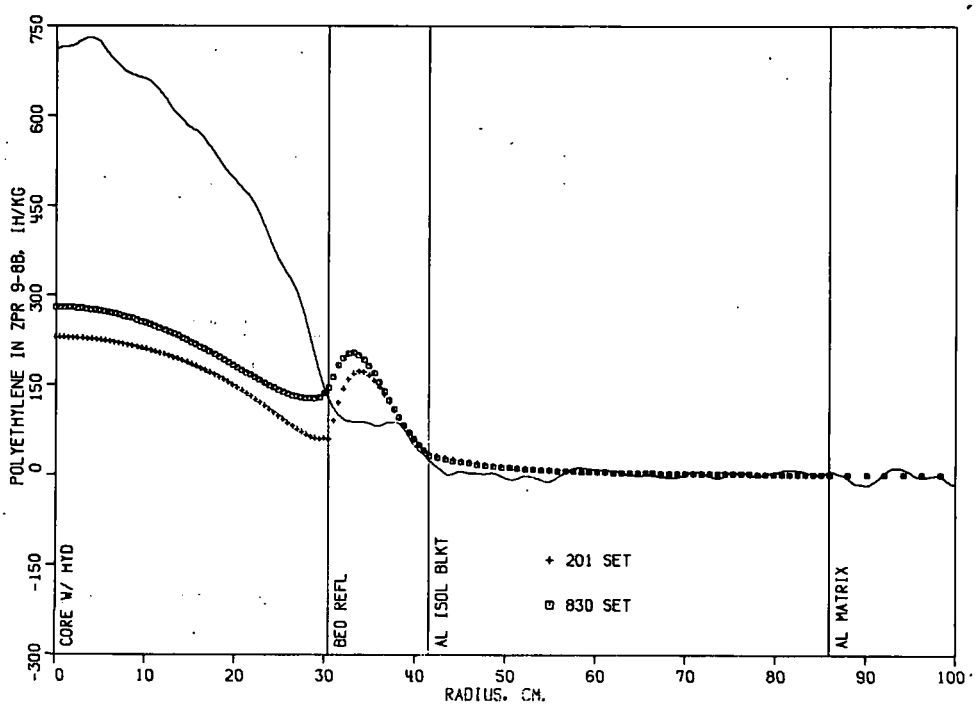


112-7736

Fig. 64. Polyethylene Reactivity Traverse in Assembly No. 8B

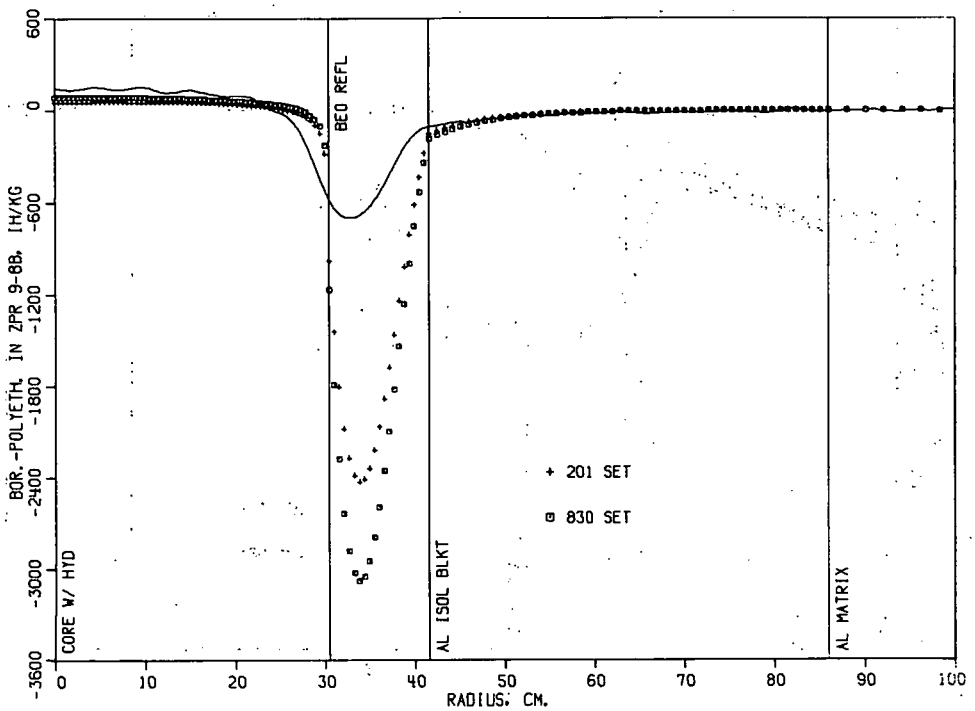


112-7350

Fig. 65. Borated Polyethylene Reactivity Traverse in Assembly No. 8B

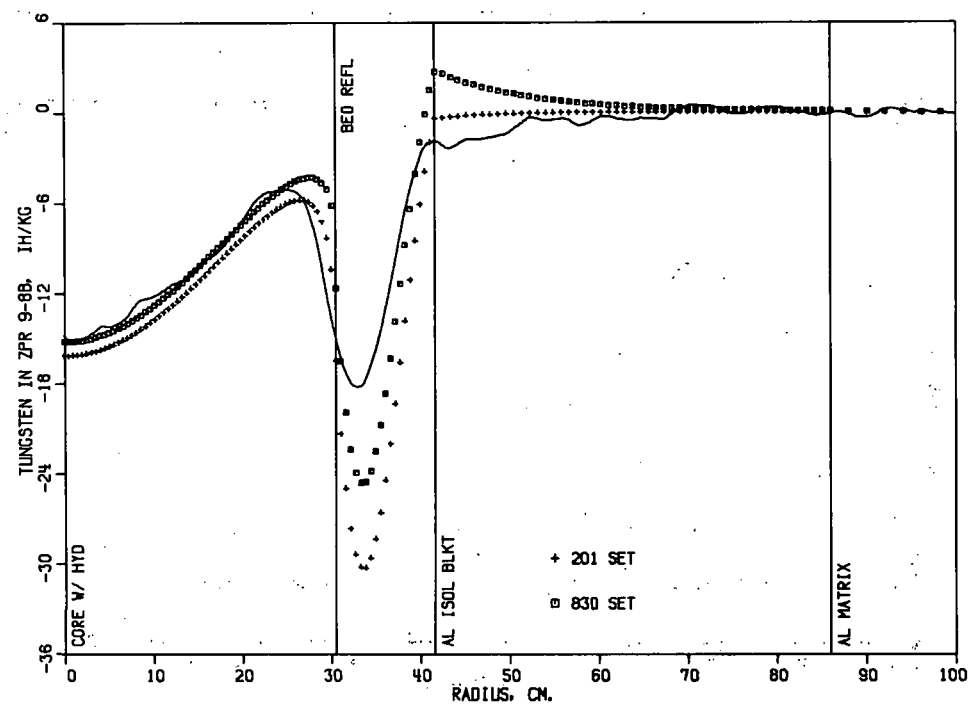


112-7337

Fig. 66. Tungsten Reactivity Traverse in Assembly No. 8B

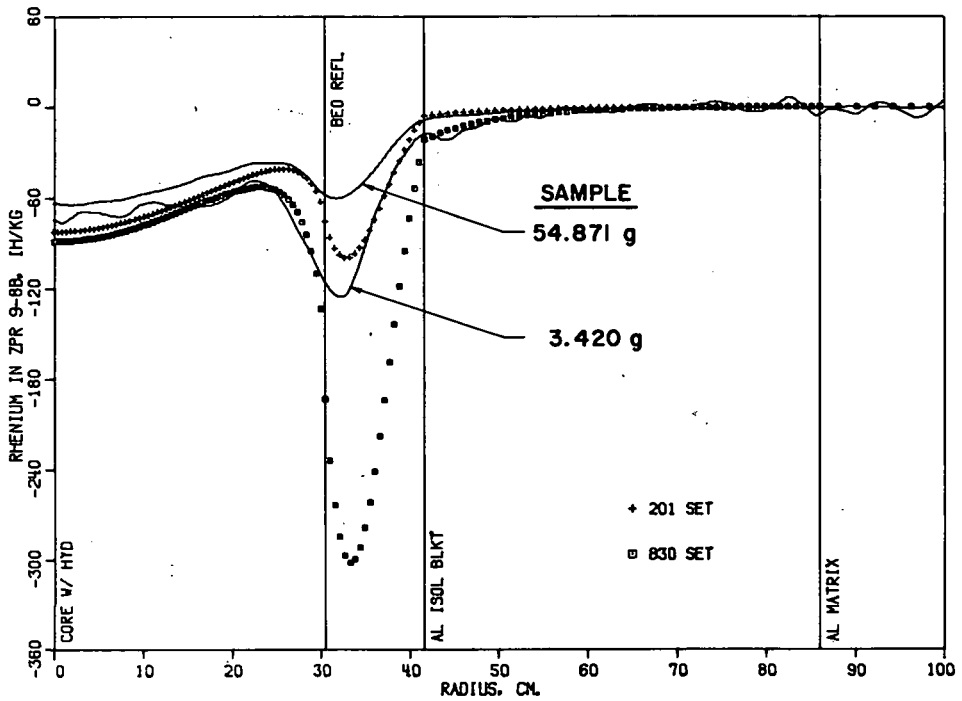


112-7341

Fig. 67. Rhenium Reactivity Traverse in Assembly No. 8B

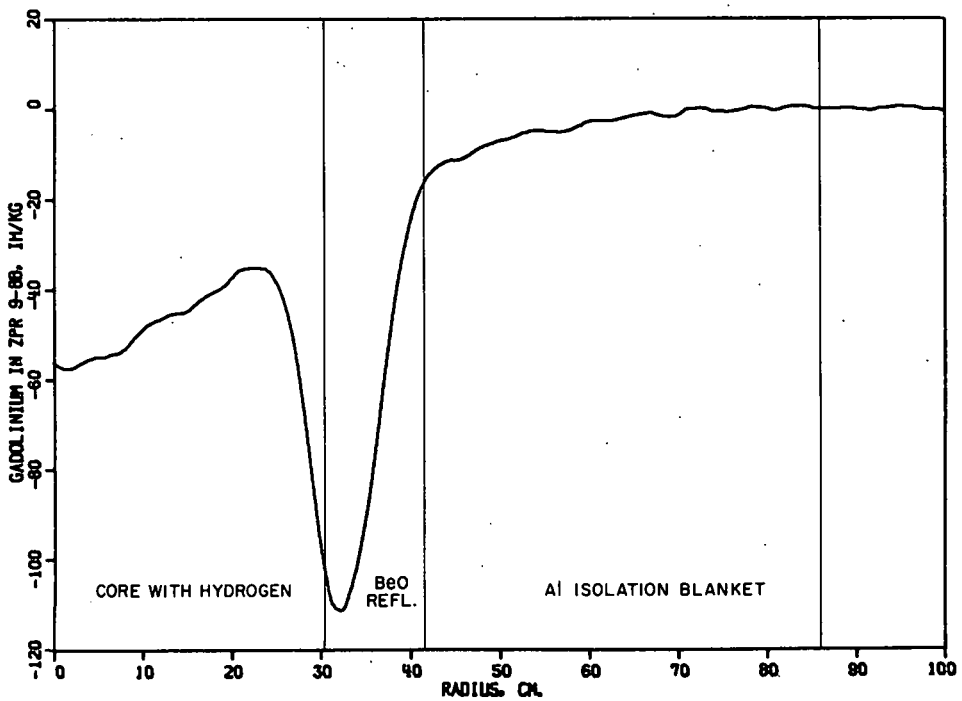


112-7716 Rev. 1

Fig. 68. Gadolinium Reactivity Traverse in Assembly No. 8B

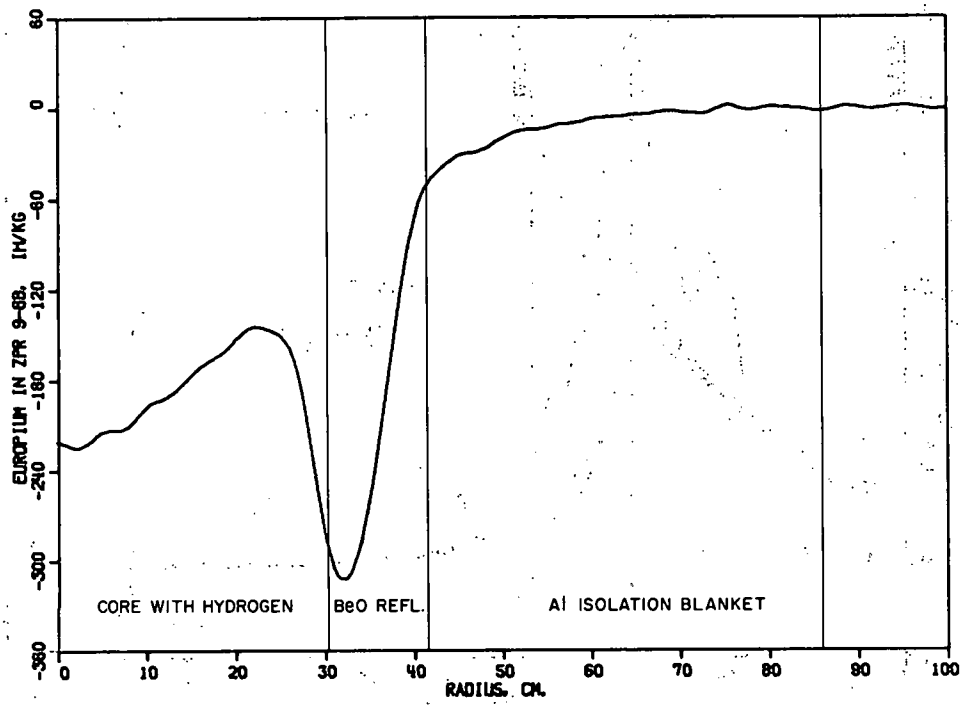


112-7717 Rev. 1

Fig. 69. Europium Reactivity Traverse in Assembly No. 8B

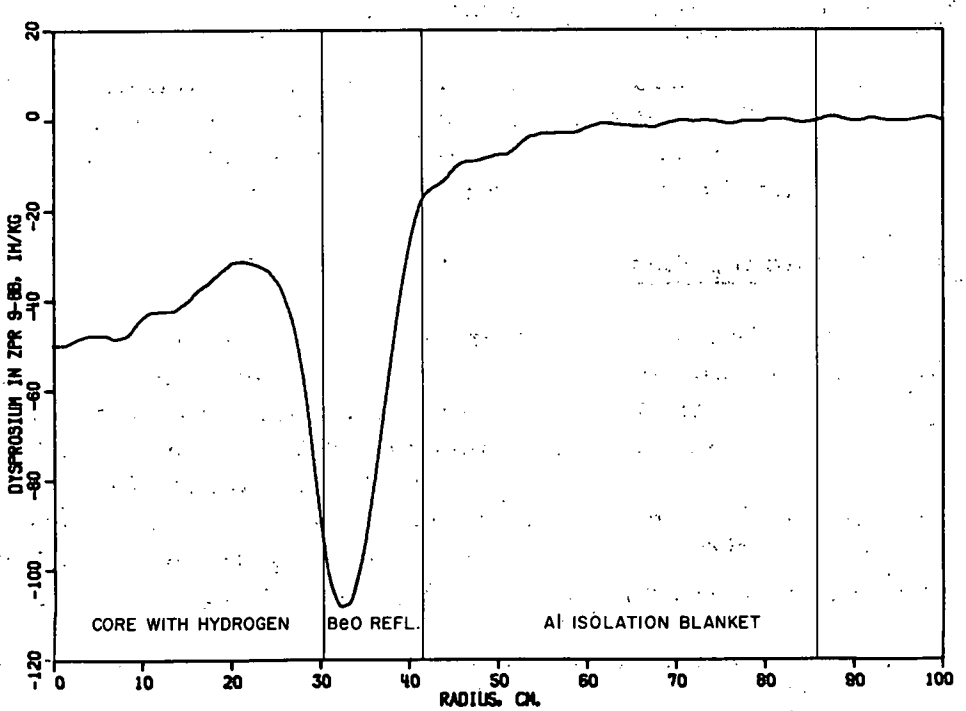


112-7708 Rev. 1

Fig. 70. Dysprosium Reactivity Traverse in Assembly No. 8B

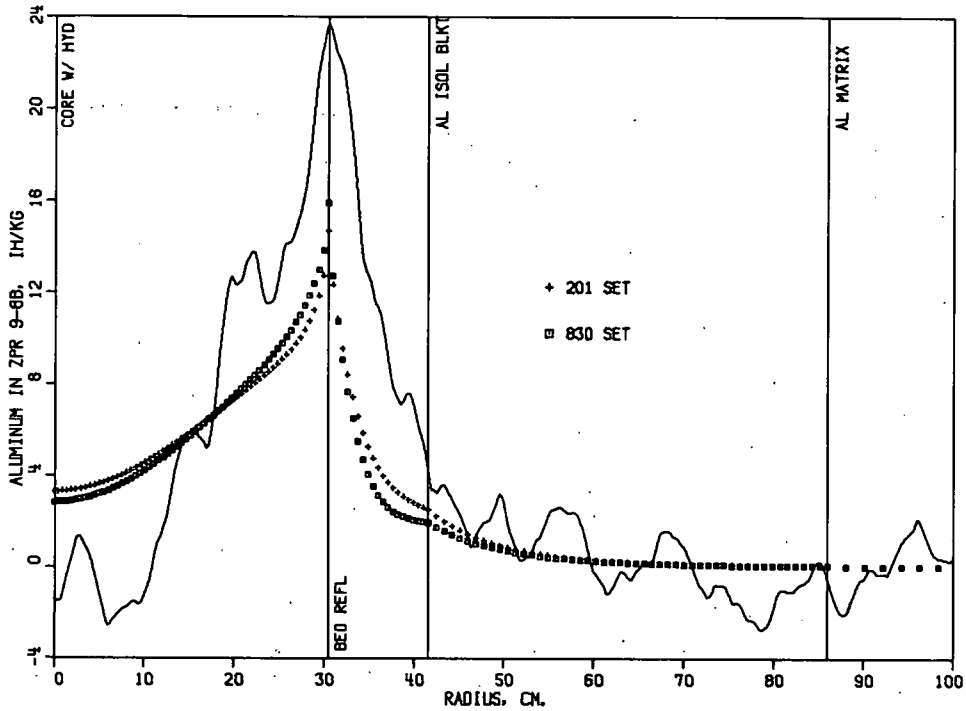


112-7735

Fig. 71. Aluminum Reactivity Traverse in Assembly No. 8B

## E. Reactivity Distributions in Assembly No. 9

Figures 72-75 show the spatially dependent reactivity worths for $U^{235}$, polyethylene, $B^{10}$, and borated polyethylene, respectively, for Assembly No. 9. Figures 76-80 show the measured distributions for tungsten, rhenium, gadolinium, europium, and dysprosium, respectively.

## F. Neutron Streaming Studies

To determine if any significant amounts of neutron streaming can be attributed to the void tube used in these traverses, measurements were made with the sample encapsuled in long lead rods which extended completely through the assembly. Comparisons of these results to those in which no lead rod filled the voided region showed no significant differences. Figures 81 and 82 show the results of the pairs of measurements in Assembly No. 8B for $U^{235}$ and $B^{10}$, respectively. Figures 83 and 84 show similar results in Assembly No. 9 for $U^{235}$ and polyethylene, respectively.

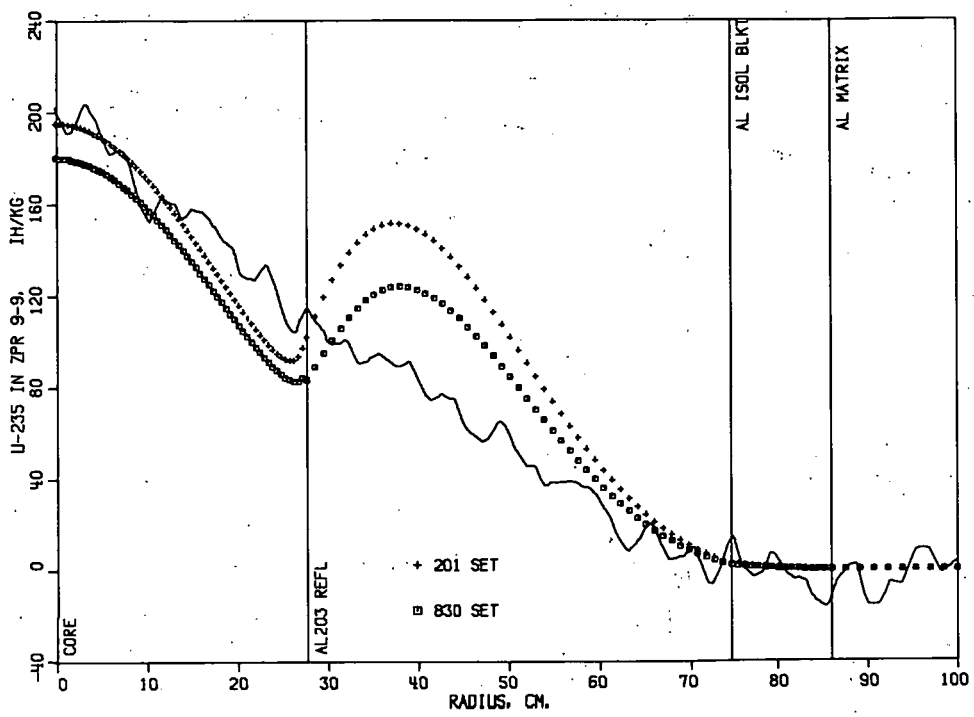


112-7725

Fig. 72. $U^{235}$ Reactivity Traverse in Assembly No. 9

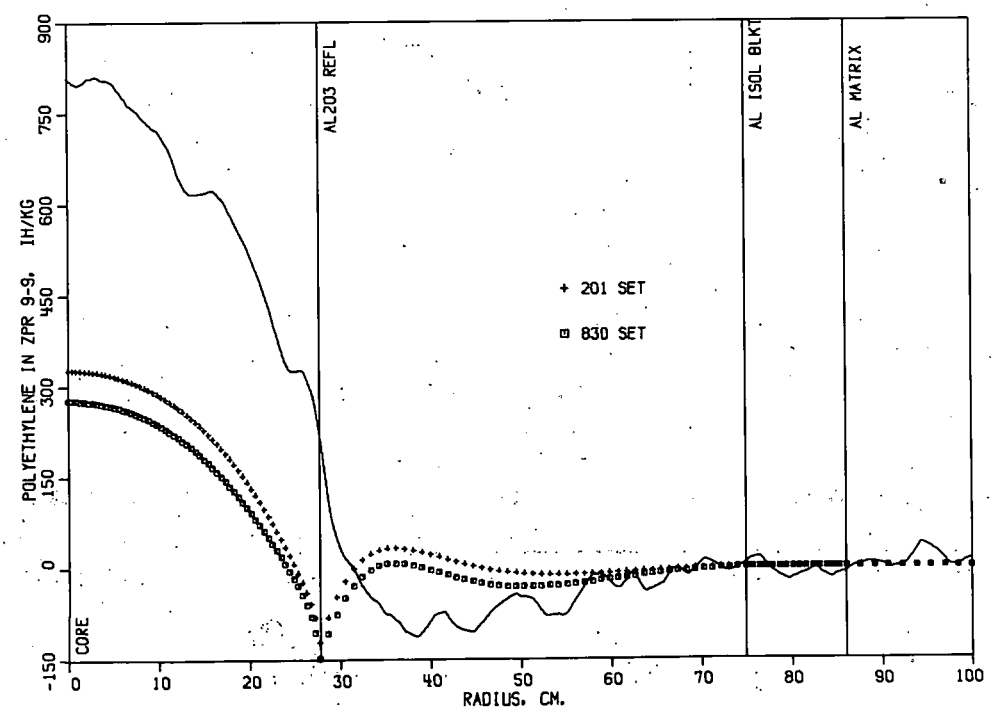


112-7723

Fig. 73. Polyethylene Reactivity Traverse in Assembly No. 9

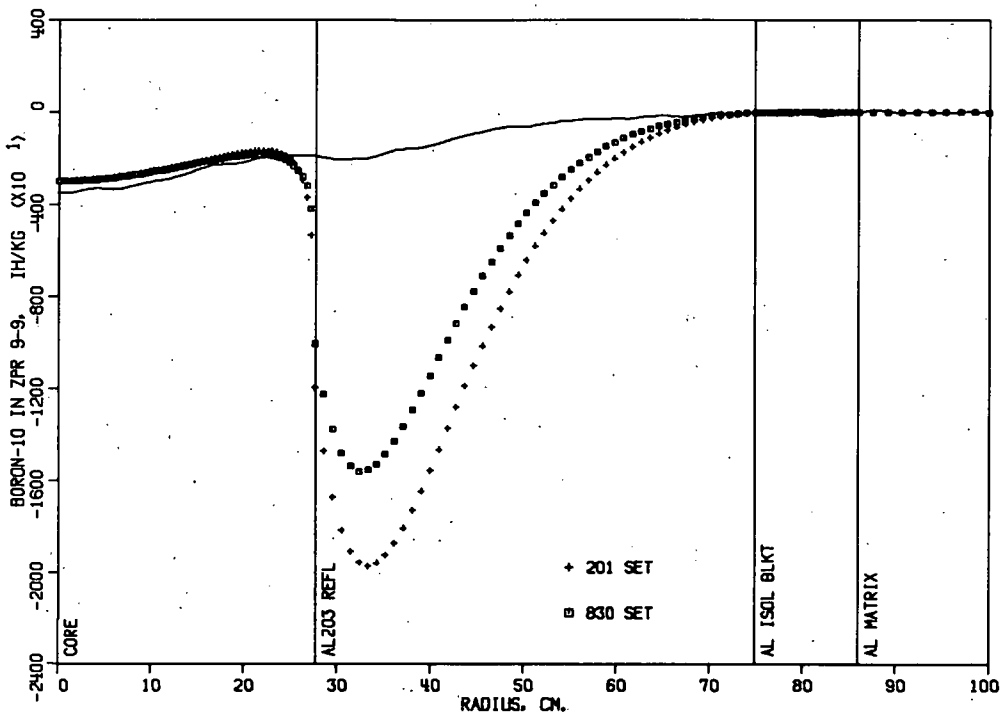


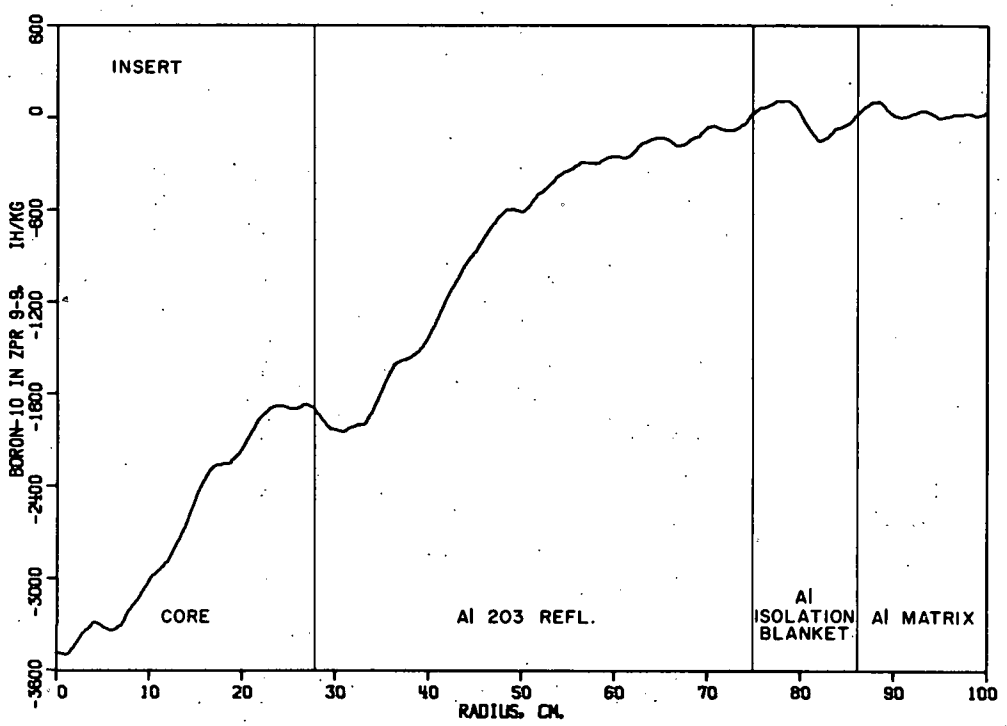


112-7926

Fig. 74. $B^{10}$ Reactivity Traverse in Assembly No. 9

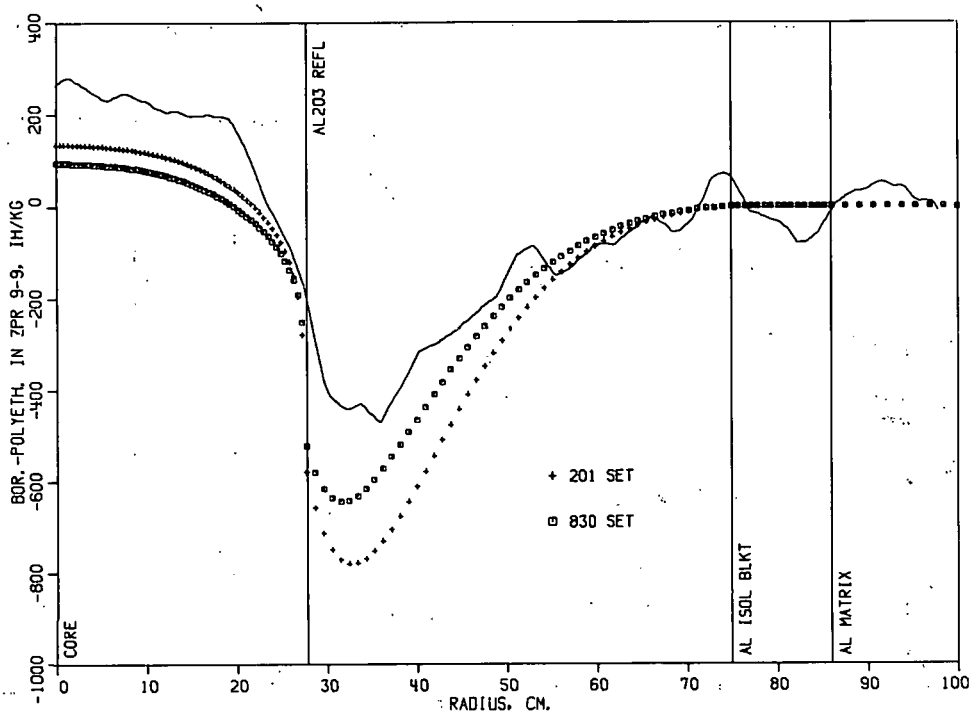


112-7349

Fig. 75. Borated Polyethylene Reactivity Traverse in Assembly No. 9

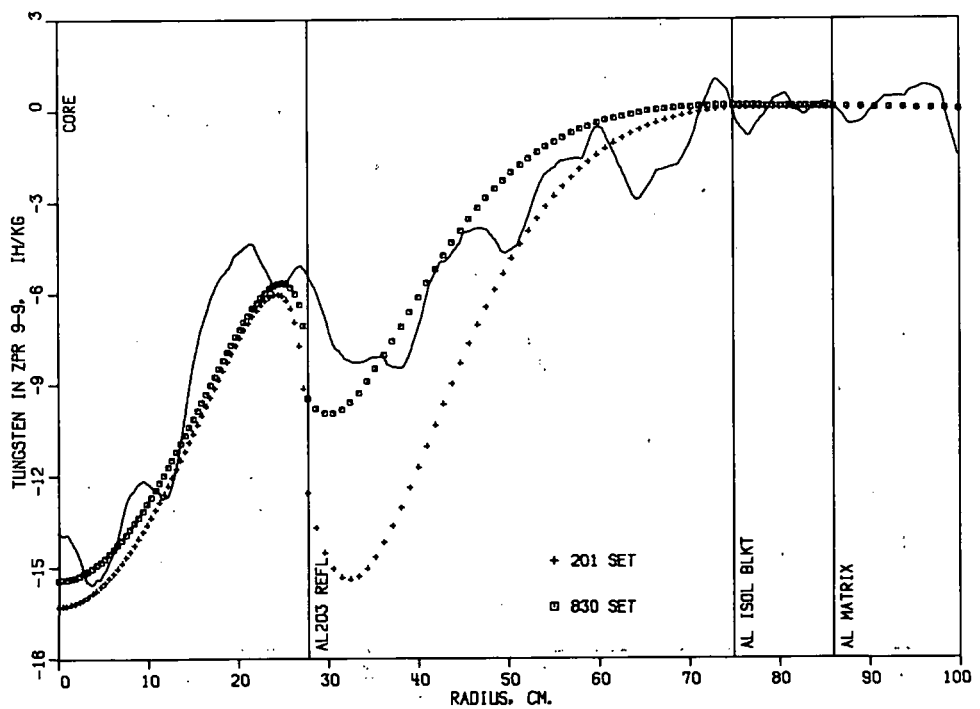


112-7732

Fig. 76. Tungsten Reactivity Traverse in Assembly No. 9

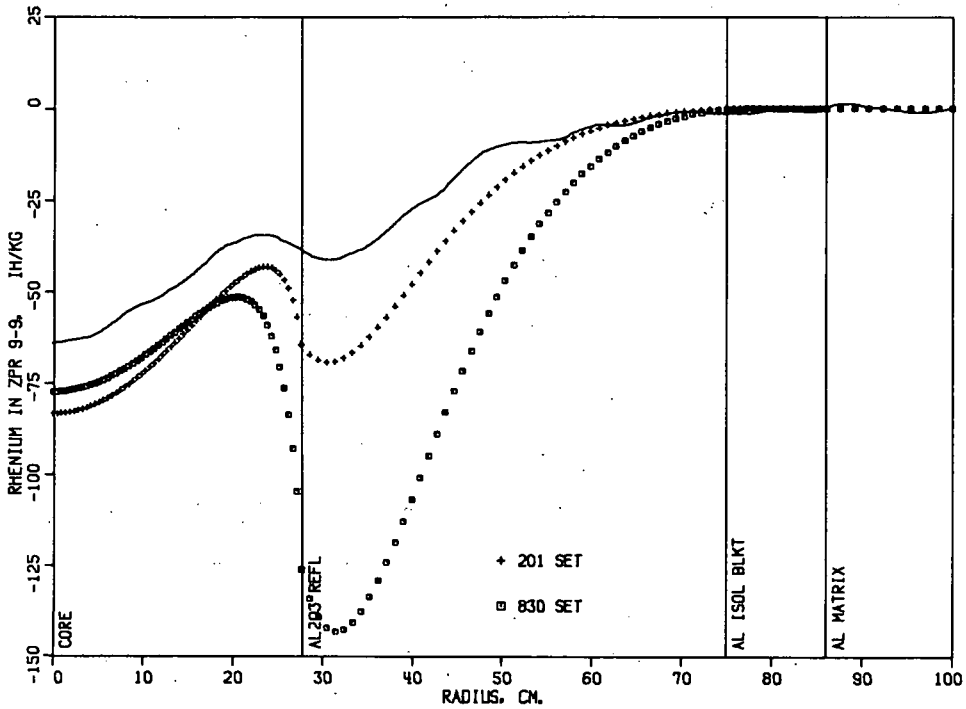


112-7718

Fig. 77. Rhenium Reactivity Traverse in Assembly No. 9

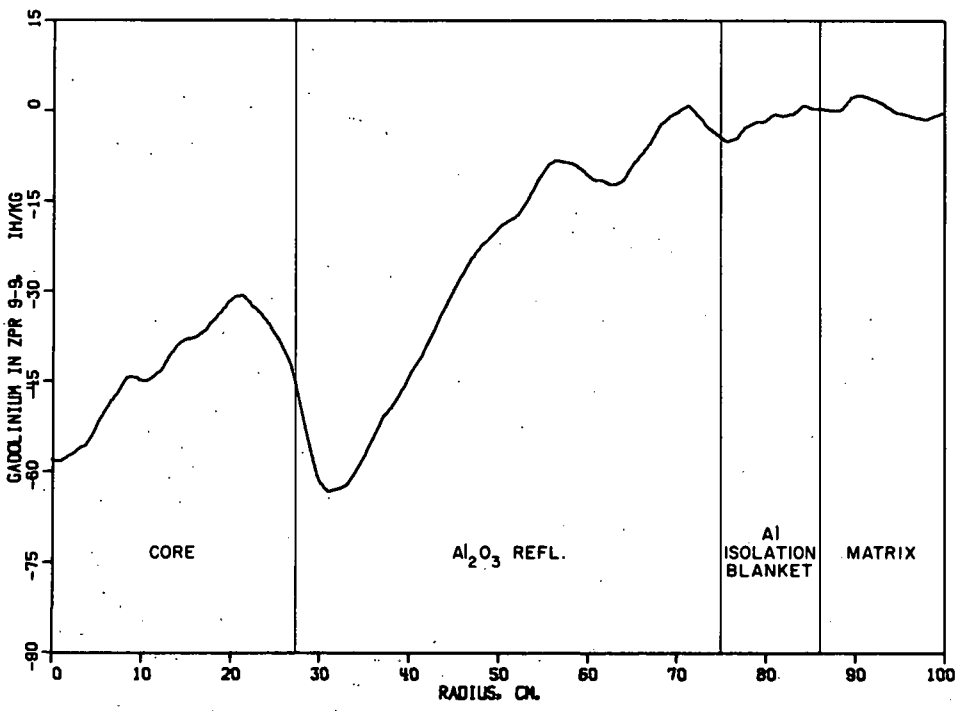


112-7710 Rev. 1

Fig. 78. Gadolinium Reactivity Traverse in Assembly No. 9

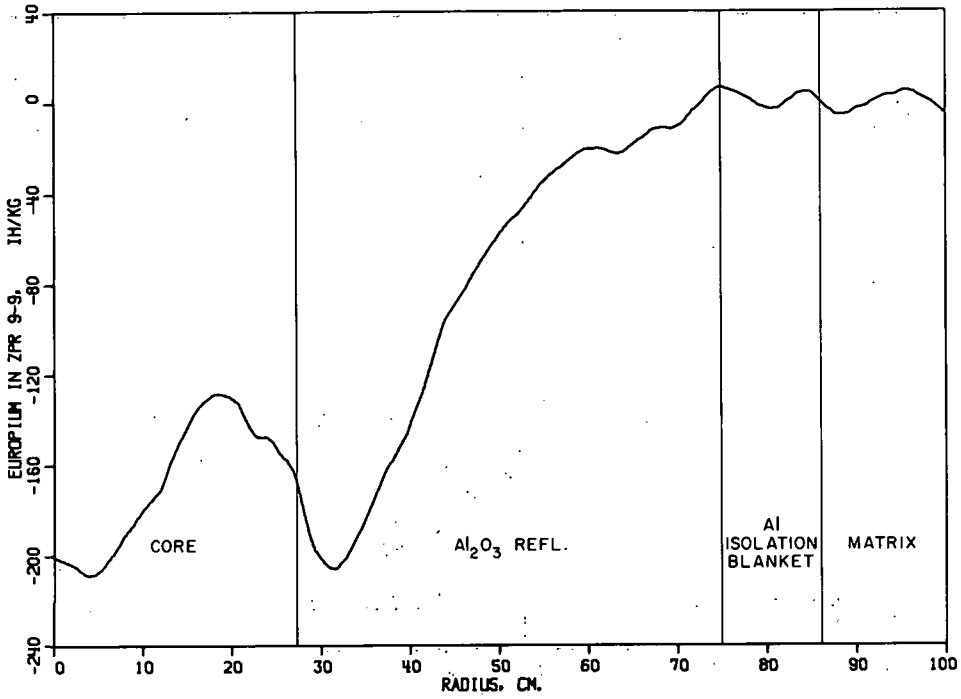


112-7722 Rev. 1

Fig. 79. Rhenium Reactivity Traverse in Assembly No. 9

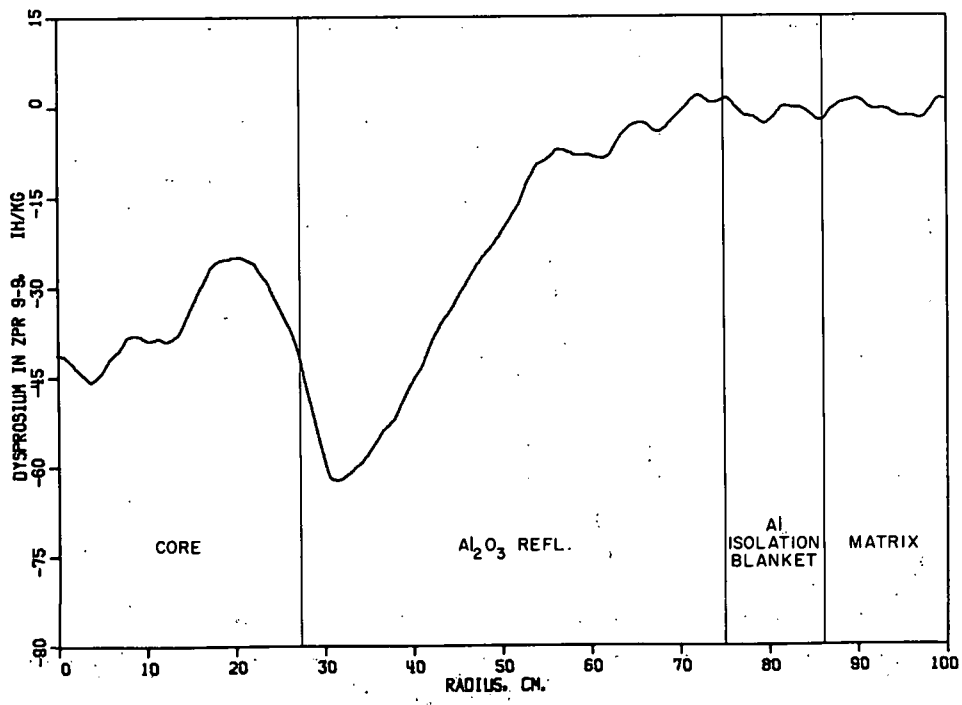


112-7734 Rev. 1

Fig. 80. Dysprosium Reactivity Traverse in Assembly No. 9

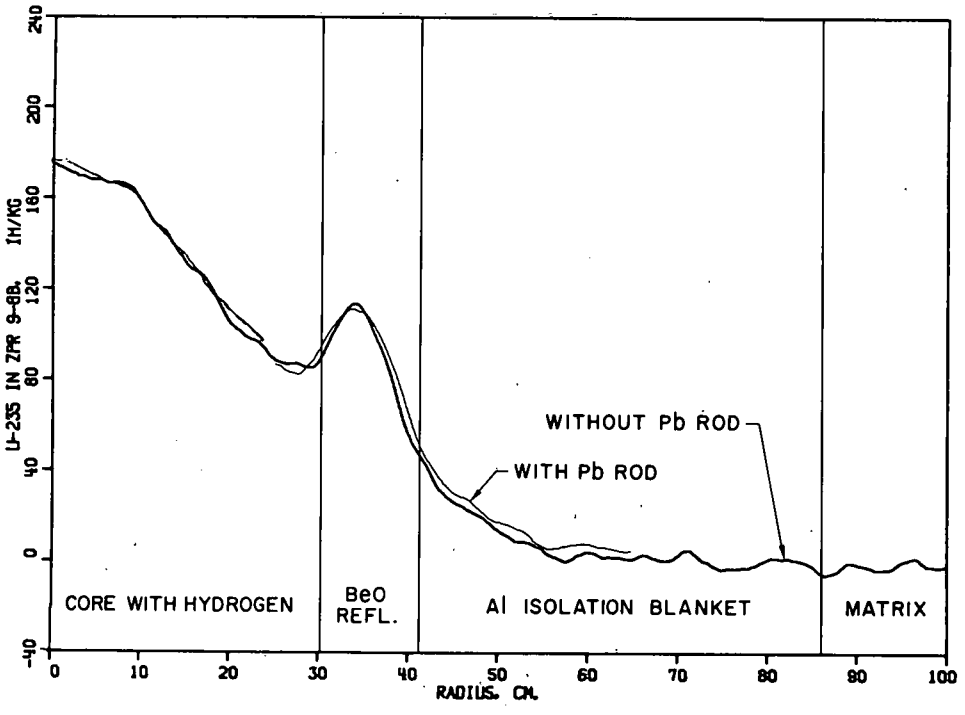


112-7336 Rev. 1

Fig. 81. $U^{235}$ Reactivity Traverse in Assembly No. 8B (with lead rod)

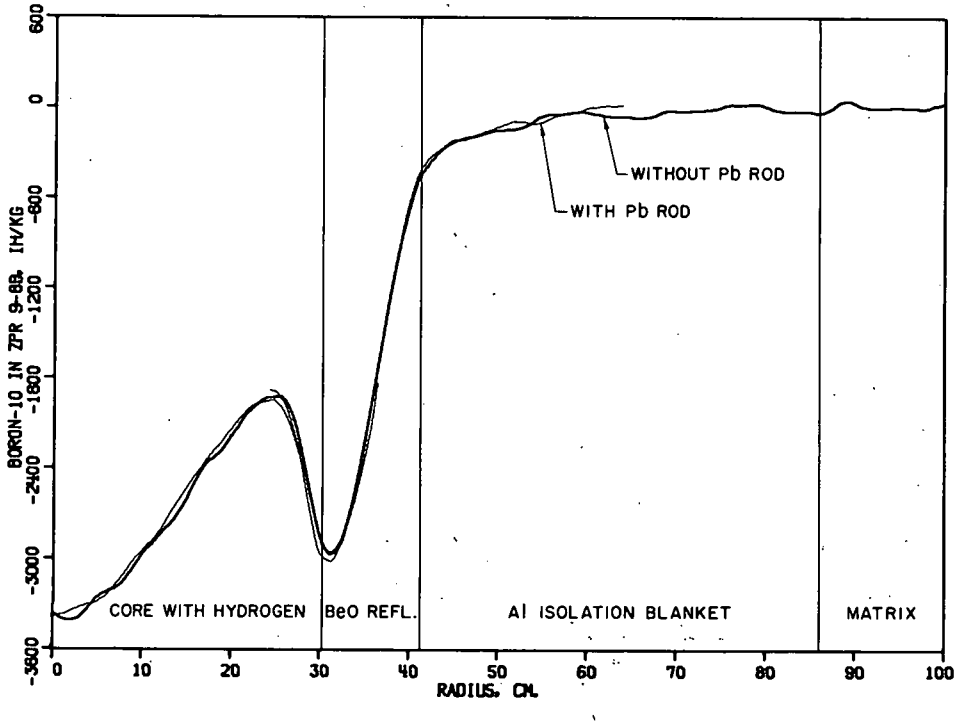


112-7733 Rev. 1

Fig. 82. $B^{10}$ Reactivity Traverse in Assembly No. 8B (with lead rod)

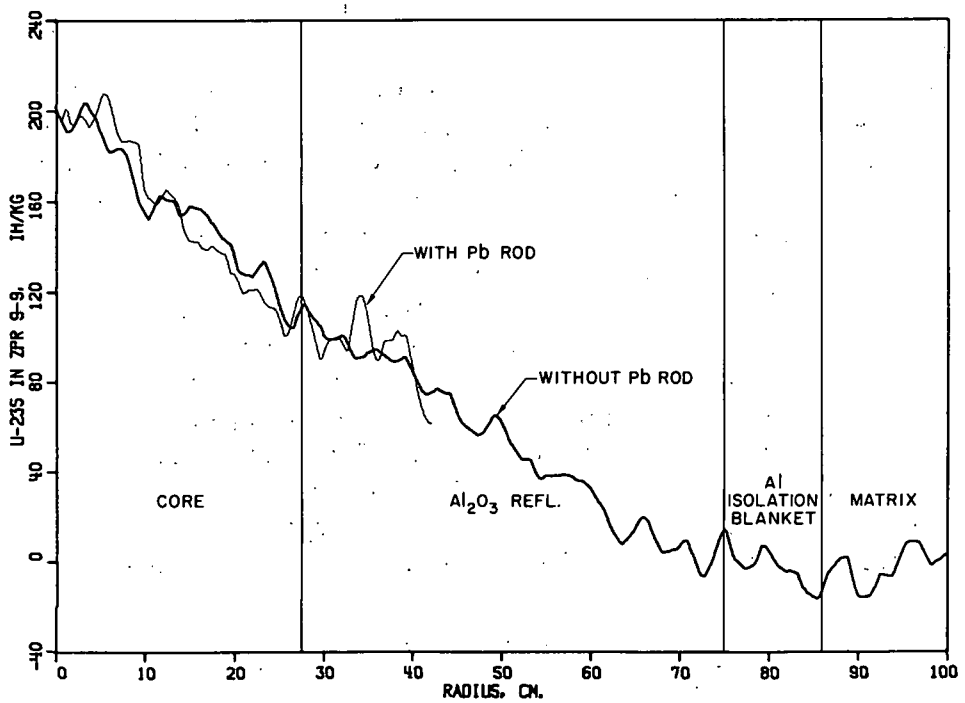


112-7712 Rev. 1

Fig. 83. $U^{235}$ Reactivity Traverse in Assembly No. 9 (with lead rod)

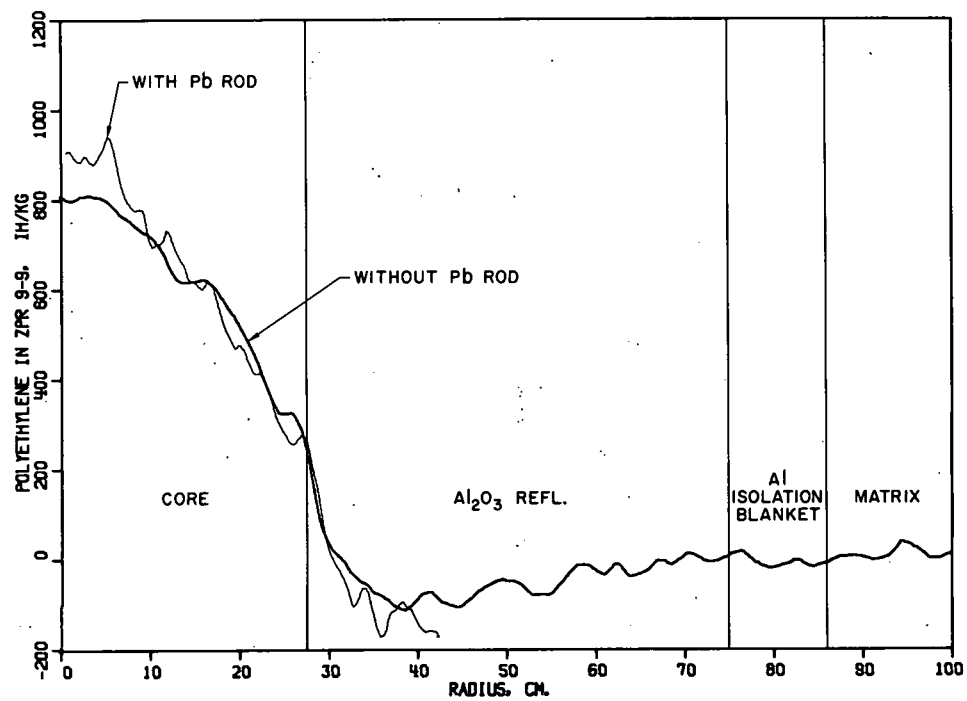


112-7727 Rev. 1

Fig. 84. Polyethylene Reactivity Traverse in Assembly No. 9 (with lead rod)

# VII. DISCUSSION

Table XXXII briefly describes the properties of the assemblies studied in this report. Assembly No. 6, reported in ANL-7207, is included as a basis for comparison. The table provides an overall picture of the general size of the core and radial and axial reflectors of the various assemblies. Detailed dimensions are given in the midregion of the table. Each assembly is divided into several radially symmetric regions or zones. Dimensions are given for three zones in the core even though most cores had only one zone. The inner reflector refers to the material between the core edge and the boron sleeve in the assemblies designated by the letter C. The two regions in the boron sleeve are with respect to Assembly No. 7C. The aluminum metal beyond the BeO reflector of Assembly No. 8 and beyond the $Al_2O_3$ of Assembly No. 7 Loading 71, and Assembly No. 9 is referred to as an isolation blanket. Table XXXIII lists the atom densities in units of $10^{24}$ atoms/cm$^3$ for the various assemblies.

TABLE XXXII. Properties of ZPR-9 Assemblies No. 6-9

| Assembly No.: / Loading No.: | 6 / 48 | 6A / 1 | 6C / 14 | 7 / 18 | 7 / 71 | 7C / 96 | 7C / 118 | 8 / 11 | 8A / 49 | 8B / 53 | 8C / 73 | 9 / 7 | 9A / 36 |
|---|---|---|---|---|---|---|---|---|---|---|---|---|---|
| Axial Reflector | 38.1 cm Al | | | 35.56 cm $Al_2O_3$ | | | | 35.56 Al | | | | 35.56 $Al_2O_3$ | |
| Core Length, cm | 61.26 | 61.26 | 61.26 | 51.1 | 51.1 | | 51.1 | 51.1 | 51.1 | 51.1 | 51.1 | 51.1 | 51.1 |
| Radial Reflector | 39.2 cm Al | | | 37.2 cm $Al_2O_3$ | 50.1 $Al_2O_3$ | | | 10.8 cm BeO | | | | 50.8 cm $Al_2O_3$ | |
| Ih/% k (calc.) | 437.4 | 437.4 | 437.3 | 433.1 | 433.1 | 433.1 | 436.1 | 431.4 | 431.0 | 431.0 | 434.3 | 431.4 | 431.4 |
| Radius, cm | | | | | | | | | | | | | |
| Central Core Zone | | 3.172 | 4.423 | | | 3.127 | 3.172 | | | | 9.382 | | 3.172 |
| Main Core | | | | | | 15.321 | 25.977 | | | | | | |
| Outer Core Zone | 36.804 | 36.804 | 36.804 | 27.884 | 27.083 | 27.442 | 27.442 | 31.892 | 31.43 | 31.43 | 31.43 | 26.35 | 26.35 |
| Inner Reflector | | | 42.483 Al | | | 32.638 | 32.638 $Al_2O_3$ | 42.651 BeO | 42.77 BeO | 42.77 BeO | 34.425 BeO | | |
| Inner Boron Sleeve | | | | | | | 33.047 | | | | | | |
| Outer Boron Sleeve | | | 42.829 | | | 33.936 | 34.566 | | | | 34.760 | | |
| Outer Reflector | 76.026 Al | 76.026 Al | 76.026 Al | 65.375 $Al_2O_3$ | 77.175 $Al_2O_3$ | 77.125 $Al_2O_3$ | 77.175 $Al_2O_3$ | 90.042 Al | 90.042 Al | 90.042 Al | 42.77 BeO | 77.175 $Al_2O_3$ | 77.175 $Al_2O_3$ |
| Isolation Blanket | | | | | 90.042 Al | 88.949 | | | | | 90.042 Al | 90.042 Al | 90.042 Al |
| Excess Reactivity, Ih | 152.40 | 188.006 | 5.01 | 151.219 | 50.876 | 90.52 | 82.038 | 69.90 | 152.86 | 200.67 | 47.8 | 106.2 | 159.0 |
| Fuel Mass, kg $U^{235}$ | 458.622 | 456.965 | 460.269 | 219.134 | 206.963 | 229.011 | 247.953 | 286.66 | 273.430 | 273.430 | 291.349 | 195.699 | 197.134 |
| Edge Worth, Ih/kg | 17.55 | | | 18.21 | 17.43 | | | 20.83 | 20.833 | 20.833 | | 32.20 | 32.2 |
| Central Fuel Worth, Ih/kg | | 113.15 | 113.50 | | 169.57 | 142.861 | 178.43 | | | | 132.910 | | 143.16 |

TABLE XXXIII. Dimensions and Atom Densities in ZPR-9 Assemblies

| Identification[a] | | Radius, cm | Atom Densities in $10^{24}$ atoms/cm$^3$ | | | | | | | | | | | | Mass/Excess, kg/lh |
|---|---|---|---|---|---|---|---|---|---|---|---|---|---|---|---|
| | | | $U^{235}$ | $U^{238}$ | Aluminum | Tungsten | Iron | Nat. B Equiv. | $B^{10}$ | $B^{11}$ | Beryllium | Oxygen | Hydrogen | Carbon | |
| 6-48 | C | 36.8 | 0.00452 | 0.00035 | 0.0159 | 0.0215 | 0.00023 | | | | | | | | 458.6222/152.40 |
| | R | 76.0 | | | 0.0566 | | | | | | | | | | |
| 6A-66 | IC | 3.17 | 0.00225 | 0.00016 | 0.0153 | 0.0223 | | | | | | | | | 456.9652/191.96 |
| | C | 36.8 | 0.00452 | 0.00035 | 0.0159 | 0.0215 | 0.00023 | | | | | | | | |
| | R | 76.0 | | | 0.0571 | | | | | | | | 0.00097 | 0.00048 | |
| 6C-14 | IC | 4.42 | 0.00563 | 0.00041 | 0.0156 | 0.0215 | | | | | | | | | 460.2691/5.01 |
| | C | 36.8 | 0.00452 | 0.00035 | 0.0159 | 0.0215 | 0.00023 | | | | | | | | |
| | IR | 42.5 | | | 0.0571 | | | | | | | | 0.00097 | 0.0048 | |
| | B | 42.8 | | | 0.0241 | | | 0.253 | 0.062 | 0.0055 | | | | | |
| | OR | 76.0 | | | 0.0571 | | | | | | | | 0.00097 | 0.0048 | |
| 7-18 | C | 27.9 | 0.00450 | 0.00033 | 0.0159 | 0.0211 | 0.0003 | | | | | | | | 219.114/151.2 |
| | R | 65.4 | | | 0.0432 | | | | | | | 0.0545 | | | |
| 7-87 | C | 27.4 | 0.00450 | 0.00033 | 0.0159 | 0.0211 | 0.0003 | | | | | | | | 212.4756/200.00 |
| | R | 77.2 | | | 0.0423 | | | | | | | 0.0547 | | | |
| | ISO | 88.9 | | | 0.0566 | | | | | | | | | | |
| 7C-96 | IC | 3.13 | 0.00450 | 0.00033 | 0.0159 | 0.0211 | | | | | | | | | 299.0111/90.510 |
| | C | 15.3 | 0.00562 | 0.00041 | 0.0094 | 0.0211 | 0.00031 | | | | | | | | |
| | OC | 27.4 | 0.00450 | 0.00033 | 0.0159 | 0.0211 | | | | | | | | | |
| | IR | 32.6 | | | 0.0432 | | | | | | | 0.0547 | | | |
| | B | 33.9 | | | 0.0241 | | | 0.253 | 0.062 | 0.0055 | | | | | |
| | OR | 77.2 | | | 0.0432 | | | | | | | 0.0547 | | | |
| | ISO | 88.9 | | | 0.0566 | | | | | | | | | | |
| 7C-118 | IC | 3.13 | 0.00225 | 0.00016 | 0.0159 | 0.0244 | | | | | | | | | 247.9526/82.038 |
| | C | 26.0 | 0.00562 | 0.00041 | 0.0094 | 0.0211 | | | | | | | | | |
| | OC | 27.4 | 0.00450 | 0.00033 | 0.0159 | 0.0211 | 0.00031 | | | | | | | | |
| | IR | 32.6 | | | 0.0432 | | | | | | | 0.0547 | | | |
| | IB | 33.0 | | | 0.0241 | | | 0.212 | 0.052 | 0.0046 | | | | | |
| | OB | 35.6 | | | 0.0223 | | 0.096 | 0.019 | 0.069 | | | | | 0.0182 | |
| | OR | 77.2 | | | 0.0432 | | | | | | | 0.0547 | | | |
| | ISO | 88.9 | | | 0.0566 | | | | | | | | | | |
| 8-11 | C | 31.9 | 0.00451 | 0.00033 | 0.0166 | 0.0214 | 0.00026 | | | | | 0.0089 | | | 286.66/69.90 |
| | R | 42.7 | | | 0.0069 | | | | | | 0.0581 | 0.0581 | | | |
| | ISO | 88.9 | | | 0.0566 | | | | | | | | | | |
| 8A-49 | C | 31.4 | 0.00451 | 0.00033 | 0.0166 | 0.0214 | 0.00026 | | | | | 0.0089 | 0.00066 | 0.00033 | 273.430/152.86 |
| | R | 42.8 | | | 0.0069 | | | | | | 0.0581 | 0.0581 | | | |
| | ISO | 90.0 | | | 0.0566 | | | | | | | | | | |
| 8B-52 | C | 31.4 | 0.00451 | 0.00033 | 0.0166 | 0.0214 | 0.00026 | | | | | 0.0089 | 0.00066 | 0.00033 | 273.430/200.67 |
| | R | 42.8 | | | 0.0069 | | | | | | 0.0581 | 0.0581 | 0.00066 | 0.00033 | |
| | ISO | 90.0 | | | 0.0566 | | | | | | | | | | |
| 8C-73 | IC | 9.38 | 0.00476 | 0.00036 | 0.0166 | 0.0214 | | | | | | 0.0089 | 0.00066 | 0.00033 | 291.437/47.80 |
| | C | 31.4 | 0.00451 | 0.00033 | 0.0166 | 0.0214 | 0.0026 | | | | | 0.0089 | 0.00066 | 0.00033 | |
| | IR | 34.4 | | | 0.0069 | | | | | | 0.0581 | 0.0581 | 0.00066 | 0.00033 | |
| | B | 34.8 | | | 0.0241 | | | 0.253 | 0.062 | 0.0055 | | | | | |
| | OR | 42.8 | | | 0.0069 | | | | | | 0.0581 | 0.0581 | 0.00066 | 0.00033 | |
| | ISO | 90.0 | | | 0.0566 | | | | | | | | | | |
| 9-17 | C | 26.4 | 0.00450 | 0.00033 | 0.0177 | 0.0213 | 0.00037 | | | | | 0.0089 | | | 195.6987/106.20 |
| | R | 77.2 | | | 0.0432 | | | | | | | 0.0545 | | | |
| | ISO | 90.0 | | | 0.0566 | | | | | | | | | | |
| 9A-36 | IC | 3.17 | 0.00225 | 0.00016 | 0.0166 | 0.0244 | | | | | | 0.0044 | 0.00066 | 0.00033 | 197.134/159.00 |
| | C | 26.4 | 0.00450 | 0.00033 | 0.0177 | 0.0213 | 0.00037 | | | | | 0.0088 | 0.00066 | 0.00033 | |
| | R | 77.2 | | | 0.0432 | | | | | | | 0.0547 | | | |
| | ISO | 90.0 | | | 0.0566 | | | | | | | | | | |

[a]Basic assemblies are identified by the numbers 6, 7, 8, or 9, and variations. A = hydrogen in reflector, B = hydrogen in core, C = with boron sleeve. The second number in the assembly identification is the loading number. Regions are identified by IC = inner core, C = core, OC = outer core, IR = inner reflector, IB = inner boron sleeve, B = boron sleeve, OB = outer boron sleeve, R = reflector, OR = outer reflector, and ISO = isolation blanket.

## A. Critical Mass

In ANL-7007, the experimental critical mass loaded into the first four assemblies was corrected for excess reactivity, heterogeneity, central gap, and noncylindrical core boundary effects to yield an equivalent, cylindrical, homogeneous critical mass. A two-step conversion factor given by Davey[11] was then used to find an equivalent spherical mass, which was compared to calculated values. At least part of the discrepancy between theory and experiment is absorbed by this shape factor since it was determined partially on a basis of a comparison between calculated and measured critical masses on a number of ZPR-3 assemblies. With the presently existing multigroup, one-dimensional diffusion code, MACH-1,[10] a two-dimensional calculation can be approximated by determining first the axial-reflector savings by a calculation in the axial direction. Using this as a transverse buckling, we can then calculate the core size in the radial direction. This type synthesis of a two-dimensional diffusion calculation is subject to some questions for the small multizone assemblies and "leaky" reflectors in the ZPR-9 program. A typical case can underestimate the axial-reflector savings by 10% and overestimate the critical mass by 35%. For this reason, the comparison between theory and experiment in terms of critical mass is made on the basis of a $k_{eff}$ calculation of the experimental assembly by a two-dimensional, multigroup diffusion code, CANDID. For the various assemblies, Table XXXIV gives results of measured and calculated $k_{eff}$.[6] The mass of fuel and equivalent radii of the various assemblies are listed in the second and third columns. Cores in which fuel adjustments were made in the central zone are designated by Z. Excess reactivity, converted to $k_{eff}$, is given in column 4. For the nonzoned systems, the excess reactivity is removed in terms of edge fuel to give a "critical mass" and "critical radius," given in columns 5 and 6. In the zoned cores, the excess reactivity was compensated for by removing fuel in the central zone giving the "critical mass" listed in column 7.

TABLE XXXIV. Critical-mass Summary

| | As Loaded | | | Corrected for $k_{ex}$ by Removal of | | | MACH-1 Calculated | | | | |
|---|---|---|---|---|---|---|---|---|---|---|---|
| | | | | Edge Fuel | | Central Fuel | | | | | |
| Assembly and Loading No. | Mass, kg $U^{235}$ | Radius, cm | $k_{eff}$ | Critical Mass, kg | Critical Radius, cm | Critical Mass, kg | Mass, kg $U^{235}$ | Radius, cm | Extrapolated Height, cm | $k_{eff}$ | Two-dimensional Calculation, $k_{eff}$ |
| 6-48 | 458.622 | 36.804 | 1.00348 | 454.60 | 36.60 | | 506 | 38.6 | 85.8 | 0.9807 | 0.999 |
| 6A-1 | 456.965 | 36.804 Z | 1.00430 | | | 455.265 | 510 | 38.9 | | 0.9788 | |
| 6C-14 | 460.269 | 36.804 Z | 1.00011 | | | 460.225 | 517 | - | | 0.9776 | |
| 7-18 | 219.114 | 27.884 | 1.00349 | 214.25 | 27.56 | | 214 | 27.6 | 93.3 | 1.0043 | |
| 7-71 | 206.963 | 27.173 | 1.00117 | 204.04 | 26.98 | | 201 | 26.7 | | 1.0090 | 0.995 |
| 7C-96 | 229.011 | 27.442 Z | 1.00207 | | | 228.403 | 248 | 30.3 | | 0.9553 | |
| 7C-118 | 247.953 | 27.442 Z | 1.00188 | | | 247.379 | 260.8 | 27.6 | | 0.9972 | |
| 8-11 | 286.66 | 31.892 | 1.00162 | 283.304 | 31.71 | | 290 | 32.1 | 71.5 | 0.9982 | 1.007 |
| 8A-49 | 273.43 | 31.43 | 1.00355 | 266.093 | 31.01 | | 275 | 31.2 | | 1.0023 | |
| 8B-53 | 273.43 | 31.43 | 1.00466 | 263.798 | 30.88 | | 271 | 31.0 | | 1.0019 | |
| 8C-73 | 291.437 | 31.43 Z | 1.00110 | | | 291.075 | 349 | 36.3 | | 0.9542 | |
| 9-17 | 195.698 | 26.35 | 1.00246 | 192.400 | 26.13 | | 198.1 | 26.5 | 85.2 | 0.9978 | 1.004 |
| 9A-36 | 197.134 | 26.35 Z | 1.00369 | | | 196.023 | 200 | 27 | | 0.9918 | |

Extrapolated heights for each of the assemblies (column 10) were calculated by a two-step process:

1. Determining the critical buckling (bare radius) for a calculation along the core axis and into the axial reflector.

2. Using the critical buckling (bare radius) to calculate the bare height of the assembly.

The extrapolated heights are then entered as transverse bucklings in a critical-radius search in the radial direction. Critical masses and radii so calculated are given in columns 8 and 9, respectively. In an analogous manner, the $k_{eff}$ has been calculated for each assembly using the calculated extrapolated height and the experimental radius of the assemblies. Column 11 shows these results. The last column shows the results of some two-dimensional calculations. The MACH-1 calculations all used the 201 cross-section set; the CANDID 2D calculations used the 830 set. Both are discussed in Section H below.

## B. Central Worths

Central worths for some of the materials measured in the four basic assemblies (Assemblies No. 6, 7, 8, and 9) have been calculated from perturbation theory using the unperturbed, one-dimensional, real and adjoint fluxes of the multigroup diffusion code MACH-1,[10] using infinitely dilute (non-self-shielded), 16-group, 201 cross-section set. Materials have been selected to show the effects of thermal fission ($U^{235}$ and $U^{233}$), fast fission plus absorption ($U^{238}$), small and large elastic downscattering (carbon and hydrogen, respectively), moderate and large resonance capture with appreciable scattering (tungsten and rhenium), and a well-behaved $1/v$ absorber ($B^{10}$). Since the denominator of the perturbation expression involves an integral over the volume of the core, it is advantageous to normalize one of the materials to unity and express the worth of others in terms of the first. This has been done in Table XXXV. The underprediction of $U^{238}$ worth in

TABLE XXXV. Normalized Worths of Materials at Center of Reactor

| | Assembly No. 6 | | Assembly No. 7 | | Assembly No. 8 | | Assembly No. 9 | |
|---|---|---|---|---|---|---|---|---|
| | Measured | Calculated | Measured | Calculated | Measured | Calculated | Measured | Calculated |
| $U^{235}$ | 1.00 | 1.00 | 1.00 | 1.00 | 1.00 | 1.00 | 1.00 | 1.00 |
| $U^{238}$ | -0.0216 | -0.0236 | -0.0151 | -0.0234 | -0.0877 | -0.0307 | -0.0276 | -0.0318 |
| Hydrogen | 24.35 | | 21.07 | 17.84 | 28.8 | 10.85 | 23.53 | 10.60 |
| $B^{10}$ | -13.95 | -12.36 | -13.97 | -12.40 | -14.71 | -13.76 | -14.87 | -13.83 |
| Tungsten | -0.0716 | | -0.0625 | -0.0785 | -0.0685 | -0.0826 | -0.0769 | -0.0835 |
| Rhenium | -0.264 | | -0.264 | -0.389 | -0.280 | -0.415 | -0.285 | -0.416 |
| Carbon | 0.0581 | 0.226 | 0.143 | 0.217 | 0.0516 | 0.169 | 0.0585 | 0.160 |
| $U^{233}$ | 1.797 | 1.74 | 1.70 | 1.74 | | 1.73 | 1.74 | 1.73 |

Assembly No. 8 may be the result of too hard a calculated spectrum, giving rise to larger positive (fission) and smaller negative (capture) contributions to the $U^{238}$ total worth. Every comparison between measured and calculated rhenium worth shows too high an assumed capture. The very large differences in carbon may be a reflection of a poor calculation of the adjoint spectrums. The calculations were made with flux-weighted cross sections; adjoint-weighted cross sections were not used in the adjoint equation.

## C. Hydrogen Worth

Measurements of hydrogen worth as a function of sample size are summarized in Fig. 85. To avoid confusion, only errors on one side of a given point are sometimes shown. Extrapolation to infinite dilution in these measurements is somewhat arbitrary since the statistical errors get quite large for the very small samples of hydrogen (polyethylene).

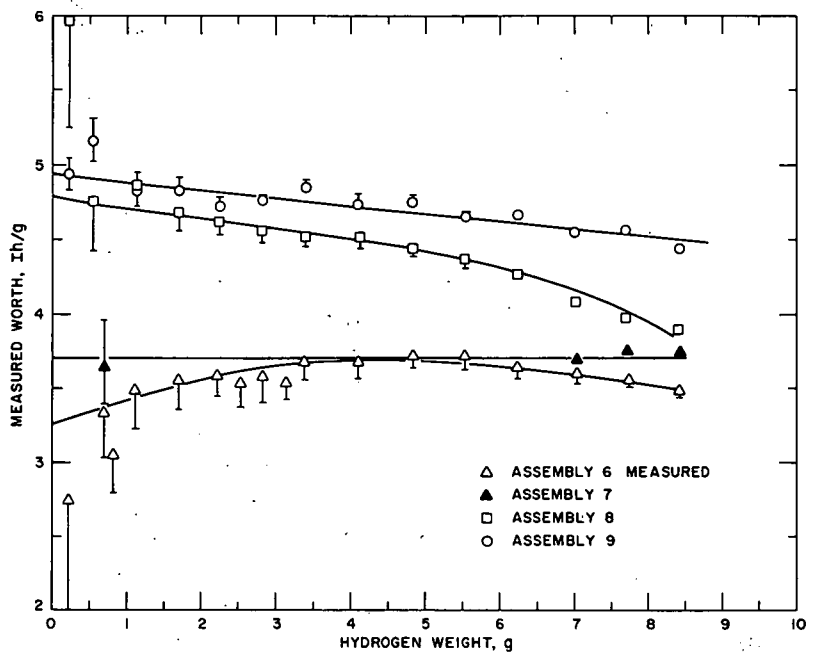


112-7507

Fig. 85. Central Hydrogen Worths

## D. Boron-Lucite Mixture Worths

Worth measurements of boron, mixed with varying amounts of Lucite, have their ultimate application in control studies. Such mixtures were studied at the core center when the flux gradient is zero, and an analysis of the measurements is somewhat simplified. Although there is considerable scatter in the measured data, no favored mixture appears to greatly enhance the mixture worth. Measured values of the different mixtures are shown in Fig. 86 for the basic assemblies.

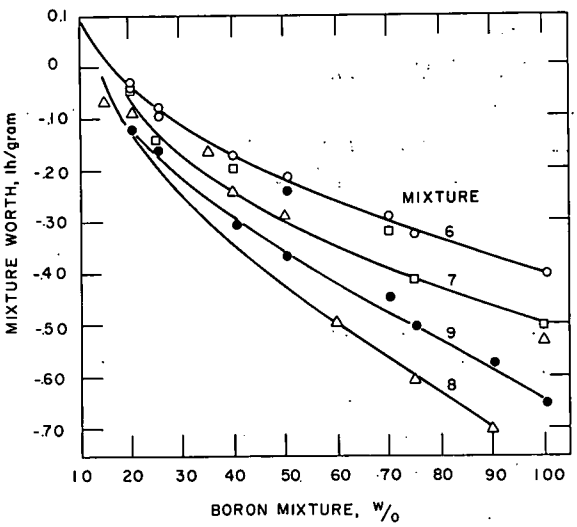


112-7758

Fig. 86. Central Worths of Boron-Lucite Mixtures

## E. Kinetic Properties

As discussed earlier, three distinct exponential terms are readily extracted from the measured Rossi-alpha data. With long-time channels in the experiment, a large portion of the data is associated with the smallest value of alpha ($\alpha_3$) and corresponds to what has been used in the usual definition of $\alpha = \alpha_3 = \beta_{eff}/\ell$, where the lifetime, $\ell$, is understood to be a characteristic of the fundamental mode of the assembly as a whole. Table XXXVI lists measured values of the three components, as well as the calculated values of $\beta_{eff}$ and $\ell$. The last two rows show values for the measured lifetimes and the relative differences between measured and calculated values. Typically, differences of 25 to 40% are encountered; most of this can be accounted for by inadequate cross sections. The factor-of-two difference in Assembly No. 7C indicates that in the calculation the boron sleeve almost completely isolates the core from the reflector, and the prompt lifetime of Assembly No. 7C is more characteristic of a bare assembly rather than a reflected one. The large differences for Assembly No. 8 may be the result of too hard a calculated spectrum--consistent with the observations regarding the central worth of $U^{238}$ in Assembly No. 8.

TABLE XXXVI. Kinetic Properties of ZPR-9, Assemblies No. 6-9

| Assembly No. | 6 | 7 | 7C | 8 | 9 |
|---|---|---|---|---|---|
| $\alpha_1$, $sec^{-1}$ | | $(8.58 \pm 0.92) \times 10^5$ | $(5.55 \pm 0.52) \times 10^4$ | $(5.8 \pm 1.7) \times 10^4$ | $>10^6$ |
| $\alpha_2$, $sec^{-1}$ | $(2.86 \pm 1.10) \times 10^6$ | $(6.86 \pm 0.58) \times 10^4$ | $(1.57 \pm 0.07) \times 10^4$ | $(3.5 \pm 0.5) \times 10^3$ | $(1.67 \pm 0.28) \times 10^5$ |
| $\alpha_3$, $sec^{-1}$ | $(4.67 \pm 0.31) \times 10^4$ | $(1.51 \pm 0.95) \times 10^3$ | $(3.65 \pm 0.01) \times 10^3$ | $(1.27 \pm 0.27) \times 10^3$ | $(1.55 \pm 0.02) \times 10^3$ |
| $\beta_{eff}$ | $6.542 \times 10^{-3}$ | $6.605 \times 10^{-3}$ | $6.563 \times 10^{-3}$ | $6.630 \times 10^{-3}$ | $6.629 \times 10^{-3}$ |
| $\ell_{calc}$, sec | $104 \times 10^{-9}$ | $3111 \times 10^{-9}$ | $902 \times 10^{-9}$ | $1445 \times 10^{-9}$ | $2502 \times 10^{-9}$ |
| $\ell_{meas} = \frac{\beta_{eff}}{\alpha_3}$, sec | $140 \times 10^{-9}$ | $4374 \times 10^{-9}$ | $1798 \times 10^{-9}$ | $5220 \times 10^{-9}$ | $4277 \times 10^{-9}$ |
| $\frac{\ell_{meas} - \ell_{calc}}{\ell_{calc}}$ | 0.35 | 0.41 | 1.9 | 2.6 | 0.71 |

## F. Reaction-rate Traverses

The reaction rates given in Section V indicate that the measured shapes in the core region are fairly well predicted by both cross-section sets used in this study. In the reflector region, the calculations underestimate the reaction rates, the 830 set appearing always to be lower than the 201 set. However, the 830 set gives values for the $U^{238}$-to-$U^{235}$ fission

ratio in better agreement with the experiment than the 201 set. Since the prompt-neutron lifetimes reported in Section VII.D above were based on the 201 cross-section set of calculations, at least part of the discrepancy between measured and calculated lifetimes can probably be attributed to the harder calculated spectrum than actually exists in the assembly.

## G. Reactivity Traverses

The various calculated and measured reactivity distributions given in Section VI show that at least the shape of these distributions in the core region are moderately well predicted by either cross-section set. In the reflector regions, however, the 201 set strongly overestimates the low-energy effects. This is most pronounced in Assemblies No. 8 and 8B. Although sample size effects probably account for some of the difference between measured and calculated distributions (see particularly Fig. 62), the 201 set consistently overpredicts both the capture and the fission effects at the lower energies.

## H. Cross-section Sets

Where data are available, all the spatial dependent reaction rates in reactivities given in Sections V and VI are compared to the older but respected 16-group Hansen-Roach[12] set, Argonne No. 201. To this have been added the Argonne-generated tungsten data.[13] All cross sections in the 201 set are neither energy nor space self-shielded.

By 1965 considerable new basic data were available on tungsten and other materials of interest in rocket systems. To see whether these new data could be used to obtain improved calculational results, a 26-group cross-section set, labeled Argonne Set No. 830, was assembled using the $MC^2$ code described in Ref. 14.

Unfortunately, the library available did not have complete cross sections for very low energies, so it proved necessary to continue use of the older Hansen-Roach cross sections below 30 eV. As a group, these cross sections show the best accuracy. However, this improvement is primarily in the calculation of assemblies having large quantities of $U^{238}$ where the new $U^{238}$ cross-section set gives improved results. Results for tungsten-based systems using the new set are actually a little poorer on the average than are the Hansen-Roach results.

# APPENDIX--MATERIAL CONSTANTS

This appendix accumulates the material constants for the various materials used in the ZPR-9 experiments. Core materials are identified in Table A-I, reflector materials in Table A-II, and miscellaneous materials in Table A-III. Table A-IV identifies samples used in the reactivity traverses. A 10-in.-long column of material might consist of two 2 x 2-in. pieces placed end to end with two 2 x 3-in. pieces.

TABLE A-I. Core-material Constants

| Material | Size, in. | Weight, g | Density, g/cm$^3$ |
|---|---|---|---|
| 45% density Aluminum | 1/8 x 2 x 2 | 9.13 | 1.135 |
| | 1/8 x 2 x 3 | 14.01 | |
| | 1/8 x 2 x 5 | 23.03 | |
| Enriched fuel[a] | 1/16 x 2 x 2 | 68.62 | 16.705 |
| | 1/16 x 2 x 3 | 103.65 | |
| $Al_2O_3$ | 1/8 x 2 x 2 | 19.41 | 2.383 |
| | 1/8 x 2 x 3 | 29.57 | |
| Tungsten | 1/8 x 2 x 2 | 146.1 | 17.831 |
| | 1/8 x 2 x 3 | 219.2 | |
| Full-density Aluminum | 1/16 x 2 x 2 | 10.62 | 2.635 |
| | 1/16 x 2 x 3 | 16.27 | |

[a]Composition is 93.24% $U^{235}$, 5.41% $U^{238}$, 0.91% $U^{234}$, 0.44% $U^{236}$. Weights and density are given for $U^{235}$ content only.

TABLE A-II. Reflector-material Constants

| Material | Size, in. | Weight, g |
|---|---|---|
| Full-density Aluminum | 1 x 1 x 5 | 217.51 |
| | 2 x 2 x 3 | 528.0 |
| | 2 x 2 x 4 | 705.1 |
| | 2 x 2 x 5 | 882.4 |
| BeO | 1 x 2 x 5 | 472.54 |
| | 1 x 2 x 3 | 283.57 |
| | 1 x 2 x 2 | 188.75 |
| | 1/8 x 2 x 3 | 34.54 |
| | 1/8 x 2 x 2 | 22.98 |
| $Al_2O_3$ | 1/4 x 2 x 2 | 60.03 |
| | 1/4 x 2 x 5 | 149.35 |
| | 2 x 2 x 1 | 237.22 |
| | 2 x 2 x 2 | 475.03 |
| | 2 x 2 x 5 | 121.31 |

TABLE A-III. Miscellaneous Material Constants

| Material | Size, in. | Weight, g | Composition | |
|---|---|---|---|---|
| Polyethylene | 0.005 x 1.994 x 15 | 2.139 | | |
| | 0.010 x 1.994 x 15 | 4.558 | | |
| | 0.020 x 1.994 x 15 | 9.427 | | |
| Enriched $B^{10}$ | 1/8 x 2 x 2 | 11.17 | Al cladding | 6.29 ± 0.05 g |
| | | | Impurities | 0.16 ± 0.01 g |
| | | | $B^{10}$ | 4.20 ± 0.12 g |
| | | | $B^{11}$ | 0.41 ± 0.02 g |
| Natural Boron | 1/8 x 2 x 2 | 12.58 ± 0.23 | Al cladding | 6.29 ± 0.05 g |
| | | | Impurities | 0.18 ± 0.01 g |
| | | | $B^{10}$ | 1.20 ± 0.05 g |
| | | | $B^{11}$ | 4.93 ± 0.23 g |
| $B_4C$ Plates | 1/8 x 2 x 2 | 10.73 ± 0.65 | $B^{10}$ | 1.62 ± 0.10 g |
| | | | $B^{11}$ | 6.67 ± 0.48 g |
| | | | C | 2.412 ± 0.18 g |
| | | | Impurities | 0.02 ± 0.00 g |

TABLE A-IV. Sample Constants for Space-dependent Worth Measurements

| Sample Identification | Sample Weight, g | Cladding | Description | Assembly No.[a] 7 | 7C | 9 | Lead 9 Rod | 8 | 8B | Lead 8B Rod |
|---|---|---|---|---|---|---|---|---|---|---|
| $B^{10}$ | 0.775 | Aluminum | Enriched $B^{10}$ Powder 0.9-cm diam x 1.4 cm long | x | x | x | | x | x | e |
| $B^{10}$ | 0.113 | Aluminum | 0.9-cm diam x 1.2 cm long | | | | | x | x | |
| $B^{10}$ | 0.045 | Aluminum | Natural Boron mixed with lead powder 0.9-cm diam x 1.4 cm long | | | | | | x | |
| $B^{10}$ | 0.009 | Aluminum | 0.9-cm diam x 1.4 cm long | | | | | | x | |
| $U^{235}$ | 6.396 | Aluminum | Stack of 0.005-in. foils 0.9-cm diam x 1.2 cm long | x | x | x | e | x | x | e |
| $U^{235}$ cyl. foil | 0.742 | Aluminum | 0.005-in.-thick sleeve inside capsule 1.2 cm long | | | | | x | x | |
| $U^{235}$ disc | 0.790 | Aluminum | 0.9-cm diam x 0.13 cm high | | | | | | x | |
| Polyethylene | 1.888 (Hydrogen = 0.272 g) | - | 1.2-cm diam x 2.5 cm with 0.6-cm axial hole part way | x<br>x | x<br>x | | | | | |
| Polyethylene | 2.014 (Hydrogen = 0.288 g) | - | 1.2-cm x 2.5 cm with 0.3-cm axial hole | | | x<br>x | e | x<br>x | x<br>x | |
| Borated Polyethylene | 2.168 ($B^{10}$ = 0.095) | - | Stack of eight 1/8-in.-thick, 1.2-cm-diam discs | x | x | x | e | c | x | |
| Rhenium | 54.871 | - | Stack of sixteen 1/16-in.-thick, 1.2-cm-diam discs | c | c | x | | x | x | |
| Rhenium | 3.420 | - | Single disc, as above | | | | | | x | |
| Tungsten | 49.750 | - | Eight 0.3-cm-thick discs, as above | c | c | x | | x | x | |
| Gadolinium | 20.317 | - | Fourteen 0.16-cm-thick discs, as above | | | e | | | e | |
| Dysprosium | 22.140 | - | As above | | | e | | | e | |
| Europium | 10.552 | - | As above | | | e | | | e | |
| Aluminum | 9.665 | Aluminum | Empty capsule | c | c | c | | c | x | |
| Lead | 3.037 | Aluminum | 0.9-cm diam x 1.4 cm long | | | | | | e | |

[a] x = both experimental and calculated worths.
e = only experimental worths.
c = only calculated worths.

Dimensions of the various assemblies were determined from the dimensions of a typical matrix position as shown in Fig. A-1. The first row of the upper right table in the figure gives the fixed weight of aluminum (drawer plus matrix) per centimeter of core length. The second row gives the fixed weight of aluminum (in the matrix) and steel (in the 10 dual-purpose rods) for each centimeter of core length.

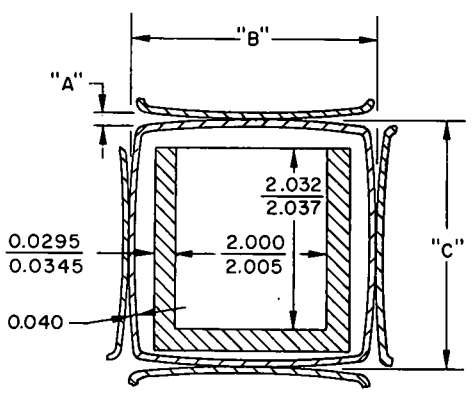


| | Aluminum | Iron |
|---|---|---|
| Fuel Drawer<br>D. P. Rod Drawer | 9.52 g/cm<br>5.80 g/cm | 15.0 g/cm |
| Average cross-sectional area of matrix position = 30.725 $cm^2$ | | |

NOTES

BOWING CONDITION OF MATRIX TUBE IS EXAGGERATED FOR THE PURPOSE OF CLARITY.

ALL DIMENSIONS IN INCHES

| "A" | "B" | "C" | CONDITION |
|---|---|---|---|
| 0.007 | 2.199 | 2.199 | CORE UNLOADED |
| 0.0002 | 2.179 | 2.186 | FULLY LOADED 200 LITER CORE |

Fig. A-1
Typical Matrix Position

112-7936 Rev. 1

## REFERENCES


1. R. C. Doerner, W. G. Knapp, K. K. Almenas, and R. A. Karam, *Physics Measurements in Tungsten-based, Aluminum-reflected Fast Reactors*, ANL-7007 (March 1967).

2. R. C. Doerner, K. K. Almenas, R. A. Karam, W. Y. Kato, W. G. Knapp, and W. B. Loewenstein, "Physics Measurements in Tungsten-based, Aluminum-reflected Fast Reactors," *Reactor Physics Division Annual Report, July 1, 1963 to June 30, 1964*, ANL-7010 (Jan 1965), pp. 116-123.

3. W. G. Knapp and R. C. Doerner, *Physics Measurements with Modified Diluent Compositions in Tungsten-based, Aluminum-reflected Fast Reactors*, ANL-7207 (Feb 1967).

4. R. C. Doerner, W. G. Knapp, K. K. Almenas, C. Cohn, R. A. Karam, W. Y. Kato, and W. B. Loewenstein, "Experimental Physics Studies in Tungsten-based Fast Reactors," *Reactor Physics Division Annual Report, July 1, 1964 to June 30, 1965*, ANL-7110 (Dec 1965), pp. 215-221.

5. D. K. Butler, R. C. Doerner, W. G. Knapp, and W. B. Loewenstein, *Physics of Fast Reactors with Tungsten-$U^{235}$ Fuel; Summary and Discussion*, ANL-7285, (in preparation).

6. Much of the experimental data has been summarized on a month-to-month basis during the past year in the monthly Reactor Development Program Progress Reports. In particular, the following references are cited:

   Assembly No. 6: *Reactor Development Program Progress Report, May 1965*, ANL-7046, pp. 17-18.

   Assembly No. 6A: *Reactor Development Program Progress Report, June 1965*, ANL-7071, pp. 18-19.

   Assembly No. 7: *Reactor Development Program Progress Report, August 1965*, ANL-7090, pp. 19-22.

   *Reactor Development Program Progress Report, October 1965*, ANL-7115, pp. 29-30.

   Assemblies No. 7 and 7C: *Reactor Development Program Progress Report, November 1965*, ANL-7122, pp. 21-31.

   Assembly No. 9: *Reactor Development Program Progress Report, December 1965*, ANL-7132, pp. 15-17.

   Assemblies No. 8 and 9: *Reactor Development Program Progress Report, January 1966*, ANL-7152, pp. 19-21.

   Assembly No. 8: *Reactor Development Program Progress Report, February 1966*, ANL-7176, p. 22.

7. C. E. Cohn, *Initial Usage of a Computer for On-line Data Reduction in Reactor Physics Experiments*, Trans. ANS *8*, No. 2, 585 (1965).

8. C. E. Cohn, *Further Use of an On-line Computer in Reactor Physics Experiments*, Trans. ANS *9*, No. 1, 262 (1966).

9. C. E. Cohn, "Automated Data Analysis and Control for Critical Facilities," *Use of Computers in Analysis of Experimental Data and the Control of Nuclear Facilities*, Argonne, May 4-6, 1966, CONF. 660527.

10. D. A. Meneley, L. C. Kvitek, and D. M. O'Shea, *MACH-1, A One-dimensional Diffusion-theory Package*, ANL-7223 (June 1966).

11. W. G. Davey, *An Analysis of 23 ZPR-3 Fast Reactor Critical Experiments*, Nucl. Sci. Eng. *19*, 259 (1964).

12. G. E. Hansen and W. H. Roach, *Six and Sixteen Group Constants for Fast and Intermediate Critical Assemblies*, LAMS-2543 (Nov 1961).

13. K. K. Almenas,"Verification of Tungsten Cross Sections," *Reactor Physics Division Annual Report, July 1, 1963 to June 30, 1964*, ANL-7010 (Jan 1965), pp. 131-134. See also *Reactor Physics Constants*, ANL-5800 (July 1963).

14. D. M. O'Shea, B. J. Toppel, and A. L. Rago, "The Automated Preparation of Multigroup Cross Sections for Fast Reactor Analysis Using the $MC^2$ Code," *Proceedings of the International Conference on Fast Critical Experiments and Their Analysis, October 10-13, 1966*, ANL-7320, pp. 27-32.